INTERNATIONAL SYMPOSIUM ON POLAR OCEAN AND GLOBAL CHANGE

RESPONSE AND FEEDBACK OF THE POLAR OCEANS TO GLOBAL WARMING

ABSTRACT

中国海洋大学
OCEAN UNIVERSITY OF CHINA

Qingdao, China
22-24 October, 2024

Contents

Keynote Lectures

Polar ocean water-mass change over the past 50 years — and projections for the future

Matthew H. England

Centre for Marine Science and Innovation (CMSI), and ARC Australian Centre for Excellence in Antarctic Science, University of New South Wales, Sydney, NSW, Australia
* Presenter's email: M.England@unsw.edu.au

By absorbing vast quantities of heat and carbon, the polar oceans play a critical role in moderating climate change. But these climate benefits do not come without cost; as the polar oceans warm, they disrupt ecosystems and melt the polar ice caps, raising sea-level globally and reshaping our coastlines. In this talk I will outline the ways in which the Southern Ocean is currently absorbing vast quantities of heat. I will also show how melting ice around Antarctica is slowing the ocean's abyssal overturning circulation, and what this means for global climate and sea-level rise. The talk will also analyze recent high-resolution model projections of a slowdown in the Atlantic Meridional Overturning Circulation (AMOC), how to monitor an AMOC slowdown using regional hydrographic observations, and what a slowdown potentially means for Pacific climate variability and change.

Antarctic shelf ocean warming and sea ice melt affected by projected El Niño changes

Wenju Cai[1], Agus Santoso[1,2,3*]

[1] Frontiers Science Center for Deep Ocean Multispheres and Earth System, Ministry of Education, Ocean University of China, 266100 Qingdao, PR China
[2] International CLIVAR Project Office, Ocean University of China, 266100 Qingdao, PR China
[3] Climate Change Research Centre, University of New South Wales, Sydney, Australia
*Presenter's email: agus.santoso@clivar.org

Antarctica is a major component of the climate system, with extensive cover of sea ice and ice sheets that maintain Earth's radiative balance, global thermohaline circulation, and the ocean's freshwater and volume budgets. In a planet that continues to warm, it is crucial to understand how Antarctica, its cryosphere, and the vast Southern Ocean surrounding it, will change in the future. While a lot is known about how this complex system will be affected by greenhouse warming in the climatological sense, a less known or underappreciated aspect is how some of the changes can be related to projected change in climate variability. The El Niño Southern Oscillation (ENSO) is the most dominant mode of year-to-year climate variability on the planet. Climate models that participated in the sixth phase of Coupled Model Intercomparison Project (CMIP6) have shown an inter-model consensus on the projected increase in ENSO variability over the 21st Century. Our analysis further showed that this projection has an impact on Antarctica. Specifically, the projected increase in ENSO variability is found to slow Southern Ocean warming and heat uptake but accelerate Antarctic shelf ocean warming. Models with greater increase in ENSO variability tend to simulate ENSO-induced high-latitude easterly wind anomalies which reduce circumpolar upwelling that plays an important role in the uptake of atmospheric heat. The reduced upwelling means that less warm shelf ocean water is transported to the surface, thus hastening ice shelf melting but slowing sea ice reduction. This has implications for global warming and the risk of future sea level rise.

Ecology of benthic ciliates in the Arctic seas: spatial patterns and long-term dynamics

Yuri Mazei[1,2*], Xiaolei Li[1,2]

[1] Shenzhen MSU-BIT University, International University Park Road, 1, Shenzhen 518172, PR China
[2] Lomonosov Moscow State University, Leninskiye gory, 1, Moscow, 119234, Russian Federation
* Presenter's email:yurimazei@mail.ru

Arctic coastal ecosystems play a major role in global environmental system and have been altered significantly by climate changes. To better understanding the response of marine coastal ecosystems towards rapid Arctic climate changes, we reviewed the available information about the spatial patterns and community structure as well as seasonal and long-term dynamics of interstitial ciliate assemblages in the intertidal and bathyal zones of the White Sea, Barents Sea and Kara Sea. We review major environmental factors that affect community structure and compositions, sediment properties, depth, beach type, salinity. Co-occurrence networks analysis indicated considerably high ration of positive correlations within the model ciliate assemblage in the White Sea in 2009–2019 that indicated low competition between interstitial ciliate species. Furthermore, we found that contribution of stochastic processes to the ciliate community assembly was insignificant. Compare with earlier data from the same ecosystem obtained in 1980s–1990s, the role of competitive factors is decreasing, and communities are becoming more spatially and temporally homogeneous. This community simplification is likely due to the response of the entire intertidal ecosystem to global climate change in Arctic.

Mid-latitude cold extremes during the recent period of Arctic amplification

Judah Cohen[1,2*]

[1] Atmospheric and Environmental Research, Inc., Lexington, Massachusetts 02421, USA
[2] Department of Civil and Environmental Engineering, Massachusetts Institute of Technology, Cambridge, MA, 02139, USA
*Presenter's email: jcohen@aer.com

Though cold extremes are expected to warm comparable to Arctic warming, cold extremes across the United States (US) east of the Rockies, Northeast Asia and Europe have remained nearly constant over recent decades, in clear contrast to a robust Arctic warming trend. Analysis of trends in the frequency and magnitude of cold extremes is mixed across the US and Asia but with a clearer decreasing trend in occurrence across Europe, especially Southern Europe. This divergence between robust Arctic warming and no detectable trends in mid-latitude cold extremes highlights the need for a better understanding of the physical links between Arctic amplification and mid-latitude cold extremes.

Therefore, in an effort to understand the relationship between Arctic temperatures and mid-latitude weather, we have extended a recently developed index of accumulated winter season severity index (AWSSI), originally based on temperature and snowfall observations from weather stations in the US only, to the entire Northern Hemisphere using reanalysis output. The expanded index (rAWSSI) is analyzed to reveal relationships between Arctic air temperatures/geopotential heights and the probability of severe winter weather across the midlatitudes. We find a direct and linear relationship between anomalously high Arctic temperatures/geopotential heights and increased severe winter weather, especially in northern and eastern continental regions. Positive temperature trends in specific Arctic regions are associated with increasing trends in severe winter weather in particular midlatitude areas.

Role of ocean heat transport in Arctic ocean and sea-ice change

Young-Oh Kwon[1], Dylan Oldenburg[1], Claude Frankignoul[1,2], Gokhan Danabasoglu[3], Stephen Yeager[3], and Who M. Kim[3]

[1] Woods Hole Oceanographic Institution
[2] Sorbonne University, LOCEAN/IPSL
[3] National Science Foundation National Center for Atmospheric Research
* Presenter's email: ykwon@whoi.edu

Arctic Ocean warming and sea ice loss are closely linked to changes in the ocean heat transport (OHT) and the surface heat fluxes. To quantitatively assess their respective roles, we use the 100-member Community Earth System Model version 2 (CESM2) Large Ensemble over the 1920 – 2100 period. We first examine the Arctic Ocean warming based on a heat budget framework by quantifying the relative contributions from heat exchanges with atmosphere and sea ice versus OHT across the Arctic Ocean gateways. Furthermore, we quantify how much anomalous heat from the ocean directly translates to sea ice loss and how much is lost to the atmosphere. We find that Arctic Ocean warming is driven primarily by increased OHT through the Barents Sea Opening, with additional contributions from the Fram Strait and Bering Strait OHTs. These OHT changes are driven mainly by warmer inflowing water rather than changes in volume transports across the gateways, while there also are significant changes in the structure of volume transport at the Fram Strait an Barent Sea Opening. The Arctic Ocean warming driven by OHT is then partially damped by increased heat loss through the sea surface. The increased heat loss to atmosphere is concentrated in the cold season, thus enhances the seasonal cycle of the ocean-atmosphere heat exchanges. We also explicitly calculate the contributions of ocean–ice and atmosphere–ice heat fluxes to sea ice heat budget changes. Throughout the entire 20th century as well as the early 21st century, the atmosphere is the main contributor to heat gain by the sea ice in summer, though the ocean's role is not negligible. Over time, the ocean progressively becomes the main source of heating for the sea ice as the ocean warms.

From enhanced Arctic amplification to Tropical Eastern Pacific and Southern Ocean cooling since 1980: The role of internal variability

Qiang Fu

Department of Atmospheric and Climate Science University of Washington, Seattle, Washington, USA
*Presenter's email: qfu@uw.edu

The Arctic has been warming at four times the global average since 1980, a phenomenon known as Arctic Amplification (AA). While climate models robustly simulate the AA, they often fail to reproduce the level of observed AA. Concurrently, the observed cooling in the Tropical Eastern Pacific and Southern Ocean since 1980 is not shown in the simulated forced trend and is rarely captured in model ensembles. Whether these discrepancies between model simulations and observations are largely due to internal variability or model biases has been a debate within the climate community. To address this, it is essential to accurately assess the role of internal variability in observed temperature changes.

In this talk, we present a machine learning method we develop to effectively separate Internally generated temperature trends in observations over the Arctic and globe. Our findings show that internal variability has enhanced Arctic warming but damped global warming since 1980. By removing the effect of internal variability, the observed AA decreases from 4.2 to 3.0, aligning with the model-simulated forced AA. Furthermore, we show that internal variability manifested as Global Cooling and Arctic Warming (i-GCAW) is rare in CMIP6 large ensembles, but simulations that do produce i-GCAW exhibit a unique and robust internally driven global surface air temperature (SAT) trend pattern. This unique SAT trend pattern features enhanced warming in the Barents and Kara Sea and cooling in the Tropical Eastern Pacific and Southern Ocean. Given that these features are imprinted in the observed record over recent decades, our study suggests that internal variability makes a crucial contribution to the discrepancy between observations and model-simulated forced SAT trend patterns.

Session

Marine Cryosphere and Ice-Ocean Interaction

Definition of sea ice concentration using satellite microwave radiometry and peculiarities of its application in scientific and practical tasks

Alekseeva T.A[1,2*], Tikhonov V.V.[1,2], Afanasyeva E.V., Sokolova Yu. V.

[1] Arctic and Antarctic Research Institute, Saint Petersburg, Russia
[2] Space Research Institute of the Russian Academy of Sciences, Moscow, Russia
[3] Institute for Water and Environmental Problems of the Siberian Branch of the Russian Academy of Science, Barnaul, Russia
* Presenter's email: taa@aari.ru

Satellite microwave radiometry (SMR) data is all-weather, the most durable, independent of the time of day and covers the entire Arctic Ocean, and, accordingly, is widely used in scientific and practical tasks around the world. Undoubtedly, these data have great value and prospects for studying sea ice: for calculating the area of ice, determining the ice concentration, ice age, melt ponds, thickness of ice and probably, in the future, a number of other ice parameters. To determine all the parameters listed above, various algorithms are used, each of which has certain advantages and disadvantages. At the moment, it is impossible to state unequivocally that any algorithm determines a given parameter of sea ice better than others. The most popular algorithms are those that create a multi-year database and open public access. To carry out a large-scale assessment of the accuracy of all existing algorithms for calculating ice parameters, it is necessary to compare them with natural data, which is difficult to obtain in freezing seas.

The long-term joint work of several Russian institutes is carried out to determine the accuracy of various algorithms, analyze the causes of errors by comparing SMR data with special ship data, satellite images in the visible and infrared ranges of various resolutions, radar images and ice maps. In the period of intense ice melt, the algorithms retrieving sea ice concentration from SMR data may fail to detect vast regions of floating ice. Late stage melt is characterized by abundance of melt ponds on ice resulting in considerable underestimation of sea ice concentration. Also, during melt, ice concentration decreases and ice breccias disintegrate, therefore the size of ice floes decreases. In winter, at river mouths in the shelf seas, ice is formed with a heavy load of terrigenous sediments carried by the rivers. Dirty ice surface becomes visible in summer when snow cover melts off. SMR techniques fail to adequately determine dirty ice concentration. We present the impact of ice melt, concentration, floe size and dirtiness on the determination of sea ice extent in the Arctic using the SMR data and how it influences on usage of SMR data for ice navigation.

Advances in Arctic sea ice microstructure and implications to thermodynamics

Lu Peng*, Yu Miao, Li Xuewei, Wang Qingkai, Li Zhijun

State Key Laboratory of Coastal and Offshore Engineering, Dalian University of Technology, Dalian 116024, China
* Presenter's email: lupeng@dlut.edu.cn

Under the background of global warming, observations on Arctic sea ice have long been focused on large-scale changes such as shrinking of ice coverage, thickness, volumes and sea ice regime shift. Physical mechanisms resulting in such changes have primarily attributed to the impact of large-scale external factors such as atmospheric and oceanic circulations, and solar radiation. In fact, Arctic sea ice also undergoes rapid micro-scale evolution such as gas bubbles formation and brine pockets migration and massive formation of surface scattering layer. Field studies like CHINARE2008–2018 and MOSAiC2019–2020 have confirmed these observations, yet the fully understanding of those changes in sea ice microstructure remain insufficient and superficial. In order to cope better with the rapidly changing Arctic Ocean, this study reviews the recent advances in the microstructure of Arctic sea ice in both field observations and laboratory experiments. The significant porosity and the annual and seasonal variations likely modify the thermal, optical, and mechanical characteristics of sea ice, further altering its energy budget and mass balance. Current sea ice thermodynamic models fail to accurately capture these microstructural changes in sea ice, leading to uncertainties in the results. The discrepancy between model predictions and actual observations strongly motivates the parameterization on the evolution in ice microstructure and development of next-generation sea ice models, accounting for changes in ice crystals, brine pockets, and gas bubbles under the warming Arctic. It helps to finally achieve a thorough comprehension of Arctic sea ice changes, encompassing both macro and micro perspectives, as well as external and internal factors.

Improved Arctic summer sea ice velocity based on FY-3D/MWRI brightness temperatures

Qian Shi[1*], Fei Shi[2], Rui Xu[1], Matti Leppäranta[3], Xiaochun Zhai[4], Jiping Liu[1], Qinghua Yang[1]

[1] School of Atmospheric Sciences, Sun Yat-sen University, and Southern Marine Science and Engineering Guangdong Laboratory (Zhuhai), Zhuhai, 519082, China
[2] Operational Oceanography Institution, School of Marine Technology and Environment, Dalian Ocean University, 116023, Dalian, China.
[3] Institute for Atmospheric and Earth System Research, University of Helsinki, 00014 Helsinki, Finland
[4] National Satellite Meteorological Center of China, Beijing, 100081, China
*Presenter's email: shiq9@mail.sysu.edu.cn

Arctic sea ice velocity (SIV) in summer plays key role in navigation safety and climate study. The quality of current Arctic SIV products in summer derived from remote sensing imagery are lower than those in winter. Our work retrieves SIV-summer based on polarization difference (PD) of brightness temperature (TB) at 36 GHz channel derived from recalibrated FY-3D/MWRI. Compared to using swath TB, using swath PD can better suppress atmospheric wetness (cloud liquid water and water vapor) noise. Moreover, different from the arbitrary template selection scheme used in current algorithms, we proposed an optimized template selection scheme considering the frequent deformation processes of sea ice in summer based on the texture of imagery. The SIV obtained using templates with irregular distribution present lower uncertainty and higher computational efficiency than that using templates with irregular distribution. Based on the improved algorithm, this study either obtained swath irregular SIV fields with nominal spatial resolution of 30 km or daily gridded SIV fields with 50 km spatial resolution in summer 2019 using 36 GHz PDs. It should be noted that the new algorithm is also applicable to AMSR2 imagery and has reference value for SIV retrieval research based on similar passive microwave imagery.

Unraveling the impact of ocean eddies on Arctic sea ice decline in the warming climate

Yingjie Liu[1], Ruijian Gou[2,3**]

[1] Department of Atmospheric and Oceanic Sciences and CMA-FDU Joint Laboratory of Marine Meteorology, Fudan University, Shanghai, China
[2] Frontiers Science Center for Deep Ocean Multispheres and Earth System and Key Laboratory of Physical Oceanography, Ocean University of China, Qingdao, China
[3] Alfred Wegener Institute, Helmholtz Centre for Polar and Marine Research, Bremerhaven, Germany
*Presenter's email: Yingjie_liu@fudan.edu.cn

The Arctic sea ice extent continues to decline at an unprecedented rate, a trend often underestimated by current climate projection models. This discrepancy suggests potential biases in the representation of processes that transport heat to the sea ice. In this study, we employ an eddy-resolving climate model, covering the period from 1920 to 2100, to investigate the role of oceanic eddies in the ongoing reduction of Arctic sea ice. Our findings demonstrate that eddies play a crucial role in diminishing sea ice extent by enhancing the vertical heat transport from deeper ocean layers to the surface, particularly within marginal ice zones. The sea ice heat budget analysis, which accounts for the interactions between ocean-ice heat fluxes, sea ice cover, and atmospheric forcing, reveals that eddy-induced processes significantly contribute to the thinning and retreat of sea ice, with the most pronounced effects observed during the latter half of the 21st century. These results emphasize the critical need to incorporate eddy dynamics in future projections of Arctic sea ice and highlight the importance of high-resolution models for accurately capturing the complex interactions between oceanic eddies and the sea ice in a warming climate.

Sea ice dynamics in the Barents and Kara Seas: influence of model parametrizations and data sources

Egorova E.[1], Akhtyamova A.[1,2], Frolova A.[1], Novikov M.[1,3], Khudyakova S.[1,4], Sukhikh N.[1]

[1] Lomonosov Moscow State University Marine Research Center, Department of Hydrometeorological modelling, 119607 Moscow, Russia
[2] Moscow Institute of Physics and Technology, Department of Thermohydromechanics of the Ocean, 141701 Dolgoprudny, Russia
[3] Shirshov Institute of Oceanology of Russian Academy of Sciences, Laboratory of Land-Ocean Interactions and the Anthropogenic Impact, 117997 Moscow, Russia
[4] Saint Petersburg State University, Department of Oceanology, 199034 Saint Petersburg, Russia
* Presenter's email: avellinnaa@gmail.com

Currently, there is an increasing interest in the Arctic region, particularly in its ice conditions and their prediction and modeling. The aim of the study was to reproduce the ice conditions (sea ice concentration and thickness) of the Barents and Kara Seas using different parametrizations. To achieve this goal, the high-resolution hydrodynamic model NEMO 4.2.2 (Nucleus for European Modelling of the Ocean) was utilized in the Stand-Alone-Surface configuration, integrating the ocean-atmosphere interaction, and incorporating the sea ice model SI^3 (Sea Ice Modelling Integrated Initiative).

The study conducted a series of experiments in the western sector of the Russian Arctic (the Barents and Kara seas) during the 2022-2023 ice season, with a focus on the average sea ice extent relative to its climatological values. The season was subdivided into eight periods representing different stages of ice formation and melting. The initial and boundary conditions were derived from GLORYS12v1 data, and several experiments were performed, revealing noteworthy findings.

Experiments involving ice ridging/rafting demonstrated the need to adjust the compressive strength parameter relative to the reference value, affecting ice concentration and thickness, with variations depending on the period. An interesting trend emerged when altering the ocean-ice drag coefficient: an increase led to better alignment between model and observed sea ice concentration, whereas a decrease improved alignment with ice thickness. Model results for the melting period showed underestimated sea ice concentration, thickness, and spatial distribution. Modifications with the melt ponds parameterization did not enhance the model performance. Adjustments to ice thickness categorization and inclusion of landfast parameterization resulted in insignificant deviations from the reference experiment. Additionally, a comparative analysis using TOPAZ5 and GLORYS12v1 data revealed better agreement with actual observations using the GLORYS12v1 dataset.

This comprehensive investigation provides valuable insights into the dynamic processes of sea ice in the Arctic, shedding light on the complex interplay of various parameters in ice modeling.

Understanding Antarctic sea ice predictability through lenses of AI modeling

Xiaojun Yuan

Lamont-Doherty Earth Observatory of Columbia University, 61 Rt. 9W, Palisades, NY 10964, USA
*Presenter's email: xyuan@ldeo.columbia.edu

Dynamic and statistical models have evaluated Antarctic sea ice concentration (SIC) seasonal predictability. However, SIC subseasonal (1-8 weeks) predictability remains unknown due to imperfect representations of sea ice physical processes in dynamic models. In this study, we developed a deep learning model named SIPNet that can predict SIC variability without the need to account for complex physical processes. Compared to mainstream dynamical models like ECMWF, NCEP, and GFDL-SPEAR, as well as a relatively advanced statistical model, namely the linear Markov model, SIPNet outperforms them all, providing the first assessment of subseasonal SIC predictability in the region. SIPNet results indicate that autumn SIC variability contributes the most to sea ice predictability, whereas spring contributes the least. In addition, the Weddell Sea displays the highest sea ice predictability, while predictability is low in the West Pacific. Furthermore, the deep-learning model reveals that sea ice nonlinear processes become predominant sources for predictability at 6-week and longer lead times. In contrast, linear processes have dominant predictability at 3-week and shorter lead times. Finally, SIPNet can predict ENSO- and SAM-associated anomalies in the sea ice field.

Impact of Antarctic ice sheet meltwater pulse on Atlantic meridional overturning circulation

Soon-Il An[1,2*], Jun-Young Moon[2], Henk A. Dijkstra[3], Young-Min Yang[4], Hajoon Song[2]

[1] Irreversible Climate Change Research Center, Yonsei University, Seodaemun-gu, Seoul, 03722, Republic of Korea
[2] Department of Atmospheric Sciences, Yonsei University, Seodaemun-gu, Seoul, 03722, Republic of Korea
[3] Department of Physics, Utrecht University, Utrecht, The Netherlands
[4] Department of Environmental Engineering, Jeonbuk National University, Jeonju, Republic of Korea
* Presenter's email: sian@yonsei.ac.kr

Due to hemispheric connections, Antarctic ice sheet melting in a warmer climate could alter the Atlantic Meridional Overturning Circulation (AMOC). In this study, we investigate the impact of an Antarctic ice sheet meltwater pulse on the AMOC using an ocean-atmosphere coupled general circulation model of intermediate complexity. Freshwater input into the Pacific sector of the Southern Ocean (SO) is transported eastward via the Antarctic Circumpolar Current. As this freshwater reaches the Atlantic sector, it travels northward along the eastern coast of South America, eventually reaching the North Atlantic. Additionally, the freshwater in the SO causes surface cooling due to increased stratification, provoking a northward shift of the Intertropical Convergence Zone (ITCZ) and resulting in more precipitation in the northern tropical Atlantic. These two effects lead to lower salinity in the North Atlantic, reducing salt advection and thereby weakening the AMOC. Further experiments, in which the duration of freshwater hosing was varied while maintaining the total amount constant, reveal that both the total freshwater input and hosing duration play crucial roles in determining the extent of AMOC reduction.

East Antarctic polynyas: a quarter century of exploration and discovery on the cold, salty heartbeat driving Antarctic Bottom Water Production

Guy D. Williams

First Institute of Oceanography, and Key Laboratory of Marine Science and Numerical Modeling, Ministry of Natural Resources, Qingdao, China
* Presenter's email: guy.darvall.williams@gmail.com

Antarctic coastal polynyas, characterized by intense sea-ice formation and salinification of underlying shelf waters, are among the most dynamic and awe-inspiring regions on Earth. The interplay between freezing winds and oceanic processes in these regions drives the production of Antarctic Bottom Water, a critical component of the lower limb of the global thermohaline circulation. Polynyas also play a vital role in biogeochemical cycling and ecosystem functions.

In this presentation, I will share my personal scientific journey with these extraordinary natural phenomena, which began 25 years ago when I joined the first winter expedition to the Mertz Glacier polynya in East Antarctica during July-September 1999. The groundbreaking results from this expedition laid the foundation for new research, focusing on detecting and monitoring polynyas via satellite and incorporating these new sources of Antarctic Bottom Water into global ocean climate models.

These efforts necessitated validation and year-round observations across the vast East Antarctic margin—observations that were often beyond the reach of traditional national Antarctic research expeditions. Remarkably, the use of instrumented southern elephant seals, originally deployed in an adjacent research area to study habitat, has filled many of these observational gaps. Over the last decade, data from this program has driven significant advances in our understanding, with each new polynya region uncovering additional complexities and nuance, particularly regarding their interaction with increasing meltwater from ocean-ice shelf interactions.

Differences Between the CMIP5 and CMIP6 Antarctic sea ice concentration budgets

Yafei Nie[1*], Xia Lin[2,3], Qinghua Yang[1], Jiping Liu[1], Dake Chen[1] and Petteri Uotila[4]

[1] School of Atmospheric Sciences, Southern Marine Science and Engineering Guangdong Laboratory (Zhuhai), Sun Yat-Sen University, Zhuhai, China.
[2] School of Marine Science, Nanjing University of Information Science and Technology, Nanjing, China.
[3] Earth and Life Institute, Université catholique de Louvain, Louvain-la-Neuve, 1348, Belgium.
[4] Institute for Atmospheric and Earth System Research/ Physics, Faculty of Science, University of Helsinki, Helsinki, Finland.
* Presenter's email: nieyafei@sml-zhuhai.cn

Compared to the Coupled Model Intercomparison Project Phase 5 (CMIP5) climate models, the Antarctic sea ice area (SIA) has been improved in Phase 6 (CMIP6). However, the lack of knowledge about the reliability of sea ice dynamic and thermodynamic processes in the CMIP6 models still limits the accuracy of Antarctic sea ice projections. Here, by using a novel and systematic statistical metric, the performance of CMIP5 and CMIP6 models with near-realistic SIAs was assessed. We found improvements in CMIP6 models relative to CMIP5. Moreover, forcing the sea ice-ocean model with atmospheric reanalysis led to excessive ice convergence compared to the fully coupled ocean-sea ice-atmosphere model, although the SIA bias could be much smaller. This prevalent insufficient ice divergence in the models is highly correlated with the negative ice thickness bias, highlighting the importance of ice thickness in the correct simulation of sea ice dynamics.

The responses of Antarctic sea ice and overturning cells to meridional wind forcing

Hajoon Song[1*], Yeonju Choi[1], Edward W. Doddridge[2], and John Marshall[3]

[1] Department of Atmospheric Sciences, Yonsei University, Seoul, South Korea
[2] Australian Antarctic Program Partnership, Institute for Marine and Antarctic Studies, University of Tasmania, nipaluna / Hobart, Tasmania, Australia
[3] Department of Earth, Atmospheric and Planetary Sciences, Massachusetts Institute of Technology, Cambridge, Massachusetts, USA
* Presenter's email: hajsong@yonsei.ac.kr

Meridional winds over the seasonal ice zone (SIZ) of the Antarctic have undergone changes and likely contributed to sea ice extent variability in recent decades. In this study, using observations and an eddy-resolving channel model of the Antarctic SIZ, we investigate the influence of meridional wind changes on the sea ice distribution, and document how the underlying ocean might change. We find that southerly wind anomalies in austral winter lead to an increase in sea ice extent by encouraging equatorward sea ice drift. This results in more leads and polynyas, ice production and buoyancy loss near the coastal region and freshening out in the open ocean near the Antarctic Circumpolar Current. In contrast, summertime southerly wind anomalies reduce sea ice extent due to warming anomalies near the sea ice edge. This is a consequence of enhanced meridional overturning circulation (MOC) triggered by enhanced buoyancy loss through surface heat flux and brine rejection, which brings relatively warm water towards the summertime sea ice edge. A water-mass transformation analysis reveals the increased deep water formation caused by brine rejection and heat loss in leads and polynyas. Changes in sea ice extent and MOC behave in the opposite way when the sign of the wind anomaly is switched from southerly to northerly. Our study shows that meridional wind anomalies can modify not only the sea ice distribution, extent of polynyas and air-sea buoyancy fluxes, but also the ocean's MOC and bottom water properties.

Ice-Ocean-Atmosphere feedbacks and teleconnections accelerating Antarctic melting and project FAST (Forecast of Antarctic Sea-ice Trend)

Emilia Kyung Jin[1*], Hyun-Ju Lee[1], and Eun-Sook Heo[1]

Korea Polar Research Institute (KOPRI), Incheon, Republic of Korea
* Presenter's email: jin@kopri.re.kr

The melting of the Antarctic ice sheet, a crucial factor in global sea level rise, along with the recent rapid decline in Antarctic sea ice extent, significantly influences future global climate change. However, due to limited observations and uncertainties in modeling, a high degree of uncertainty remains in future projections. To address this issue, we analyzed both remote and regional ice-ocean-atmosphere interactions that affect the melting of the Antarctic ice sheet, utilizing a range of observational data and modeling techniques. Our focus was particularly on the Thwaites Glacier region in West Antarctica, where ice is melting most rapidly, and the eastern part of East Antarctica, where a notable reduction in ice extent is observed. External forcings that cause teleconnections, such as El Niño, the Indian Ocean Dipole (IOD), the Atlantic Multidecadal Oscillation (AMO), as well as major regional climate variabilities in Antarctica including the Southern Annular Mode (SAM) and the Amundsen Sea Low (ASL), were considered. Based on these studies, we aim to introduce Project FAST (Forecast of Antarctic Sea ice Trend), designed to enhance understanding of the unprecedented reduction in Antarctic sea ice extent observed in recent years and to improve future predictions of sea ice. In particular, this project focuses not only on the variations in sea ice extent in the open waters of the Southern Ocean, as analyzed in previous studies, but also on the analysis and prediction of fast ice, which is crucial for supporting Antarctic activities and infrastructure.

Session

Polar Ocean Dynamics and Thermodynamics

Variability of warm water intrusion and bottom water export off East Antarctic coasts

Shigeru Aoki

Institute of Low Temperature Science, Hokkaido University, 2060-0819 Sapporo, Japan
*Presenter's email: shigeru@lowtem.hokudai.ac.jp

The Antarctic margin largely controls global climate elements such as mean sea level and meridional overturning circulation. Environmental settings of the Antarctic coastal shelf region are key factors of the continental ice melt and dense water formation. Warm water intrusion onto the West Antarctic shelf is known to trigger melt of continental ice. In contrast, East Antarctic shelf has been paid less attention, but its huge potential and recent sign of ice mass loss demands intensive research. Totten Glacier is one of the hotspots for the ice sheet instability. General structure of the shelf bathymetry has been clarified and details such as zig-zag conduit of deep valleys have been revealed. Ubiquitous presence of warm water and significant temporal variabilities from the tidal to interannual time scares have been detected. The change in the warm shelf can have far-reaching influence.

General freshening, warming, and volume reduction have been recognized for Antarctic Bottom Water, and recent hydrographic surveys have clarified the presence of spatial and temporal dependence in those changes off East Antarctica. Decadal upturn in salinity has been observed in the eastern side of the Australian–Antarctic Basin, and the signature can be traced back to the Ross Sea shelf. In the western side the decadal flip is less pronounced and the longer-term trend is clear even for the lighter density further into South Australian Basin. To the west Cape Darnley Bottom Water revealed general freshening, with its magnitude somewhat suppressed compared to those changes in the east. Some numerical models reproduce similar changes, while still many models do not. Although the quantitative assessment is needed, many aspects of bottom water formation, spreading, and change remain insufficiently known due to the paucity of in situ observation. Sustained observations are indispensable in understanding the mechanism and global impact of the Antarctic margin.

Variability of Antarctic Dense Water Overflows observed from space

Matthis Auger[1,2] Paul Spence[1,2,3,4]*,Adele Morrison[5],Alberto Naveira Garabato[6,3], Alessandro Silvano[6]

[1] Institute for Marine and Antarctic Studies, University of Tasmania, nipaluna / Hobart, Tasmania, Australia.
[2] The Australian Centre for Excellence in Antarctic Science, University of Tasmania, nipaluna / Hobart, Tasmania, Australia.
[3] The Australian Antarctic Partnership Program, University of Tasmania, nipaluna/Hobart, Tasmania, Australia.
[4] The Australian Centre of Excellence for Weather of the 21st Century, University of Tasmania, nipaluna / Hobart, Tasmania, Australia.
[5] Research School of Earth Sciences and Australian Centre for Excellence in Antarctic Science, Australian National University, Canberra, Australia.
[6] Ocean and Earth Science, University of Southampton, Southampton, UK.
*Presenter's email: paul.spence@utas.edu.au

Around the margins of Antarctica, dense waters formed on the continental shelf are exported to oceanic depths. This overflow of dense waters to the abyss ventilates the ocean, and is vital to the global overturning circulation. Accurately quantifying the variability in the transport of dense waters exported from the Antarctic continental shelf poses substantial challenges, due to the reliance on costly, carbon-emitting and sparse observations or on models that do not capture complete dynamics. Here, we demonstrate that Antarctic dense water overflows can be monitored from space, using year-round sea surface height (SSH) observations from satellite altimetry. We employ high-resolution simulations to characterize the SSH signature of the dense waters crossing the Ross Sea continental shelf break. This allows us to find an SSH proxy that captures the dense water transport variability, even when model outputs are subsampled to the sparse satellite observation coverage. When applied to the existing satellite record, this proxy reveals interannual variability that aligns with changes in dense water properties measured from moorings and hydrographic surveys. Our findings suggest that satellite-based monitoring can effectively complement and enhance existing in situ observing systems, by providing long-term and extensive spatial coverage of Antarctic dense water transports. For example: The variability of Arctic sea ice contributes to heat reduction (albedo) and gas exchange between the ocean and the atmosphere, and further affects the deep-water formation.

Interannual salinity variability on the Ross Sea Continental Shelf in a regional Ocean-Sea Ice-Ice Shelf Model

Zhaomin Wang[1*], Liangjun Yan[1], Chengyan Liu[1]

Southern Marine Science and Engineering Guangdong Laboratory (Zhuhai), Zhuhai, Guangdong, 519082, China
* Presenter's email: wangzhaomin@sml-zhuhai.cn

We analyze the processes that control interannual salinity variability on the Ross Sea continental shelf in a high-resolution regional coupled ocean-sea ice-ice shelf model with constant boundary conditions. We show that both brine rejection and salt advection jointly dictate the interannual salinity variability. The surface salinity variability is driven by both brine rejection and the import of the upper layer water across the shelf break. Enhanced sea ice production does not necessarily increase the salinity in High Salinity Shelf Water (HSSW). This is because the salt input into the lower layer from brine rejection cannot exceed the salt export associated with the outflow of High Salinity Shelf Water (HSSW) when the surface salinity is relatively low and the vertical salt gradient is relatively large. The east-west sea level pressure gradient across the Ross Sea significantly shapes the surface wind patterns over the Ross Sea continental shelf and hence controls sea ice production on the continental shelf. The enhanced (reduced) HSSW production and the increase (decrease) in the salinity of the HSSW can increase (decrease) the outflow of saltier lower layer water and the inflow of the upper layer water across the shelf break, tending to make a larger (smaller) vertical salt gradient. Thus, wind-forced brine rejection acts to drive the interannual salinity variability, while the responding overturning circulation tends to damp the variability.

Evidence for large-scale climate forcing of dense shelf water variability in the Ross Sea

Zhaoru Zhang[1,2,3,4*], Chuan Xie[1], Pasquale Castagno[5], Matthew H. England[6], Xiaoqiao Wang[1], Michael S. Dinniman[7], Alessandro Silvano[8], Chuning Wang[1], Lei Zhou[1], Xichen Li[9], Meng Zhou[1,2,3,4,], Giorgio Budillon[10]

[1] School of Oceanography, Shanghai Jiao Tong University, China
[2] Key Laboratory of Polar Ecosystem and Climate Change, Ministry of Education, Shanghai Jiao Tong University, Shanghai, China
[3] Shanghai Key Laboratory of Polar Life and Environment Sciences, Shanghai Jiao Tong University, Shanghai, China
[4] Key Laboratory for Polar Science, Polar Research Institute of China, Ministry of Natural Resources, China
[5] Department of Mathematical Sciences and Informatics, Physics and Earth Sciences, University of Messina, Italy
[6] Centre for Marine Science and Innovation (CMSI) and Australian Centre for Excellence in Antarctic Science, University of New South Wales, Sydney 2052, Australia
[7] Center for Coastal Physical Oceanography, Old Dominion University, USA
[8] Ocean and Earth Science, National Oceanography Centre, University of Southampton, Southampton, UK
[9] Institute of Atmospheric Physics, Chinese Academy of Sciences, China
[10]Department of Sciences and Technologies, Parthenope University, Italy
* Presenter's email: zrzhang@sjtu.edu.cn

Antarctic Bottom Water (AABW), which supplies the lower limb of the thermohaline circulation, originates from dense shelf water (DSW) forming in Antarctic polynyas. Combining the longest mooring record of DSW measurements in the Southern Ocean, numerical simulations and satellite data, we show that significant correlation can exist between interannual variability of DSW production in polynyas of the Ross Sea that contributes between 20–40% of the global AABW production and the Southern Annular Mode (SAM). The correlation is largest when the Amundsen Sea Low (ASL) is weakened and further away from the Ross Sea. During positive SAM phases, enhanced offshore winds over the western Ross Sea increase sea ice production and promote DSW formation, with the opposite response occurring during negative SAM phases. These processes finally modulate AABW thickness in the open ocean of the Pacific sector. The projected trend in SAM toward its positive phase and ASL moving further from the Ross Sea has implications for the future of DSW and AABW.

Instabilities of the Antarctic Slope Current along an idealized continental slope

Chengyan Liu[1*], Zhaomin Wang[1*], Xi Liang[2], Xiang Li[1], Xianxian Han[1], Wenjin Sun[3], Yang Wu[4], Xichen Li[5], and Chen Cheng[1]

[1] Southern Marine Science and Engineering Guangdong Laboratory (Zhuhai), China.
[2] Key Laboratory of Marine Hazards Forecasting, National Marine Environmental Forecasting Center, Ministry of Natural Resources, Beijing, China.
[3] School of Marine Sciences, Nanjing University of Information Science & Technology, Nanjing, China.
[4] School of Information Engineering, Nanjing Xiaozhuang University, Nanjing, China.
[5] Institute of Atmospheric Physics, Chinese Academy of Sciences, Beijing, China.
* Presenter's email: liuchengyan@sml-zhuhai.cn

The Antarctic Slope Current (ASC), coupled with the Antarctic Slope Front (ASF), encircles Antarctica and is a roughly alongshore flow. Yet, the instabilities of the ASC/ASF can induce cross-slope exchanges. The ASC/ASF instabilities excited by external forcing have been studied extensively in previous literature. However, the mechanisms responsible for the intrinsic instabilities are still not clear. Based on an idealized eddy-resolving model, this study focuses on the intrinsic instabilities of the ASC/ASF. The ASC/ASF is classified into three types: Fresh Shelf, Warm Shelf, and Dense Shelf. Focused on the Fresh Shelf and Dense Shelf cases, two high-resolution process-oriented numerical experiments are conducted to reveal the typical characteristics, the dynamic mechanisms, and the influences of intrinsic instabilities. In the Fresh Shelf case, the intrinsic instabilities are characterized by a submesoscale vortex train over the middle-lower slope, associated with the Topographic Rossby waves. In the Dense Shelf case, a mesoscale vortex train is present over the lower slope, and abundant filaments and jets can flow across the shelf break. The baroclinic instability greatly contributes to the generation of intrinsic instabilities in the two cases, yet the barotropic instability contributes less to the intrinsic instabilities in the Fresh Shelf case. As an important feature of the instabilities, coherent eddies have been identified and significantly favor the cross-slope exchanges by the advection of water boluses retaining source water. Intrinsic instabilities only contribute to exchanges across the continental rise in the Fresh Shelf case but effectively result in cross-slope exchanges in the Dense Shelf case.

Mechanisms and impacts of extreme high-salinity shelf water formation in the Ross Sea

Xiaoqiao Wang[1], Zhaoru Zhang[2**, 3, 4, 5], Chuan Xie[2]

[1] College of Meteorology and Oceanography, National University of Defense Technology, Changsha, China
[2] Key Laboratory of Polar Ecosystem and Climate Change, Ministry of Education and School of Oceanography, Shanghai Jiao Tong University, 1954 Huashan Road, Shanghai, 200030, China
[3] Shanghai Key Laboratory of Polar Life and Environment Sciences, Shanghai Jiao Tong University, Shanghai, China
[4] Shanghai Frontiers Science Center of Polar Science, Shanghai Jiao Tong University, 1954 Huashan Road, Shanghai, 200030, China
[5] Key Laboratory for Polar Science, Polar Research Institute of China, Ministry of Natural Resources, Shanghai, 200136, China
* Presenter's email: wangxiaoqiao23@nudt.edu.cn

High-salinity shelf water (HSSW) acts as a precursor to Antarctic Bottom Water (AABW) and plays a critical role in regulating the global ocean circulation system. This study utilizes a high-resolution Ross Sea-Amundsen Sea ocean-sea ice-ice shelf model to analyze the variability in HSSW formation in the Ross Sea from 2003 to 2019, with a focus on the extreme HSSW event during the winter of 2007. The results indicate that during the winter of 2007, synoptic-scale cyclones were predominantly located near the front of the Ross Ice Shelf. Under the influence of local topography, the western flanks of these cyclones significantly enhanced offshore winds, leading to a sharp increase in ice production within the Ross Ice Shelf polynya, which directly contributed to the substantial HSSW formation. However, despite this increase in HSSW, the salinity and density of the Ross Sea decreased significantly during the same period. Further investigation revealed that this anomaly was due to a rapid increase in ice shelf melting in the Amundsen Sea and Ross Seas during 2006-2007, with annual cumulative melt rates reaching up to 600 Gt yr^-1, the highest in recent decades. The resulting large inflow of meltwater was transported westward into the Ross Sea by a strong coastal current, leading to an increase in freshwater in the region. This increase in freshwater flux, combined with the increased production of HSSW, created a dynamic interplay that ultimately altered the hydrographic characteristics of the Ross Sea.

Emergence of Top-down Controls on Southern Ocean Biomass in the 21st Century

Tyler Rohr[1,2]

[1] Institute for Marine and Antarctic Science, University of Tasmania, Hobart, TAS, Australia
[2] Australian Antarctic Program Partnership, Hobart, TAS, Australia
*Presenter's email: Tyler.rohr@utas.edu

Accurately predicting climate-driven changes to Southern Ocean marine biomass is essential to protecting fragile ecosystems and managing fisheries. The canonical wisdom holds that higher temperatures will drive weaker conductive mixing, shallower mixed layers, relived phytoplankton light limitation, higher primary productivity, and ultimately more marine biomass. Consistent with this framework, CMIP6 models generally agree that phytoplankton growth conditions (i.e. specific cell division rates) will increase under high emissions scenarios (SSP585). However, only a subset of models actually exhibit increasing phytoplankton biomass. Many others simulate decreasing phytoplankton biomass despite improving growth conditions. This paradox is only possible if increasing phytoplankton loss rates become decoupled from biomass, allowing them to outpace increasing cell division rates. Interestingly, this phenomenon typically only occurs in the Southern Ocean when biogeochemical models include multiple phytoplankton and zooplankton functional groups. I will show mechanistically how shifting planktonic community composition in a changing climate can drive decreasing phytoplankton biomass despite faster cell division more efficient trophic transfer. This is critical because most marine ecosystem models used to project Southern Ocean fisheries are forced only with phytoplankton biomass, and thus could mistake increasing secondary production for decreasing biomass at the base of the food chain. These results raise questions about the true fate of Southern Ocean biomass and how best to predict -and protect- it.

Oceanic teleconnections from the tropics to the Southern Ocean

Zhi Li[1,2,3], Ivana Cerovečki[4], Sjoerd Groeskamp[5], Matthew H. Englanda[2], F. AlexanderHaumann[6,7]

[1] Centre for Marine Science and Innovation, University of New South Wales, NSW 2052, Australia.
[2] Australian Centre for Excellence in Antarctic Science, University of New South Wales, NSW 2052, Australia.
[3] Climate Change Research Centre, University of New South Wales, NSW 2052, Australia.
[4] Scripps Institution of Oceanography, University of California, San Diego, La Jolla, California, USA
[5] NIOZ Royal Netherlands Institute for Sea Research, Department of Ocean Systems, 1790 AB, Den Burg, Texel, The Netherlands.
[6] Alfred Wegener Institute, Helmholtz Centre for Polar and Marine Research, Bremerhaven, Germany.
[7] Ludwig-Maximilians-Universität München, Munich, Germany.
* Presenter's email: zhi.li4@unsw.edu.au.

Mode waters in the Southern Ocean form a major sink for both anthropogenic heat and carbon, yet little is known about the oceanic mechanisms that control its variability. In this study, we use observationally based data to examine the oceanic teleconnections from the tropics to the Southern Ocean along a pathway from the Indonesian Throughflow (ITF) to the South Equatorial Current, the Agulhas Current, then around the Southern Ocean via the Antarctic Circumpolar Current (ACC). Our analysis reveals propagation of ITF water and its interannual variations into the Southern Ocean along this pathway, taking approximately 2–3 years from the Indonesian exit passages to the Agulhas Retroflection region. The Agulhas water combines with ACC water entering from the Atlantic basin to govern the temperature–salinity pattern and variability of ACC waters in the western Indian Ocean, over which the mixed-layer depth (MLD) and Subantarctic Mode Water (SAMW) volume and properties all show strong quasi-biennial variability. These temperature–salinity, MLD, and SAMW anomalies introduced in the western Indian Ocean are then advected eastward with the ACC and re-emerge in the eastern Indian Ocean in approximately one year, reaching the southeast Pacific in 4–5 years and further to the east of Drake Passage a year later. The propagation speed of these anomalies is around 40–55 degrees longitude per year along the ACC, or equivalently 0.15–0.2 m s-1, matching the advective time-scale and pathway of variability along the ACC. A Lagrangian particle tracking analysis shows this route matches the trajectory of particles driven by geostrophic currents in the ACC.

Drivers of the Southern Ocean salinity changes under anthropogenic warming

Kewei Lyu

State Key Laboratory of Marine Environmental Science, Center for Marine Meteorology and Climate Change, College of Ocean and Earth Sciences, Xiamen University, 361102 Xiamen, PR China
* Presenter's email: kewei.lyu@xmu.edu.cn

The Southern Ocean has experienced considerable salinity changes. In this study, specifically designed numerical perturbation experiments based on a global ocean-sea ice model were conducted to distinguish contributions from different types of surface flux forcing to the Southern Ocean salinity changes under anthropogenic climate change. We find that in addition to the freshwater flux forcing, the heat flux and wind stress forcing also have significant contributions to the Southern Ocean salinity changes, especially for those seen in the interior ocean. Particularly, the heat flux forcing is mainly responsible for the deep-reaching salinification in the high-latitude Southern Ocean through the enhanced stratification and suppressed diffusive vertical exchange, as well as the subtropical freshening in the SAMW and AAIW through the poleward migration of surface outcropping and resulting subduction of fresher water.

Enhanced ocean heat storage efficiency by Southern Ocean warming and AMOC weakening during the last deglaciation

Chenyu Zhu[1*], Saray Sanchez[2], Zhengyu Liu[3, 4], Peter U. Clark[2], Chengfei He[5], Lingfeng Wan[6], Jiuyou Lu[7], Chenguang Zhu[8], Lingwei Li[3, 9], Shaoqing Zhang[6], Lijing Cheng1[10]

[1] Earth System Numerical Simulation Science Center, Institute of Atmospheric Physics, Chinese Academy of Sciences, Beijing, China
[2] College of Earth, Ocean, and Atmospheric Sciences, Oregon State University, Corvallis, OR 97331, USA
[3] Department of Geography, Ohio State University, Columbus, OH 43210, USA
[4] School of Geography Science, Nanjing Normal University, Nanjing, China
[5] Rosenstiel School of Marine, Atmospheric, and Earth Science, University of Miami, Miami, Florida
[6] Frontier Science Center for Deep Ocean Multispheres and Earth System (DOMES), Institute for Advanced Ocean Study (IAOS) and Key Laboratory of Physical Oceanography, MOE (POL), Ocean University of China, Qingdao, China
[7] Laoshan Laboratory, Qingdao, China
[8] School of Ocean Sciences, China University of Geosciences (Beijing), Beijing, China
[9] Institute of Arctic and Alpine Research, University of Colorado Boulder, Boulder, CO 80303, USA
[10]International Center for Climate and Environment Sciences, Institute of Atmospheric Physics, Chinese Academy of Sciences, Beijing, China
* Presenter's email: zhuchenyu@mail.iap.ac.cn

Proxy reconstructions suggest that increasing global mean sea-surface temperature (GMSST) during the last deglaciation was accompanied by a comparable or greater increase in global mean ocean temperature (GMOT), corresponding to a large heat storage efficiency (HSE, ΔGMOT/ΔGMSST). An increased GMOT is commonly attributed to surface warming at sites of deepwater formation, but winter sea-ice covered much of these source areas during the last deglaciation, which would imply a HSE much less than 1. Here we use climate model simulations and proxy-based reconstructions of ocean temperature changes to show that an increased deglacial HSE is achieved by warming of intermediate-depth waters, especially those sourced from the Southern Ocean. The warming is forced by mid-latitude surface warming in response to greenhouse gas and ice-sheet forcing as well as by reduced Atlantic meridional overturning circulation associated with meltwater forcing. These results, which highlight the role of surface warming pattern and oceanic circulation changes, have implications for our understanding of long-term ocean heat storage change.

Mesoscale eddies inhibit intensification of the Subantarctic Front under global warming

Dapeng Li[1*], Zhao Jing[1,2], Wenju Cai[1,2], Zhengguang Zhang[1], Jiuxin Shi[1], Xiaohui Ma[1], Bolan Gan[1], Haiyuan Yang[1], Zhaohui Chen[1], Lixin Wu[1,2]

[1] Frontiers Science Center for Deep Ocean Multispheres and Earth System and Key Laboratory of Physical Oceanography, Ocean University of China, Qingdao, China
[2] Laoshan Laboratory, Qingdao, China.
*Presenter's email: lidapeng@ouc.edu.cn

Oceanic mesoscale eddies are important dynamical processes in the Southern Ocean. Using high-resolution (~0.1。for the ocean) Community Earth System Model (CESM-HR) simulations under a high-carbon emission scenario, we investigate the role of mesoscale eddies in regulating the response of the Subantarctic Front (SAF) to global warming. The CESM-HR simulates more realistic oceanic fronts and mesoscale eddies in the Southern Ocean than a coarse-resolution (~ 1。for the ocean) CESM. Under global warming, the SAF is projected to intensify. The mean flow temperature advection intensifies the front, whereas the mesoscale-eddy-induced temperature advection and atmospheric dampening play primary (~67%) and secondary (~28%) roles in counteracting the effect of mean flow temperature advection. Our study suggests the importance of mesoscale eddies on inhibiting the SAF intensification under global warming and necessity of mesoscale-eddy-resolving simulations for faithful projection of future climate changes in the Southern Ocean.

Ageostrophic meridional eddy-induced heat flux in the Southern Ocean

Ruiyi Chen and Yiyong Luo

[1] Key Laboratory of Physical Oceanography and Frontiers Science Center for Deep Ocean Multispheres and Earth System, China
[2] College of Oceanic and Atmospheric Sciences, Ocean University of China, Qingdao, Shandong, China
*Presenter's email: yiyongluo@ouc.edu.cn

Eddy-induced heat flux (EHF) convergence plays an important role in balancing the cooling of mean flows in the heat budget of the Southern Ocean. This study investigates the EHF in the Southern Ocean and the surface ocean heat budget over the Antarctic Circumpolar Current (ACC) estimated through a high-resolution ocean assimilation product. In contrast to previous studies in which the estimation of the EHF in the Southern Ocean was based on the assumption that mesoscale eddies are quasigeostrophic turbulence, we find that more than one-third of the total meridional EHF in the surface layer is attributed to ageostrophic currents of eddies and that the ageostrophic component of the EHF convergence is as important as its geostrophic component for the surface ocean heat budget over the ACC. In particular, the ageostrophic meridional EHF convergence accounts for 22% of the warming needed to balance the cooling from the mean flows during winter, equivalent to warming the surface ocean of the ACC by 0.14°C. The ageostrophic meridional EHF is likely caused by the stirring effect of ageostrophic secondary circulations in mesoscale eddies, which are induced by the turbulent thermal wind balance to restore the vertical shear of the upper layer in mesoscale eddies destructed by intense winter winds.

Eddies regulate the ocean heat advection to the Arctic

Bashmachnikov I.[1,2*]

[1] Saint Petersburg State University, 7/9 Universitetskaya nab, St. Petersburg, 199034, Russian Federation
[2] Nansen International Environmental and Remote Sensing Centre, 7, 14-th Line V. O., Saint Petersburg, 199034, Russian Federation
*Presenter's email: i.bashmachnikov@spbu.ru, igorb1969@mail.ru

Oceanic heat enters the Arctic mainly through the Nordic Seas, advected by two main branches of the Norwegian Atlantic Current: the Norwegian Atlantic Slope Current and the Norwegian Atlantic Front Current. The Norwegian Atlantic Current, on its way through the Nordic Seas to the Arctic, loses over 50% of its heat. In this study it is shown that a large portion of this heat loss is due to generation of mesoscale eddies.

Three-dimensional properties of mesoscale eddies in the Norwegian and Greenland Seas were studied using satellite altimetry data and in situ observations. Eddies in the Norwegian Sea generally have significantly bigger volume, rotation velocity, and core temperature anomalies compared to eddies in the Greenland Sea. The likely reason for this difference is that eddy generation mechanisms in the Greenland Sea are different from those in the Norwegian Sea. The large-scale pattern of eddy translations was estimated. Eddies move counterclockwise around the Norwegian-Greenland region, and are organized in an intensified regional circulation pattern in the Lofoten Basin.

Mesoscale eddies are shown to have a significant impact on heat redistribution in the Lofoten Basin, extracting and dispersing over the Basin approximately 1/3 (60 TW) of the heat, brought into the Basin by the Norwegian Atlantic Slope Current.

The interannual variability of the eddy heat transport, which is linked to the observed variability in the number of generated eddies, accounts for only 10 TW. However, an increase in the temperature in the eddy cores by 1°C leads to an increase of the eddy heat flux by 50 TW. Thus, the variability in the eddy heat transport can effectively damp the water temperature anomalies entering the Norwegian Sea from the south.

The seasonal variability of the Chukchi Slope Current

Wenli Zhong[1,2*], Luyang Ye[1], Zichen Liu[1], Maxime Ballarotta[3], …

[1] Frontier Science Center for Deep Ocean Multispheres and Earth System (FDOMES) and Physical Oceanography Laboratory, Ocean University of China, Qingdao, Shandong, China.
[2] Laoshan Laboratory, Qingdao, Shandong, China.
[3] Collecte Localisation Satellites, 31520 Ramonville-Saint-Agne, France.
* Presenter's email: wlzhongouc@ouc.edu.cn

The Chukchi Slope Current (CSC) is an important channel for transporting freshwater and heat that originates from the Pacific Ocean into deep Arctic basins. The variation of its intensity is influenced by ice-ocean interaction processes. This talk will analyze the seasonal variations of the CSC from an observational perspective, revealing its variability under different forcing fields and exploring the interaction between CSC and eddies via examining the wind-power input.

Upper-layer Circulation at the Mouth of Amundsen Gulf, Arctic Ocean

Peigen Lin[1,2*], Robert S. Pickart[3], Maria Pisareva[4], Bill Williams[5]

[1] School of Oceanography, Shanghai Jiao Tong University, Shanghai, China
[2] Key Laboratory of Polar Ecosystem and Climate Change, Ministry of Education, China
[3] Woods Hole Oceanographic Institution, Woods Hole, USA
[4] Deutsches Geodätisches Forschungsinstitut, Technical University of Munich, Munich, Germany
[5] Institute of Ocean Sciences, Sidney, Canada
* Presenter's email: plin@sjtu.edu.cn

Amundsen Gulf, located between the Canadian north slope and Banks Island, is the first gateway to the Canadian Arctic Archipelago, providing a bridge between the western Arctic Ocean and the North Atlantic. Using timeseries from 13 moorings in the vicinity of the mouth of Amundsen Gulf deployed from 2003-2004, we investigate the mean state and dominant variability of the circulation in the upper layer which consists of boundary currents on both sides of the gulf and anticyclonic recirculation in the interior. We find that the flow at the western side of the gulf switches directions in response to the wind: inflow under northwesterly winds and outflow under southeasterly winds. Such a relationship persists throughout the year, except during periods of full ice coverage. By contrast, the current on the eastern side of Amundsen Gulf consistently flows into the gulf for most of the year and is only weakly correlated with the western boundary current or local winds. Instead the flow aligns more with the circulation along the eastern side of Banks Island which is linked to the southeastern extension and movement of the Beaufort Gyre, and, in turn, the basin-scale wind stress curl. Three distinct water masses were observed at the mouth of the gulf mouth during the year-long period: fresh water in late fall that originates in the basin and penetrates into the gulf; cold/salty water in winter that is intermittently advected into the gulf from the eastern boundary current; and warm water in summer that appears in open ocean regions where atmospheric heating occurs, independent of the detailed circulation structure.

Arctic marine heatwave and total heat exposure projections based on CMIP6 Models

Yan He[1*], Qi Shu[1], Qiang Wang[2], Zhenya Song[1], Min Zhang[1], Shizhu Wang[1], Lujun Zhang[3], Haibo Bi[4], Rongrong Pan[1], Fangli Qiao[1]

[1] First Institute of Oceanography, Ministry of Natural Resources, Qingdao, China.
[2] Alfred Wegener Institute, Helmholtz Centre for Polar and Marine Research (AWI), Bremerhaven, Germany.
[3] School of Atmospheric Sciences, Nanjing University, Nanjing, China.
[4] Key Laboratory of Marine Geology and Environment, Institute of Oceanology, Chinese Academy of Sciences, Qingdao, China.
* Presenter's email: heyan@fio.org.cn

Marine heatwaves (MHWs) and total heat exposures (THEs), extreme warming events occurring across the global oceans, seriously threaten marine ecosystems and coastal communities as the climate warms. However, future changes in MHWs and THEs in the Arctic Ocean, where unique marine ecosystems are present, are still unclear. Here, based on the latest CMIP6 climate simulations, we find that both MHWs and THEs in the Arctic Ocean are anticipated to intensify in a warming climate, mainly due to Arctic sea ice decline and long-term warming trend, respectively. Particularly striking is the projected rise in MHW mean intensity during the 21st century in the Arctic Ocean, surpassing the global average by more than sevenfold under the CMIP6 SSP585 scenario. This phenomenon, coined the 'Arctic MHW Amplification', underscores an impending and disproportionately elevated threat to the Arctic marine life, necessitating targeted conservation and adaptive strategies.

Climate Variabilities of polar ocean across scales

Ruijian Gou[1,2*], Gerrit Lohmann[2], Lixin Wu[1,3]

[1] Frontiers Science Center for Deep Ocean Multispheres and Earth System, Ministry of Education, Ocean University of China, 266100 Qingdao, PR China
[2] Alfred Wegener Institute, 27570 Bremerhaven, Germany
[3] Laoshan Laboratory, 266100 Qingdao, PR China
* Presenter's email: rgou@foxmail.com

High-resolution climate models can resolve more climate variability, including ocean eddies and climate extremes, and are therefore important for studying the interactions of polar climate variability at different scales. We found that although the meridional overturning circulation in high-resolution climate model shows a smooth weakening, there are abrupt shifts on regional scales only in the high-resolution model, such as a strengthening toward the Arctic. The Arctic marine heatwaves, as resolved in high-resolution climate models, would induce even stronger future Arctic ocean warming, and therefore the currently expected ocean warming is underestimated. In the Southern Ocean, marine cold spells are projected to intensify in the future. This is due to the resolved eddies that show a strengthening of northward movement and carry high-latitude cold water.

Thermodynamic and dynamic contributions to the abrupt increased winter Arctic sea ice growth since 2008

Daling Li Yi[1*], Ke Fan[1], and Shengping He[2,3]

[1] School of Atmospheric Sciences, Sun Yat-sen University, and Southern Marine Science and Engineering Guangdong Laboratory (Zhuhai), Zhuhai, PR China
[2] Geophysical Institute, University of Bergen and Bjerknes Centre for Climate Research, Bergen, Norway
[3] Nansen Environmental and Remote Sensing Center, Bergen, Norway
*Presenter's email: yildling@mail.sysu.edu.cn

The area of Arctic winter sea ice growth (WSIG) has expanded dramatically since winter 2008. Yet the thermodynamic and dynamic contributions to the abrupt increase in WSIG remain unclear. Here using an ice concentration budget, we characterized quantitatively the increasing WSIG and revealed the relative contributions of dynamics during 1985–2021. Ice dynamics related to ice convergence/divergence are compared in two representative regions. The northern Laptev Sea is a freezing-dominated ice growth region and is competitively driven by the ice convergence. While in northwest Beaufort Gyre (BG), the combined effects of freezing and ice divergence have both enhanced since 2008, and the dynamics contribute 84% to the significant WSIG intensification since 2008. Comparison of thermodynamic and dynamic contributions emphasized that the winter sea-ice expansion is influenced not only by winter freeze, but also by convergence/divergence relative to newly formed thinner and mobile ice. Furthermore, the amplified summer Beaufort High in the mid-2000s and its long-lasting memory of the wind-driven strengthened BG are partially attributed to the abrupt increased WSIG since 2008.

Nonstationary thermodynamic and dynamic contributions to the interannual variability of winter sea ice growth in the Kara–Laptev Seas

Anjie Zhang, Daling Li Yi and Ke Fan

School of Atmospheric Sciences, Sun Yat-sen University, and Southern Marine Science and Engineering Guangdong Laboratory (Zhuhai), Zhuhai, People's Republic of China
* Presenter's email: zhanganj3@mail2.sysu.edu.cn

The Kara–Laptev Seas (KLS), known as the 'Ice Factory of the Arctic', witnesses rising instead of falling winter sea ice growth (WSIG) under the shrinkage of Arctic ice. However, knowledge of the large year-to-year variation is still unclear. Combining a seasonal ice concentration budget, a composite analysis, and a typical case study, we study both the interannual variability of WSIG in the KLS and the associated air-sea forcings during 1985–2021. Results quantitatively reveal that, during 1985–2021, thermodynamic melt in the melting season (April–August) contributed 80.3% to the interannual ice loss difference and promoted the subsequent WSIG by the recovery mechanism in the KLS. This consistent thermodynamic melt is caused by the strengthened summer Beaufort High, transporting heat and introducing a locally positive ice-albedo feedback. However, since 2010, the dynamic growth during the freezing season (October–February) has increasingly stimulated the WSIG. Typical cases in 2013 and 2017 indicate that the overlying anticyclonic atmospheric regime restricts the ice drift from the KLS and contributes to the dynamic growth of 41.6% of the WSIG difference, while the turbulent-heat-induced thermodynamic growth in winter is down to 58.4%. In short, we reveal an unstable relationship between the summer ice loss and the subsequent WSIG under the background of Arctic warming. Our study points out that the distinct dynamic ice growth driven by surface winds or ocean currents during the freezing season is likely to increase in the near future, with thinner and more mobile seasonal ice predominating in the Arctic.

Deep Atlantic multidecadal variability

Yang Jiajun[1*], Li Jianping[1,2], An Qirong[1,2]

[1] Frontiers Science Center for Deep Ocean Multi-spheres and Earth System (DOMES)/Key Laboratory of Physical Oceanography/Academy of Future Ocean/College of Oceanic and Atmospheric Sciences, Ocean University of China, 266100 Qingdao, PR China
[2] Laboratory for Ocean Dynamics and Climate, Qingdao Marine Science and Technology Center, 266237 Qingdao, PR China
* Presenter's email: yjj@stu.ouc.edu.cn

Investigating deep - sea temperature variability is essential for understanding deep - sea variability and its profound impacts on climate. The first mode in the Atlantic is referred to as Deep Atlantic Multidecadal Variability (DAMV), characterized by a north - south dipole pattern in the mid - high latitudes with a quasi - period of 20 – 50 years. The DAMV and Atlantic Multidecadal Variability, despite a statistical discrepancy, may be different responses to ocean heat transport (OHT) driven by the Atlantic Meridional Overturning Circulation (AMOC) at distinct depths separately. The relationship between the DAMV and the AMOC is established, indicating the AMOC is likely to transport surface heat downwards by deep convection and contribute to such dipole pattern in the deep Atlantic. Furthermore, meridional OHT proves the AMOC can explain the DAMV variation as a dynamic driver. These results reinforce the importance of deep-sea studies concerning the Atlantic climate system.

Session

Polar Marine Ecosystem and Biogeochemistry

Temporal and spatial patterns in biogeochemical variables as elucidated by Biogeochemical Argo Floats

Walker O. Smith, Jr., Ruobing Cao, and Yisen Zhong

School of Oceanography, Shanghai Jiao Tong University, Shanghai, PR China
* Presenter's email: wos@vims.edu

Seasonal patterns in seasonally frozen waters have largely been derived from composites of analyses conducted in different years and largely have been confined to ice-free periods. We present the first continuous measurements of hydrographic and biogeochemical variables collected over an entire year by Biogeochemical-Argo (BGC-Argo) profiling floats on the continental shelf of the Ross Sea. Analyses were divided into two periods: autumn/winter and spring/summer. Mixed layers increased rapidly upon ice cover, and nitrate, oxygen, and dissolved inorganic carbon vertical distributions were strongly influenced by this deeper mixing. Rates of nitrification in autumn were substantial and similar to rates measured in other areas of the ocean. Organic carbon disappearance was also most rapid in March. Changes in all variables slowed considerably after May. The largest mixed layer depths occurred at the southern floats and were from 400 - 500 m. Spring/summer patterns were similar to those observed during individual cruises, with rapid nitrate removal beginning in late November, continuing through early January, but ceasing during austral summer. The most rapid accumulations of chlorophyll occurred prior to complete ice retreat. Substantial spatial differences were noted that were likely related to both mixed layer depths and phytoplankton composition. Particulate matter accumulated throughout the summer below 100 m, although the rates of change suggested substantial remineralization in the water column. The temporal patterns observed show the importance of relatively short periods that markedly influence the vertical distribution of biogeochemical parameters.

The future of Arctic Ecosystems: differential responses of phytoplankton and zooplankton communities to environmental change

Russell R Hopcroft

Department of Oceanography, University of Alaska, Fairbanks, Alaska, USA 99775
* Presenter's email: rrhopcroft@alaska.edu

The ongoing reduction in the extent and duration of sea ice coverage in the Arctic Ocean appears to have resulted in increased biomass and production of phytoplankton along with a shift away from ice-associated algae. Phytoplankton increases have occurred within both the inflow seas, as well as over the interior shelves. Observations suggest there has been concurrent increases in the abundance of zooplankton, although such data remains spotty in its coverage. Here we discuss the factors that have led to these increases in phytoplankton and how zooplankton communities have responded. Not all zooplankton species have benefited equally due to differences in their life history strategies. For both components, we consider how these trends will continue into the future, and what can be expected for community structure and their seasonal cycles in the future Arctic Ocean. Such trends will ultimately determine the ability of the Arctic to support upper trophic levels including fisheries in the future.

Zooplankton of the Arctic Ocean: patterns of diversity and productivity

Ksenia Kosobokova

Shirshov Institute of Oceanology RAS Nakhimovskiy Prospekt 36, Moscow 117997, Russia
* Presenter's email: xkosobokova@ocean.ru

A review of the current state of knowledge on the structure and productivity of zooplankton communities in the Arctic Ocean is presented. The review is based on extensive sampling data collected during expeditions by research icebreakers, including the RV "Polarstern" (1995-2016) and the USCGC "Healy" (2005). Data from over 170 sampling locations, where stratified samples were collected from the bottom to the surface, allow us to compare species diversity, vertical structure, and biomass distribution of zooplankton across the entire Arctic Ocean. This large dataset clearly demonstrates that Arctic zooplankton are less diverse than those in other oceans. Only approximately 180 metazoan species have been identified in the four deep basins of the Arctic: the Nansen, Amundsen, Makarov, and Canada basins. The list of species is now believed to be nearly complete, with the exception of the deepest water layers where new species continue to be discovered. The use of modern quantitative sampling techniques in combination with consistent and standardized methods for zooplankton processing allowed for a comparison of regional variability in zooplankton stock distribution. Consistent observations across all four Arctic Ocean basins revealed two main components contributing to zooplankton biomass and productivity: a locally reproducing autochthonous community and an allochthonous community comprised of species transported into the Arctic by the Atlantic current. A strong correlation was demonstrated between regional variation in biomass and water circulation patterns, bottom topography, and life cycle traits of both autochthonous and allochthonous species.

The role of viruses in marine polar environments and their response to change

Andrew McMinn [1,2*]

[1] Institute of Marine and Antarctic Studies, University of Tasmania, Hobart, Tasmania, Australia
[2] College of Marine Life Sciences, Ocean University of China, Qingdao, Shandong, China
*Presenter's email: andrew.mcminn@utas.edu.au

Viruses are the most abundant life form on earth with an estimated total abundance in the oceans of ~1030. They are responsible for 10-30% of bacterial mortality, known to control harmful algal blooms and can reduce photosynthesis by up to 78%.

In Prydz Bay, eastern Antarctica, their abundance at all depths is closely correlated with both chlorophyll*a* and bacterial abundance. Metagenomic analyses of surface seawater from the Scotia Ridge and Prydz Bay, identified bacteriophages of the *Caudovirales*, especially the Podoviridae, as the most abundant. Microalgal viruses belonging to the Phycodnaviridae family, which contains most microalgal viruses, especially *Phaeocystis* viruses, were also identified.

Sea ice algae communities comprises a globally significant photosynthetic biofilm. While their microalgal and bacterial constituents are well characterized, there is very little information on their associated viral communities or on the virus-bacteria and virus-algae interactions within them. While high levels of interaction might be expected because of the high density of cells, infection rates, particularly of microalgae, have been found to be low. It remains unclear whether this is a result of environment characteristics, developed resistance or because of the small number of studies. However, research to date has focussed exclusively on DNA viruses. Recent research has shown that key eukaryote group, including diatoms, are mostly infected with RNA viruses. Our most recent research is showing that RNA viruses are abundant and diverse in sea ice.

We are investigating how projected global change, including ocean acidification temperature and nutrient availability, will change infection rates in ice edge blooms and sea ice ecosystems.

Impact of sea ice on the physicochemical characteristics of marine aerosols in the Arctic Ocean

Shanshan Wang[1,2*], Jinpei Yan[1,2*], Shuhui Zhao[3], Rong Tian[1,2], Xia Sun[1,2], Siying Dai[1,2], Xiaoke Zhang[1,2], Miming Zhang[1,2]

[1] Key Laboratory of Global Change and Marine Atmospheric Chemistry, MNR, China.
[2] Third Institute of Oceanography, Ministry of Natural Resources of China.
[3] School of Tourism, Taishan University, Tai'an, China.
* Presenter's email: wangshanshan1336@tio.org.cn; jpyan@tio.org.cn

Marine aerosols (MA) can be influenced by sea ice concentration, potentially playing a pivotal role in the formation of cloud condensation nuclei and exerting an impact on regional climate. A high-resolution aerosol observation system was employed to measure the concentration and size of aerosols in the floating ice region and seawater region of the Arctic Ocean during the 8th and 9th Chinese Arctic Expedition Research Cruise. The identification of aerosol sources was conducted using a modified positive definite matrix factorization method and a backward air mass trajectory model. Two types of MA including the sea-salt aerosol (SSA) and the marine biogenic aerosol (BA) were identified and their concentrations were calculated. Then the physical-chemical characteristics of MA in the floating ice region and seawater region were compared under normalized conditions (-2.5℃ < T < -0.1℃; 5.80 m/s < WS < 10.95 m/s) to discern the impact of sea ice. A unimodal distribution was observed for MA number concentration with a dominant peak ranging from 0.5 μm to 1.0 μm in size range. The findings revealed that the presence of sea ice cover led to a significant reduction of 52.2% in the number concentration of SSA, while exerting minimal influence on its composition. BA number concentration in the floating ice region was 33.3% higher than that in the seawater region. Strong winds (wind speed > 6.5 m s-1) transported organic matter and nutrients entrapped in sea ice into the atmosphere, leading to an increase in BA concentration. However, the presence of sea ice cover hampered the exchange of biogenic gases between the ocean and air, resulting in a reduction of secondary BA formation. Our study elucidates the correlation between MA release and sea ice coverage in the Arctic Ocean, thereby establishing a theoretical foundation for climate prediction models.

Sedimentary particle flux and composition in the Amundsen Sea, Antarctica: seasonal variations and regional differences

Jun Zhao[1*], Wenhao Huang[1,2], Jiaying Guo[1], Jianming Pan[1]

[1] Key Laboratory of Marine Ecosystem Dynamics, Second Institute of Oceanography, Ministry of Natural Resources, Hangzhou 310012, China
[2] School of Ocean Sciences, China University of Geosciences (Beijing), Beijing 100083, China
* Presenter's email: jzhao@sio.org.cn

The Southern Ocean is an important carbon sink globally, with significant seasonal, inter-annual, and regional variations in the sedimentary particle flux and composition. However, there is insufficient understanding of its ecological and environmental control factors. Here, based on one-year time series particle samples collected by sediment traps deployed inside and outside the Amundsen Sea Polynya, we analyzed the seasonal and regional variations in sedimentary particle flux and composition. We also discussed inter-annual differences and controlling factors, and evaluated the impact on carbon sequestration. The results showed that the sediment flux in the polynya was significantly higher than the open ocean (3.2-276 vs. 0.5-38.3 mg m-2 d-1), and higher in summer and lower in winter. The sedimentary particles in the polynya during summer are mainly organic matter (46.4%-50.5%), while terrestrial materials (65.2%-72.4%) in winter. The seasonal differences in the composition of sedimentary particles in open ocean are relatively small, with opal being the main component (7.7%-79.8%), and the proportion of terrestrial materials (1.1%-8.4%) being significantly lower than that of polynya. The summer sedimentary particles in the Amundsen Sea were mainly contributed by phytoplankton. In the polynya, the dominant species shifted from Phaeocystis antarctica to diatoms, while in the open ocean, diatoms were the main species. In winter, the primary production of phytoplankton slows down, and the flux of particulate organic carbon in polynya is mainly contributed by polychaete zooplankton, while in open ocean it is mainly contributed by pteropod zooplankton. The ratio of particulate organic carbon deposition flux to net primary productivity in the Amundsen Sea Polynya (0.77%-1.85%) is significantly lower than the Ross Sea (0.87%-17.64%) and the Prydz Bay (1.81%-4.20%). This is related to the presence of *P. antarctica* as the main phytoplankton and CDW upwelling obstructing the deposition of particulate organic carbon in the Amundsen Sea Polynya.

Comparison of oceanic tintinnid biogeography in Arctic and Southern Ocean

Wuchang Zhang

Institute of Oceanology, Chinese Academy of Sciences, Qingdao 266071, PR China
* Presenter's email: Wuchangzhang@qdio.ac.cn

Polar oceans are experiencing rapid warming. Plankton biogeography is the basis to understand the response of plankton to climate change on plankton. Oceanic tintinnids are planktonic loricate ciliate which could be taxonomically identified. Before 2012, tintinnid in the polar oceans were not further divided into different belts as in the zooplankton. In recent years, tintinnid biogeography was revealed in several transects penetrating different water masses. Here we review tintinnid biogeographic pattern in the polar oceans in the past ca. 10 years. Boreal tintinnids in Dolan (2012) could be divided into three belts: subarctic belt, subarctic-arctic transition belt and arctic belt. Austral tintinnids had more belt than Boreal tintinnids: subantarctic belt, subantarctic-antarctic transion belt, Antarctic belt and Antarctic slope belt. Compared with the nine-belt pattern of zooplankton, tintinnid had three more belts in the polar oceans: subpolar-polar transiton belts in both hemisphere and Antarctic slope belt. The tintinnid Arctic belt is confined in the Beaufort Gyre while the zooplankton Arctic belt is in whole Arctic Ocean. There are more tintinnid Antarctic species than in the Arctic possibly due to the young geological history of Arctic. The bipolar tintinnid *Acanthostomella norvegica* is in fact confined to subpolar regions. The Weddell Gyre and Ross Gyre are two anticyclonic gyres with upwelling in their centers. Tintinnid *Salpingella gausii* was the dominant species edge of the two gyres.

Session

Coupling of Atmosphere and Polar Ocean and its Global Effect

Embracing physical constraints: Reducing uncertainties in projecting a summer Ice-Free Arctic Ocean

Xiao Zhou and Bin Wang

Department of Atmospheric Sciences, University of Hawaii, Honolulu, HI 96822, USA
*Presenter's email: wangbin@hawaii.edu

The pace at which the Arctic Ocean will be free of summer ice has been a pressing societal concern. Climate models have consistently struggled to accurately project the rate of decline in the September Sea Ice Area (SIA), and the time the Arctic Ocean becomes ice-free in summer. This study indicates that the decrease in September SIA is predominantly influenced by winter Arctic warming and the subsequent response in sea ice thickness, along with the rate at which summer sea ice melts due to feedback from ice thickness. The study found that the 40 CMIP6 models have significant errors in simulating the growth rate of winter sea ice thickness and the impact of summer ice thickness on melting, leading to uncertainties in future projections. The study introduces a set of metrics, incorporating three physical constraints, to confidently classify CMIP6 models as good, fair, or poor. The good models predict the first ice-free year as 2049 with a standard deviation of inter-model spread of 10 years under the SSP2-4.5 scenario. In contrast, the fair (poor) models predict 2076 (2060) with a spread standard deviation of 23 (42) years. The findings demonstrate that variations in sea ice thickness during both freezing and melting seasons are pivotal in driving the long-term decline of September SIA. Understanding these deficiencies and sources of uncertainty can confidently enhance the prediction of sea ice in climate models.

Roles of large scale circulation in shaping Arctic climate variability over recent decades

Qinghua Ding

Department of Geography and Earth Research Institute, University of California Santa Barbara, Santa Barbara, CA, USA
* Presenter's email: Qinghua@ucsb.edu

Arctic warming has been primarily attributed to anthropogenic forcing as well as significant changes in large scale circulation patterns in the high latitudes on low frequency time scales. In this talk, I will highlight a series of my recent work to reveal how these circulation changes regulate various aspects of the Arctic climate system over recent decades and the fact that our current models still lack sufficient skill to fully capture these impacts exerted by large scale circulation changes. To overcome this challenge, which hinders us from achieving better projections of future Arctic climate, we may need to put more effort into improving models' capabilities in simulating the sources of this low frequency circulation variability, such as the impact of low frequency SST variability in the tropics and subtropics, and the simulation of teleconnections linking these remote forcing to the Arctic. This roadmap may offer new possibilities for improving future climate projections not only within the Arctic but also beyond.

Unraveling the forcings behind West Antarctic summer melt: CMIP6 perspectives on remote climate drivers

Song Yang [1*], Yingfei Fang [1], Xiaoming Hu [1], James A. Screen [2] and Shuheng Lin [3]

[1] School of Atmospheric Sciences, Sun Yat-sen University, Zhuhai, China
[2] Department of Mathematics and Statistics, University of Exeter, Exeter, Devon, UK
[3] School of Geographical Sciences, Fujian Normal University, Fuzhou, China
* Presenter's email: yangsong3@mail.sysu.edu.cn

The atmospheric circulation favorable for Ross Ice Shelf summer surface melt could be influenced by both the El Niño-related sea surface temperature (SST) anomalies in the tropical central-eastern Pacific and the atmospheric heating anomalies over western Australia through generating Rossby wave trains. Here we analyze output from 60 CMIP6 models and reveal their ability to effectively simulate these primary drivers that affect the circulation pattern over West Antarctica.

El Niño emerges as a crucial force shaping atmospheric circulation anomalies over the Ross Sea through inducing two distinct wave trains toward West Antarctica: one originating from the central Pacific and the other from the Maritime Continent. It is further found that, independent from El Niño, the anomalous atmospheric heating over western Australia provides another significant forcing and initiates a Rossby wave train that extends from subtropical Australia to the Ross Sea. Overall, the CMIP6 models could simulate the wave train patterns associated with these drivers; however, they underestimate the intensity of the teleconnection.

This comprehensive assessment advances our understanding of the remote forcings steering climate variability in West Antarctica during austral summer. Moreover, it instills confidence in the predictability of future changes in the regional climate.

Impacts of Arctic sea ice on East Asian winter monsoon and related seasonal and subseasonal prediction models

Jianping Li[1,2*] and Zhiwei Wu[3]

[1] Frontiers Science Center for Deep Ocean Multispheres and Earth System-Key Laboratory of Physical Oceanography-Institute for Advanced Ocean Studies-Academy of Future Ocean, Ocean University of China, Qingdao 266100, China.
[2] Laoshan Laboratory, Qingdao 266237, China.
[3] Department of Atmospheric and Oceanic Sciences, Institute of Atmospheric Sciences, and Shanghai Frontiers Science, Center of Atmosphere-Ocean Interaction, Fudan University, Shanghai 200438, China
*Presenter's email: ljp@ouc.edu.cn

This presentation introduces the principal modes of the East Asian winter monsoon (EAWM) variability, the northern (N-) mode, southern (S-) mode and east-west dipole mode of surface air temperature anomalies in the EAWM region. The Arctic sea ice exerts important impacts on the EAWM at seasonal and subseasonal time scales. The possible physical mechanisms on how preceding Arctic sea ice anomalies impact on these modes of the EAWM are discussed. The results show that Arctic sea ice provides predictable signal for seasonal and subseasonal variations of the EAWM. Thus, the related physically-based empirically seasonal and subseasonal prediction models of three modes of the EAWM are established. Hindcast experiments shows good skills of these models for predicting seasonal and subseasonal variabilities of the EAWM, implying these physically-based empirical models provides useful forecast tools for seasonal and subseasonal prediction of the EAWM.

Interglacial warming intensity controlled by Antarctic ice sheet changes

Xu Zhang[1*], Evan Gowan[2], Steve Barker[3], Gregor Knorr[4], Eric Wolff[5], Chronis Tzedakis[6]

[1] British Antarctic Survey, Cambridge, UK
[2] University of Kumamoto, Kumamoto, Japan
[3] Cardiff University, Cardiff, UK.
[4] Alfred Wegener Institute, Bremerhaven, Germany.
[5] University of Cambridge, Cambridge, UK
[6] University College London, London, UK
* Presenter's email: xuang@bas.ac.uk

Interglacial intensity in past 800 kyr is characterized by a transition, about 430 kyr ago, between the older ones, which were relatively cool, and the more recent ones, which were relatively warm. This transition, as identified in Antarctic ice core records and benthic calcite d18Oc records, corresponds to the so-called mid-Brunhes Transition (MBT). However, its origin and underlying dynamics and its association with global ice volume/sea level remain elusive. Here we show, based on a start-of-art, stable water isotope enabled climate model, that MBT is in a close association with changes in Antarctic ice sheet during Termination (T) V and Marine Isotope Stage (MIS) 11c. Our results elaborate that reduction in Antarctic ice sheet strengthens vertical mixing in Southern Ocean by redistributing meltwater distribution. Our marine carbon cycle model further shows that such process promotes additional degassing of deep sea carbon, accounting for the high interglacial atmospheric CO_2 levels after the MBT. We propose that the unique orbital configurations during TV-MIS11c is the cause of extra Antarctic ice sheet decrease, accounting for the systematic change in interglacial climates in the late Pleistocene Epoch.

Teleconnections impact on Antarctic sea ice, ice shelf, and snow accumulation

Xichen Li

Institute of Atmospheric Physics, Chinese Academy of Sciences
* Presenter's email: lixichen@mail.iap.ac.cn

Tropical-Polar teleconnections play important role in driving the recent observed Antarctic climate changes. In particular, the decadal sea surface temperature variabilities over tropical Pacific and Atlantic drives the east warming, west cooling pattern over the Antarctic during the past several decades through Rossby wave dynamics. This teleconnection also leads to a dipole sea ice pattern between Amundsen Sea and Ross Sea. Recent study indicated that the tropical-polar teleconnection may further impact on the atmosphere-ice-ocean interactions over Antarctica and Southern Ocean. Tropical SST variability may drive a dipole like sea ice distribution around East Antarctica, similar to that around the west. It also accelerates the surface warming over the Ross Ice Shelf. More importantly, the tropical-polar teleconnections adjust the moisture transport over the Antarctic continent, further contribute to the snowfall pattern and thus the surface mass balance of the Antarctic icesheet.

Atmospheric rivers in the Arctic and its impact on sea ice

Pengfei Zhang

Department of Meteorology and Atmospheric Science, The Pennsylvania State University, PA US
* Presenter's email: zpengfei1006@gmail.com

In recent decades, Arctic sea-ice coverage underwent a drastic decline in winter, when sea ice is expected to recover following the melting season. It is unclear to what extent atmospheric processes such as atmospheric rivers (ARs), intense corridors of moisture transport, contribute to this reduced recovery of sea ice. Here, using observations and climate model simulations, we find a robust frequency increase in ARs in early winter over the Barents– Kara Seas and the central Arctic for 1979–2021. The moisture carried by more frequent ARs has intensified surface downward longwave radiation and rainfall, caused stronger melting of thin, fragile ice cover and slowed the seasonal recovery of sea ice, accounting for 34% of the sea-ice cover decline in the Barents–Kara Seas and central Arctic. A series of model ensemble experiments suggests that, in addition to a uniform AR increase in response to anthropogenic warming, tropical Pacific variability also contributes to the observed Arctic AR changes.

Arctic and Pacific Ocean conditions were favourable for cold extremes over Eurasia and North America during Winter 2020/21

Ruonan Zhang[1,2*], James A. Screen[3], Renhe Zhang[1,4]

[1] Department of Atmospheric and Oceanic Sciences and Institute of Atmospheric Sciences, Fudan University, Shanghai, China
[2] CMA-FDU Joint Laboratory of Marine Meteorology, Shanghai, China
[3] College of Engineering, Mathematics and Physical Sciences, University of Exeter, Exeter, UK
[4] Shanghai Frontiers Science Center of Atmosphere-Ocean Interaction, Shanghai, China
* Presenter's email: rn_zhang@fudan.edu.cn

The ongoing reduction in the extent and duration of sea ice coverage in the Arctic Ocean appears to have resulted in increased biomass and production of phytoplankton along with a shift away from ice-associated algae. Phytoplankton increases have occurred within both the inflow seas, as well as over the interior shelves. Observations suggest there has been concurrent increases in the abundance of zooplankton, although such data remains spotty in its coverage. Here we discuss the factors that have led to these increases in phytoplankton and how zooplankton communities have responded. Not all zooplankton species have benefited equally due to differences in their life history strategies. For both components, we consider how these trends will continue into the future, and what can be expected for community structure and their seasonal cycles in the future Arctic Ocean. Such trends will ultimately determine the ability of the Arctic to support upper trophic levels including fisheries in the future.

POSTER

Connections between the summertime Arctic Oscillation and the sea ice dipole mode in the Barents-Kara Seas

Shutao Cao[1], Anmin Duan[1*], Chao Zhang[1]

[1]State Key Laboratory of Marine Environmental Science, College of Ocean and Earth Sciences, Xiamen University, Xiamen, China

** Correspondence: amduan@xmu.edu.cn*

Introduction

- AO is a key atmospheric circulation mode in the Northern Hemisphere, significantly affecting sea ice variability.
- Previous studies have established a physical framework for how the memory of preceding wintertime AO influences subsequent summertime sea ice.
- There is still room for improving understanding of the relationship between the summer-time AO and Arctic sea ice, especially at the regional scale.

Methods

- Composite and regression analysis are employed to investigate the statistical relationship between the Barents-Kara Sea (BKS) ice and AO during summertime.
- Numerical experiments using CESM2.1.3 is designed to replay the observed atmospheric patterns and validate the response of the Barents-Kara Sea (BKS) ice to AO.

EXP Name	Nudging or not	Nudging horizontal domain	Nudging vertical levels	Initial conditions	Number of members	Length
CLIM-CTRL	No nudging	None	None	Branch from CESM2-CMIP6 year 2000	1	50 years
NG-POS	Nudging U/V to composite of AO positive years	60°-90°N	850hpa to surface	Branch from the last thirty years of CLIM-CTRL	30	3 months, from 1 Jun to 31 Aug
NG-NEG	Nudging U/V to composite of AO negative years	60°-90°N	850hpa to surface	Branch from the last thirty years of CLIM-CTRL	30	3 months, from 1 Jun to 31 Aug

Acknowledgments

This work was funded by the National Natural Science Foundation of China (42030602, 42305016). Chao Zhang was supported by the Chinese Scholarship Council (File No. 202306310194) and the Outstanding Postdoctoral Scholarship, State Key Laboratory of Marine Environmental Science at Xiamen University.

Results

➢ *Statistical Relationship between AO and SIAD*

- The MCA1 exhibits a SIC anomaly dipole (SIAD) mode in the BKS.
- The MC1 of SLP exhibits a pattern highly resembles AO.
- SIAD is closely related to AO at interannual timescale.

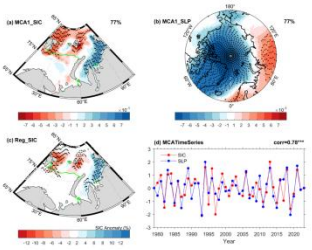

➢ *Physical mechanism linking AO to SIAD*

- Cyclonic wind anomalies trigger southeastward Ekman transport, leading to eastward sea ice drift.
- The simulation results reproduce the SIAD mode in the BKS, confirming the causal relationship between the AO and SIAD.

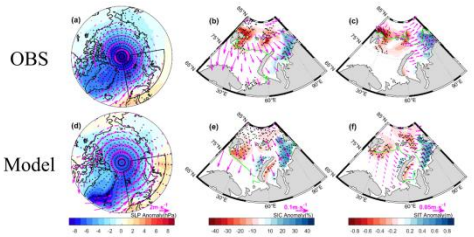

➢ *Dynamics vs. Thermodynamics*

- The AO-induced dynamics are the dominate driver of SIAD.
- As a result of the ice thickness-growth rate feedback, thermodynamics partially suppress SIAD.

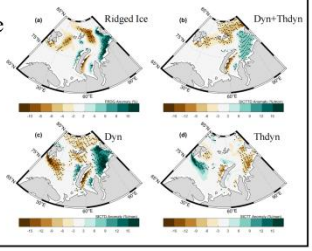

Conclusions

- A dipole mode of sea ice anomaly (SIAD) in BKS is identified, which exhibits a significant correlation with the simultaneous AO.
- The anomalous Pan-Arctic cyclonic circulation associated with the positive phase of the AO generates westerly wind anomalies over the Barents-Kara Sea surface, resulting in Ekman transport anomalies southeastward and sea ice drift eastward.
- Numerical simulations demonstrate that sea ice transport due to dynamics is the dominant factor contributing to SIAD.

Iceberg Detection Based on Swin Transformer Algorithm and SAR Imagery: case studies off Prydz Bay and Ross Sea, Antarctica

Fangru Mu[1, 2], Zhiyuan Shao[1, 2], Bin Cheng[3], Keguang Wang[4], Caixin Wang[4], Yuhan Chen[1, 2], Jiechen Zhao[1, 2, *]

Email: mufangru@hrbeu.edu.cn

[1]Qingdao Innovation and Development Base of Harbin Engineering University, Qingdao, Shandong, 266400, China

[2]Key Laboratory for Polar Acoustics and Application of Ministry of Education (Harbin Engineering University), Harbin, 150001, China

[3]Finnish Meteorological Institute, Helsinki, Finland

[4]Department of Research and Development, Norwegian Meteorological Institute, Oslo, Norway

Introduction

1. Drifting icebergs pose a great threat to polar research vessels and other marine structures.
2. Melting icebergs affect the stability of ocean layers and sea ice characteristics, thus influencing coastal ocean circulation and sea ice dynamics.

Accurate and timely information on iceberg distribution, and even predictive capabilities regarding their temporal variability

Contribution of our work

1. Focusing on the vicinity of the Chinese scientific research stations in Antarctica, the Swin Transformer for the first time was employed for iceberg detection based on Synthetic Aperture Radar (SAR) images under noisy backgrounds and various ice conditions (named AISS-Transformer).
2. The concept of iceberg concentration was introduced to express the relationship between the number of icebergs and their sizes within unit grids.

Data and Methods

Table 1. The detailed information of four AOIs.

NO.	Latitude	Longitude	Time	Regions	SIC
AOI1	67.03°S-67.91°S	69.14°E-71.44°E	September 30, 2023	Prydz Bay	75%
AOI2	74.08°S-74.82°S	175.51°W-178.27°W	December 27, 2023	Ross Sea	73%
AOI3	69.81°S-70.54°S	175.83°W-177.99°W	December 27, 2023	Ross Sea	21%
AOI4	64.15°S-64.97°S	76.09°E-77.93°E	March 26, 2023	Prydz Bay	0%

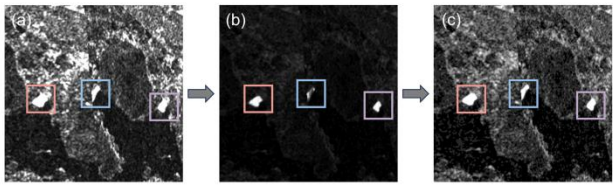

Figure 1. An example of the SAR imagery preprocessing.

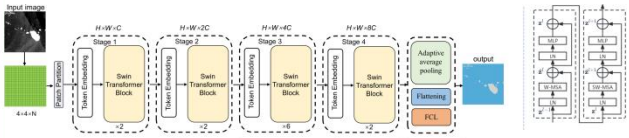

Figure 2. Overall framework of the AISS-Transformer.

Results

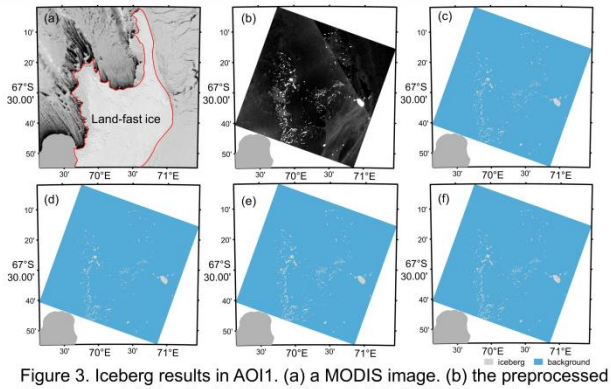

Figure 3. Iceberg results in AOI1. (a) a MODIS image. (b) the preprocessed SAR image. (c) visually. (d) SVM. (e) ResNet18. (f) AISS-Transformer.

Table 2. F1 scores and Kappa coefficients (%) for three models in four AOIs.

NO.	F_1			*Kappa* coefficients		
	SVM	ResNet18	AISS-Transformer	SVM	ResNet18	AISS-Transformer
AOI1	86.02	84.23	97.76	85.82	83.91	87.53
AOI2	80.50	82.84	96.46	80.46	82.81	86.44
AOI3	72.34	83.80	85.51	72.31	83.78	85.50
AOI4	89.19	83.08	90.89	89.19	83.07	90.89

Table 3. The detailed metrics of iceberg detection.

Research area		AOI1	AOI2	AOI3	AOI4
Iceberg number	AISS-Transformer	594	109	115	14
	Visual interpretation	582	98	105	14
Total iceberg area (%)	AISS-Transformer	1.92	0.18	0.14	3.65×10^{-4}
	Visual interpretation	1.82	0.18	0.15	3.20×10^{-4}
Number bias rate (%)		2.1	11.2	9.5	0
Precision (%)		85.62	86.74	89.25	85.59
Recall (%)		90.01	86.19	82.08	96.89
F1 (%)		97.76	96.46	85.51	90.89
Kappa coefficient (%)		87.53	86.44	85.50	90.89

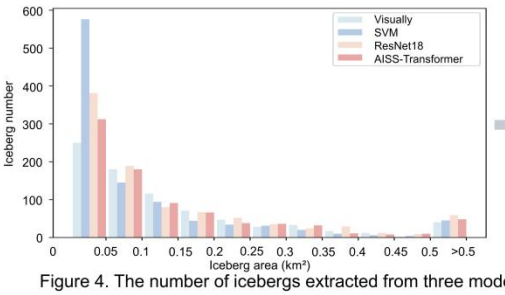

The challenge remains to distinguish small icebergs from ice floes.

Figure 4. The number of icebergs extracted from three models and visual interpretation within various iceberg area ranges.

Conclusions

1. AISS-Transformer can reliably identify icebergs in SAR images within noisy backgrounds, with F1 scores and Kappa coefficients exceeding 85% across different ice conditions.
2. Ocean models generally do not account for icebergs. Incorporating results from iceberg detection can enhance our understanding of the interactions between the ocean, sea ice, and icebergs.

A quantitative analysis of climate feedbacks in recent changes of the Southern Ocean and Antarctic sea ice

Yanchi Liu[1], Jiping Liu[1,2*], Matthew H. England[3], and Qinghua Yang[1,2]

1School of Atmospheric Sciences, Sun Yat-sen University and Southern Marine Science and Engineering Guangdong Laboratory (Zhuhai), Zhuhai, China

2Guangdong Province Key Laboratory for Climate Change and Natural Disaster Studies, Zhuhai, China

3Climate Change Research Centre and Australian Centre for Excellence in Antarctic Science, University of New South Wales, Sydney, NSW, Australia

Introduction

Since 2017, the Southern Ocean has experienced surface warming and a large reduction in sea ice, which is opposite to the situation over previous decades.

There is limited research on the mechanisms for recent warming in the Antarctic and no consensus has been reached yet. Moreover, it is widely accepted that sea-ice loss is the main contributing factor to the rapid surface warming of the Arctic.

This study aims to examine feedback processes linked to surface warming in the Southern Ocean from 2017 to 2023 and its relationship to Antarctic sea-ice change.

Data

Datasets	Variables
ERA5	2-metre temperature, specific humidity, cloud amount, cloud liquid/ice water content, solar energy flux at the TOA, and surface sensible and latent heat fluxes
NSIDC	Sea ice concentration

Analyzed area: South of 55°S (mask land)
Analyzed period: 2017-2023
Climatological reference period: 1979-2008

Method

We applied the CFRAM analysis method to decompose the total surface warming into temperature changes due to changes in CO_2 (CO_2), albedo (AL), water vapor (WV), cloud (CLD), atmospheric heat transport (ATM), oceanic transport and heat storage (OCH), surface heat fluxes (SH and LH), namely,

$$\Delta T_{Total} = \Delta T_{CO_2} + \Delta T_{AL} + \Delta T_{WV} + \Delta T_{CLD} + \Delta T_{ATM} + \Delta T_{OCH} + \Delta T_{SH} + \Delta T_{LH} + \Delta T_{ERR} = \Delta T_{SUM} + \Delta T_{ERR}$$

Δ corresponds to the difference between the two equilibrium states

Overview

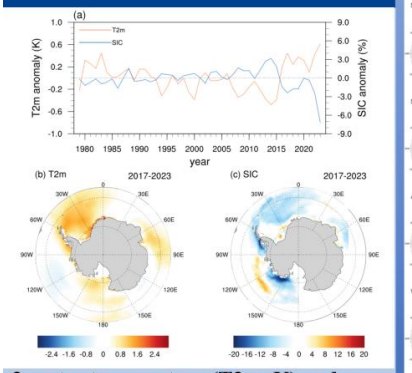

2-metre temperature (T2m, K) and sea ice concentration (SIC, %) anomalies

The Southern Ocean has warmed up and Antarctic sea ice has decreased recently. There is a strong negative correlation between the changes in surface temperature and sea ice over the Southern Ocean.

Results

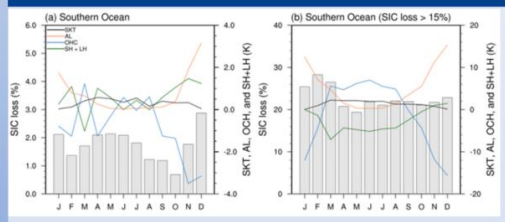

Seasonality of temperature changes (K) due to individual climate feedback

The cooling effect caused by the oceanic heat storage process offsets the warming caused by albedo feedback, resulting in weak summer warming. In winter, part of the energy released by the ocean leads to warming.

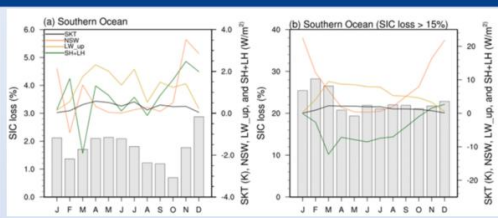

Seasonality of surface heat fluxes anomaly (W/m²)

The lack of sea ice isolation allows for enhanced air-sea heat exchange. The increase in latent and sensible heat flux is more significant in areas experiencing more sea ice melting, indicating that sea ice loss can promote the ocean to release heat to the atmosphere, leading to surface warming.

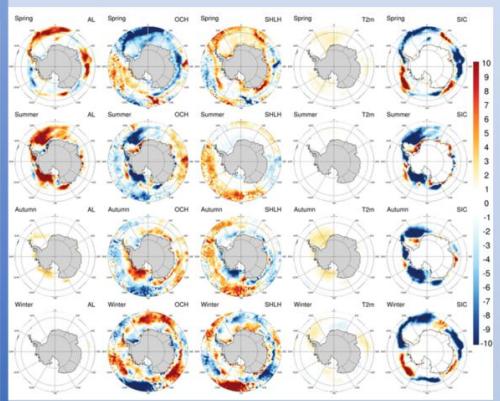

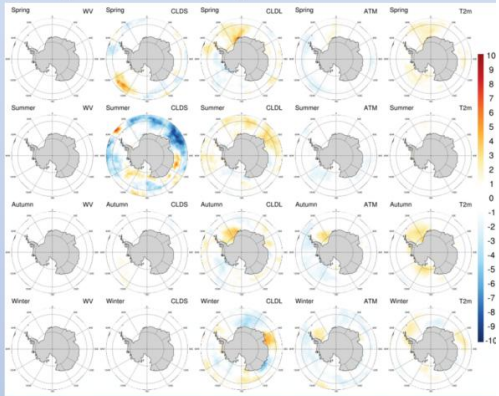

Spatial distribution of temperature changes (K) due to individual climate feedback

Sea ice loss affects surface temperature changes in the Southern Ocean by influencing albedo feedback, the oceanic heat transport and storage process, and the sea-air heat exchange process, especially during warm seasons.

In cold seasons, the heat released by the ocean can only partially explain the warming in the Ross Sea, while the long-wave cloud feedback and the atmospheric heat transport are responsible for the surface warming of the Weddell Sea.

Summary

- Weak summer warming in the Southern Ocean is mainly due to intense subsurface heat uptake by the ocean
- Part of the stored energy is released by the ocean in winter due to the re-emergence of subsurface heat, and the associated increase in outgoing longwave radiation and heat fluxes leads to maximum winter warming
- The areas experiencing more sea ice melting have stronger albedo feedback, and the exposed open ocean can absorb more heat in summer and release more heat in winter

Contact: Yanchi Liu, Sun Yat-sen University; E-mail: liuych37@mail2.sysu.edu.cn

Three phases of Arctic amplification under global warming

Fuda Yu dayu@stu.pku.edu.cn
Xinyu Wen xwen@pku.edu.cn
Department of Atmospheric and Oceanic Sciences, School of Physics, Peking University, Beijing, China.

1. Overview

Arctic Amplification(AA) refers to the phenomenon where the surface temperature in the Arctic region warms or cools at a rate accelerated relative to the global average, a trend evident in both observational data and model simulations. Previous research has highlighted that the global w arming of the current century has triggered AA and proposed various physical mechanisms to explain it. This study introduces a new insight: During the current process of global warming, AA is not a constant phenomenon but occurs in three distinct phases, each with its own defining characteristics.

Specifically, this paper analyzes the Berkeley Earth Surface Temperature (BEST) data and the simulation results from the Coupled Model Intercomparison Project Phase 6 (CMIP6) to discover: In the initial phase, changes in sea ice are minimal and global warming is not pronounced, resulting in fluctuating AA. The impact of global warming on the Arctic region is minor during this phase, with fluctuations mainly driven by short-term internal variability. In the phase of stable change, a significant increase in global temperatures leads to rapid sea ice melting, causing a significant increase in heat flux in related areas and leading to more pronounced warming. Consequently, the AA index reaches its peak and then declines. In the final phase, as sea ice melts completely, the AA disappears. At this time, land warming rates surpass those of the oceans, presenting a "land amplification" characteristic.

2. Data and methods

Observation:

-BEST: Berkeley Earth Surface Temperature dataset

-HadISST : Hadley Centre Sea Ice and Sea Surface Temperature data set

Model:

-ACCESS-CM2
-ACCESS-ESM1-5
-CanESM5
-MRI-ESM2-0

} CMIP6: *Coupled Model Intercomparison Project Phase 6* historical+SSP585

$$AA\ index = \frac{trend(Arctic)}{trend(North\ hemisphere)}$$

3. Arctic Amplification: Three Phases

3.1 Distributional characteristics of the AA index

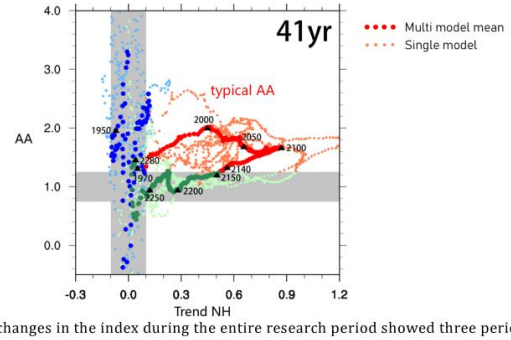

The changes in the index during the entire research period showed three periods with significantly different characteristics: violent fluctuations in the early stage, a steady rise in the middle stage and a decline after reaching a peak, and a close to 0 in the late stage, indicating the disappearance of AA.

3.2 Time series: characterization of typical phases

(Using the 41-year sliding window as an example)

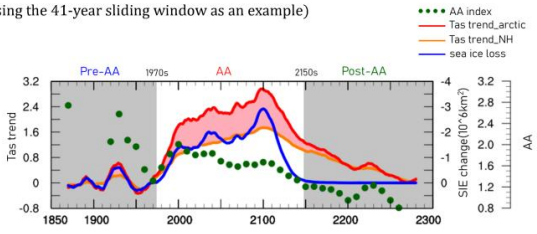

The AA index distribution is characterized as before, while an extremely high correlation between sea ice loss and the Arctic-Northern Hemisphere temperature difference can be found, and the two levels are highly consistent. At the same time the peak of the index does not coincide with the peak of the temperature difference? This provokes us to think about the time of AA peaking.

Key findings at a glance

- The Arctic amplification typical of the global warming process is not always present, but is one of three main phases.
- Sea ice loss is the underlying cause of Arctic amplification, and there would be no Arctic amplification without the ice-albedo feedback caused by sea ice loss.

Key1:The centrality of sea ice loss to AA

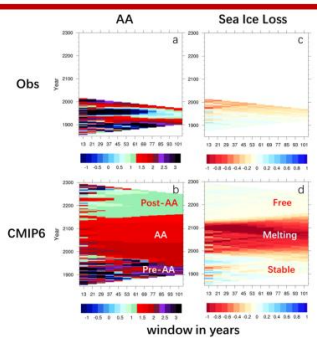

Significant sea ice loss is observed during typical AA periods, and if the sea ice is relatively stable, or if it is all melted out, there is no strong ice albedo feedback, and thus Arctic amplification does not persist, which again emphasizes the key role of sea ice loss in driving the AA.

Key2:AA's Footprints

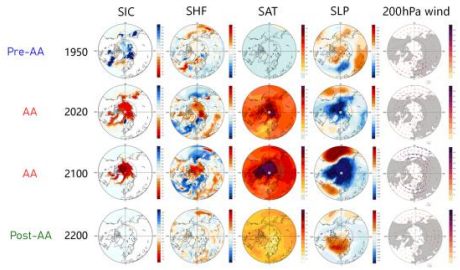

Both the response of the surface heat flux and the response of the sea-level pressure, which represents the mass of the whole atmosphere, and the upper-air wind field of the upper atmosphere are the strongest at the end of the century, reflecting the influence of the AA on them, and we can assume that the Arctic amplification phenomenon peaks at the end of the century from the point of view of air-sea interactions.

4. Conclusion

1. Contrary to previous understanding, the typical AA does not persist throughout the course of global warming. Instead, it is phased, occurring only during periods of substantial sea ice loss.
2. The occurrence of AA is always associated with a loss of sea ice, and the greater the loss of sea ice, the greater the temperature difference between the Arctic and the Northern Hemisphere. Areas of significant sea ice loss are characterized by rising sensible heat fluxes and enhanced warming. Without the loss of sea ice, the typical AA would not exist.
3. Previous studies have shown that the peak of the index, based on past AA definitions, has peaked at the beginning of the century. We argue that the greater the loss of sea ice, the stronger the feedback mechanism, given the physical processes driven by sea ice albedo feedback. Therefore, it is more appropriate to measure its strength based on the difference between the temperature trends in the Arctic and the Northern Hemisphere. Based on this definition, the peak intensity of the AA is expected to occur around 2100.

Projected Antarctic Land warming and Uncertainty Driven by Atmospheric Heat Transport

Yihan Zhang[1], Yunqi Kong[2], Song Yang[1,3], Xiaoming Hu[1,3]

Email: zhangyh339@mail2.sysu.edu.cn

1 School of Atmospheric Science, Sun Yat-sen University, Zhuhai, China
2 Guangdong Ecological Meteorology Center, Guangzhou, China
3 Guangdong Province Key Laboratory for Climate Change and Natural Disaster Studies, Sun Yat-sen University, Zhuhai, China

Introduction

- Warming in the Arctic has been faster than the global mean, a phenomenon known as Arctic Amplification (AA). In contrast, Antarctic Amplification (ANA) has been less prominent in both observations and climate simulations.
- Polar warming shows a seasonality with strong winter warming and weak summer warming, which arises from seasonal energy transfer mechanism (SETM). The asymmetric Arctic and Antarctic warming is mainly caused by different intensities of SETM in two poles.
- The warming of the Antarctic ocean and land surface exhibits significant differences and is accompanied by substantial uncertainty.

Data & Method

Data:

CMIP6

- piControl → basic climate state (the mean of last 50 years)
- abrupt-4×CO2 → warming climate state (the mean of last 20 years)

No.	Model	Resolution
1	BCC-CSM2-MR	100 km
2	FGOALS-g3	250km
3	MPI-ESM-1-2-HAM	250km
4	NorESM2-MM	100 km
5	FGOALS-f3-L	100 km
6	CMCC-CM2-SR5	100 km
7	MPI-ESM1-2-LR	250km
8	GFDL-ESM4	100 km
9	CMCC-ESM2	100km
10	GFDL-CM4	100 km
11	IPSL-CM6A-LR	250km
12	CESM2-WACCM-FV2	100km
13	TaiESM1	100km
14	CESM2-FV2	100km
15	NorESM2-LM	250 km
16	SAM0-UNICON	100 km
17	CESM2-WACCM	100 km
18	CESM2	100 km

Method:

CFRAM: Coupled Atmosphere-Surface Climate Feedback-Response Analysis Method (Lu and Cai, 2009; Cai and Lu, 2009)

$$\Delta T = \Delta T^{CO_2} + \Delta T^{AL} + \Delta T^{WV} + \Delta T^{CLDS} + \Delta T^{CLDL} + \Delta T^{ATM} + \Delta T^{OCH} + \Delta T^{SH+LH}$$

Eq. (1) enables us to calculate grid by grid. The inter-model spread is defined as the difference between each individual model's simulation and the multi-model ensemble (MME) mean.

Meridional Atmospheric Heat Transport

$$AHT = \frac{2\pi a^2}{10^{15}} \int_{-90}^{\varphi} \cos(\varphi) \cdot R(\varphi)\, d\varphi$$

R(φ) is the atmospheric energy imbalance at latitude φ. a is the radius of the Earth. AHT consists of latent heat energy (LE) and dry-static energy (DSE) transport. LE can be inferred from the moisture imbalance, while DSE is recognized as the residual between the AHT and LE.

Results

Dominant Role of Atmospheric Heat Transport in Antarctic Land Warming

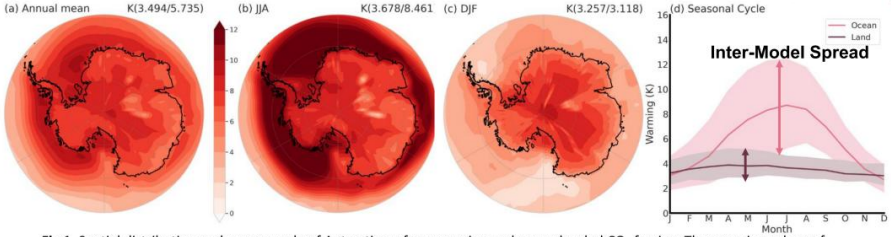

Fig 1. Spatial distribution and season cycle of Antarctic surface warming under quadrupled CO_2 forcing. The warming values of the land (former) and ocean surface (latter) are indicated at the upper right of each panel.

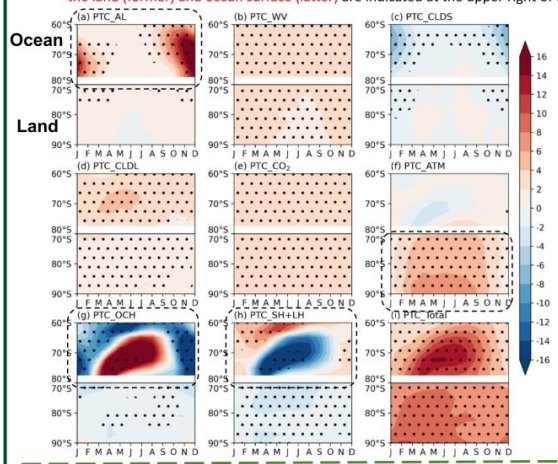

Fig 2. Seasonal cycles of zonal-mean total and partial temperature changes (PTCs) due to individual processes over land (top panel) and ocean (bottom panel) surface.

- Warming of Antarctic land surface is attributed to poleward AHT.

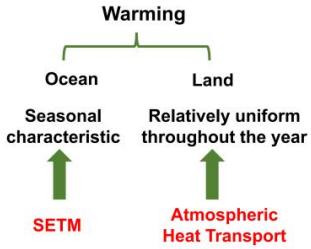

Latent Energy Transport and Its Contribution to Water Vapor Feedback

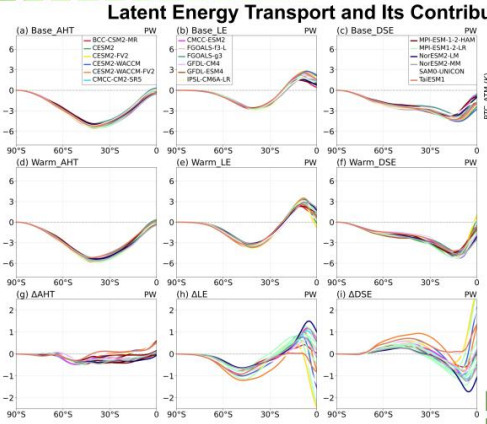

Fig 3. Meridional atmospheric heat transport (AHT), latent energy transport (LE), and dry-static energy transport (DSE) in the Southern Hemisphere.

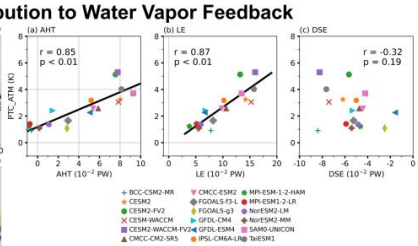

Fig 4. Relationship between partial temperature changes due to meridional heat transport and water vapor feedback.

Drivers of Inter-Model Spread in Antarctic Land Warming Projections

- Inter-model spread in poleward AHT, especially in LE transport, emerges as the primary driver of the inter-model spread in Antarctic land warming projections

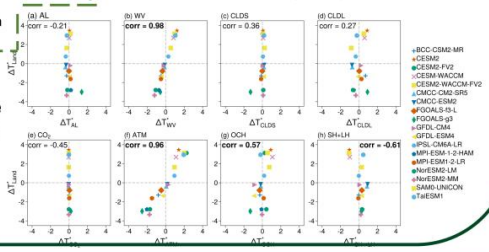

Fig 5. Uncertainties of annual mean total and partial surface temperature changes over the Antarctic land surface.

Results

- Poleward AHT, particularly the transport of LE, plays a dominant role in Antarctic land warming. The moisture-related transport enhances water vapor feedback, which significantly amplifies surface warming.
- The inter-model spread in poleward AHT is the key to the uncertainty of Antarctic land warming projection.

iSPOGOC2024, Qingdao, Oct23-24, 2024

Hydrography in the northern Bering and Chukchi Seas in the wintertime

Min Li [a,b,*], Robert S. Pickart[b], Peigen Lin[b,c]

[a] College of Ocean and Meteorology, Guangdong Ocean University. [b] Woods Hole Oceanographic Institution. [c] School of Oceanography, Shanghai Jiao Tong University.
*CONTACT: limin_gdou@hotmail.com

Background

Pacific water flowing through Bering Strait (Fig. 1a), plays a vital role in the Chukchi Sea ecosystem. During December 2020 - January 2021, the USCGC *Polar Star* conducted a mission across the northern Bering and Chukchi Seas, which provided an opportunity to collect hydrographic profiles using expendable conductivity-temperature-depth (XCTD) probes (Fig. 1b). During leg 1 of the mission, 28 hydrographic profiles were obtained on the Chukchi shelf and in the vicinity of Bering Strait, while 42 profiles were observed on the northern Bering shelf during leg 2. The observations are analyzed along with GLO12 reanalysis.

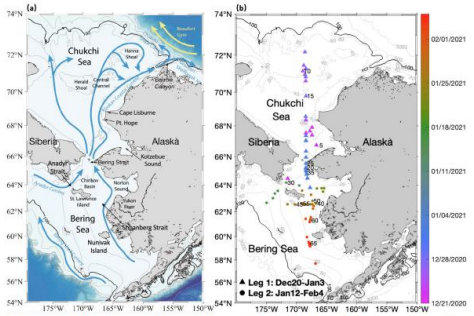

Fig.1 (a) Schematic circulation in the northern Bering and Chukchi Seas. (b) Location and time of the XCTD profiles obtained during the cruise. The station number for every other five stations is marked on the right of the station.

Primary features

The temperature, salinity, and density profiles showed nearly vertically uniform properties at most of the stations, implying the water was well mixed. Cold water with temperatures lower than -1.6°C was dominant during both legs (Fig 3).

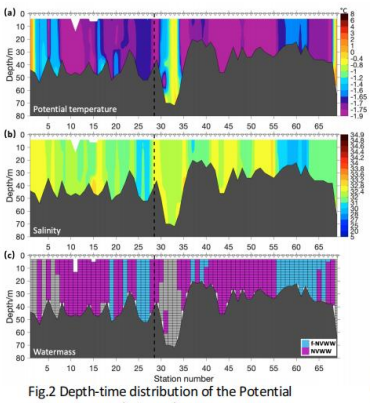

Fig.2 Depth-time distribution of the Potential temperature, salinity and watermasses.

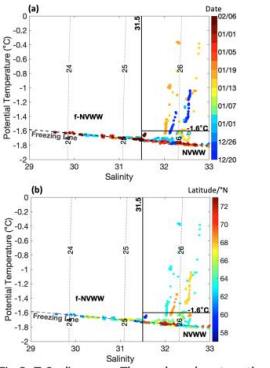

Fig.3 T-S diagram. The color denotes the observational date in (a) and latitude in (b). NVWW: newly-ventilated winter water; f-NVWW: f a fresh precursor to NVWW.

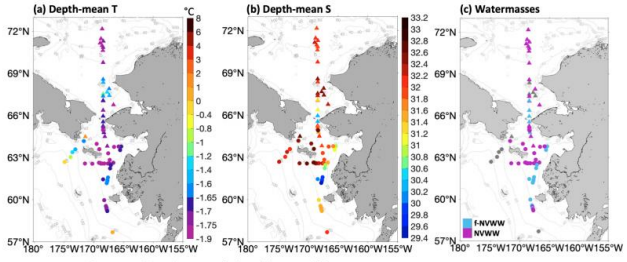

Fig.4 Distribution of depth-mean (a) T, (b) S, and (c) watermasses.

Regimes of the cold water

Three regimes of the cold water were found during observation: on the northern Chukchi shelf, in the south of the Bering Strait, and around the St. Lawrence Island (Fig 5-7). The 30 days back-tracking analysis shows the water originated from the east, the south, and the southwest, respectively. The water were all warm a month ago and cooled to the temperature near freezing point, along with ice production at the surface. The salinity increased when the ice produced.

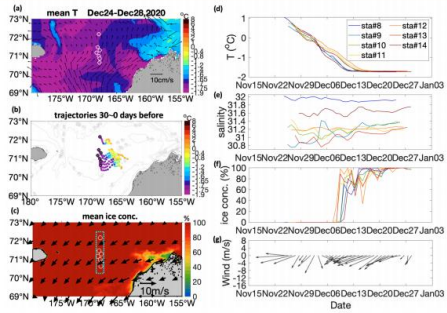

Fig.5 Cold winter on the northern shelf. (a) Mean temperature and current (b) trajectories 0~30 days before observation with temperature shown as color (c) Mean ice concentration during observations (from AMSR2) (d) Along-track temperature (e) Along-track salinity (f) Along-track ice concentration (AMSR2) (g) Along-track mean wind (from ERA5)

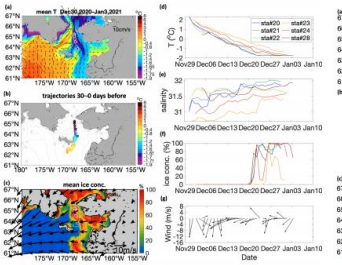

Fig.6 Cold winter water south of Bering Strait.

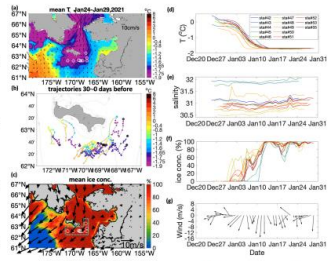

Fig.7 Cold winter water around St. Lawrence Island.

Cold water in different years

Results from the reanalysis reveal different distributions of the cold water during the same period in the winter of 2020, 2021, and 2022, implying its interannual variability. The mechanism is to be investigated.

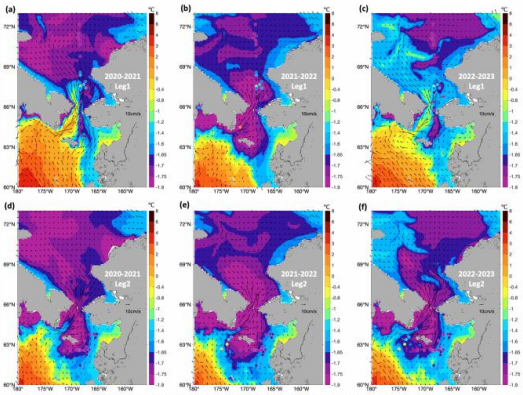

Fig.8 Time averaged and the upper 50m averaged potential temperature and current during the leg1 and leg 2 periods in the winter 2021, 2022 and 2023

Summary

- A rare hydrographic dataset of winter profiles from the northern Bering and Chukchi Seas has been analyzed to investigate the hydrography in winter.
- Much of the water column was well mixed. Three regimes of the cold water were found during observation. The back-tracking analysis shows the water were warm a month ago and cooled to temperature near freezing point along with ice production.
- The cold water in different years reveals interannual variability which is to be investigated.

2024 | INTERNATIONAL SYMPOSIUM ON POLAR OCEAN AND GLOBAL CHANGE

Antarctic sea ice surface temperature bias in atmospheric reanalyses induced by the combined effects of sea ice and clouds

Zhaohui Wang (zhaohui.wang1@unsw.edu.au)[1,2], Alex Fraser[2], Phil Reid[2,3], Siobhan O'Farrell[4] and Richard Coleman[2]

[1]University of New South Wales, [2]University of Tasmania, [3]Australian Bureau of Meteorology, [4]CSIRO

Strong warm biases in recent atmospheric reanalyses

- Sea-ice surface temperature (IST) serves as an indicator of ice melt and climate change.
- However, its in atmospheric reanalyses is not fully understood in Antarctica.

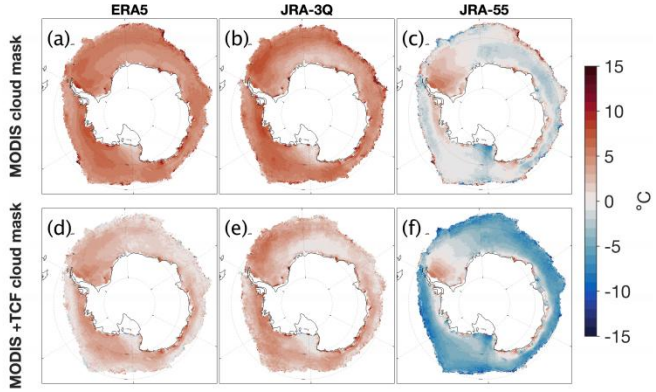

Fig. 1: IST bias for each reanalysis under different cloud masks.

- Strong and persistent warm biases in most recent reanalyses.
- JRA-55 exhibits weaker biases with notable spatial variation.
- Substantial warm bias reduction observed after TCF cloud masking.

Effects of cloud representation on IST estimation

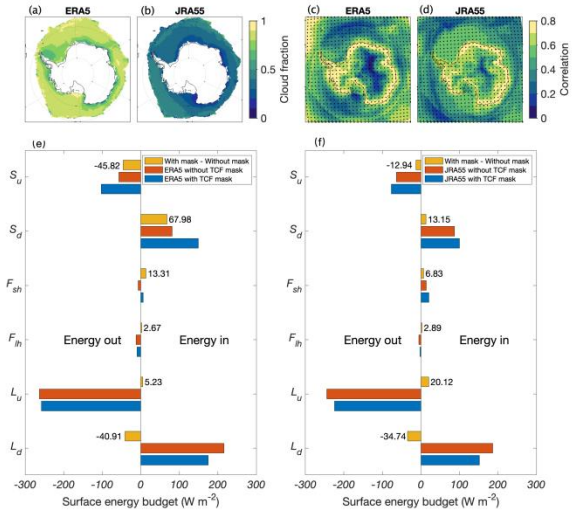

Fig. 2: The difference between JRA-55 and ERA5 in simulating clear-sky conditions and surface energy budget.

- The accuracy of modelled cloud strongly affects the simulation of surface radiative heat fluxes, consequently impacting surface temperature estimation

Effects of reanalysis sea-ice representation on IST estimation

Experiment	Sea-Ice Representation	Bias
ERA5	No snow/1.5 m SIT/Fraction SIC	4.89 K
JRA-55	No snow/2 m SIT/Binary SIC	-0.41 K
(a) Quasi-ERA5	No snow/1.5 m SIT/Fraction SIC	3.97 K
(b) Quasi-JRA-55	No snow/2 m SIT/Binary SIC	1.68 K

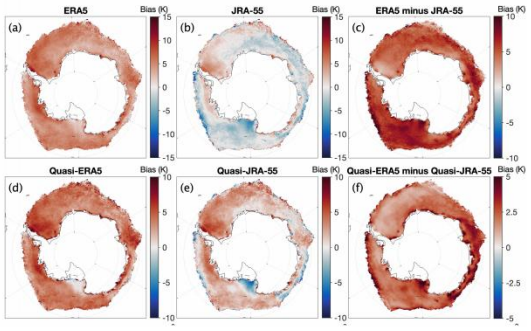

Fig. 3: The response of IST to different sea-ice representations.

The combined effects of sea ice-cloud coupling on IST estimation

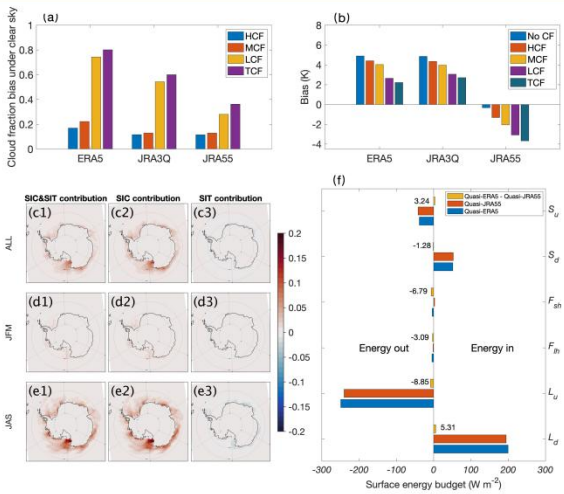

Fig. 5: The response of IST and SEB to sea ice-cloud coupling interactions.

- The representation of SIC regulates upward turbulent heat flux, influencing cloud formation and thereby surface radiation.

Conclusion

- Strong and persistent warm biases in most reanalyses.
- A compensatory relationship leads to smaller biases in JRA-55.
- The coupling between sea ice and clouds modulates IST bias.

Reference

Wang, Z., Fraser, A.D., Reid, P. *et al.* Antarctic sea ice surface temperature bias in atmospheric reanalyses induced by the combined effects of sea ice and clouds. *Commun Earth Environ* **5**, 552 (2024). https://doi.org/10.1038/s43247-024-01692-1

Strong Eddy Kinetic Energy Anomaly Induced by Baroclinic Instability in the Southwest Region of the Kerguelen Plateau, East Antarctic

Yunzhu He[1], Meng Zhou[1], and Dujuan Kang[1]

[1]Key Laboratory of Polar Ecosystem and Climate Change, Ministry of Education; and School of Oceanography, Shanghai Jiao Tong University, Shanghai, China

SCHOOL OF OCEANOGRAPHY
SHANGHAI JIAO TONG UNIVERSITY

Introduction

- Eddy activity is particularly prominent in the Southern Ocean (SO) due to the instabilities of the Antarctic Circumpolar Current (ACC).

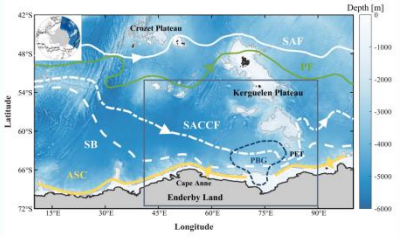

Figure 1. Bathymetry and main currents. The gray box outlines **a typical eddy-rich region** with **strong Eddy Kinetic Energy (EKE)** and associated energy conversions.

- Analyzing the dynamical processes could provide insights into underlying mechanisms and potential connections with climate variability and oceanic changes.

Data and Method

➢ **Energetics analysis framework**

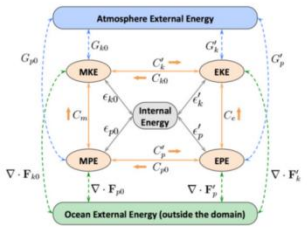

Figure 2. Energy exchange diagram (Kang and Curchitser, 2015).

$$\overline{\mathrm{MKE}} = \frac{1}{2}(\bar{u}^2 + \bar{v}^2) \qquad \overline{\mathrm{EKE}} = \frac{1}{2}\overline{u'^2 + v'^2}$$

$$\overline{\mathrm{MPE}} = \frac{g^2\bar{\rho}_a^2}{2\rho_0 N^2} \qquad \overline{\mathrm{EPE}} = \frac{g^2\overline{\rho_a'^2}}{2\rho_0 N^2}$$

$$\mathrm{MPE} \rightarrow \mathrm{EPE}: \quad \mathbf{BC} = -\frac{g^2}{\rho_0^2 N^2}\overline{\rho_a' \mathbf{u}'} \cdot \nabla\overline{\rho_a},$$

$$\mathrm{MKE} \rightarrow \mathrm{EKE}: \quad \mathbf{BT} = -\left[\overline{u'\mathbf{u}'} \cdot \nabla\bar{u} + \overline{v'\mathbf{u}'} \cdot \nabla\bar{v}\right]$$

$$\mathrm{EPE} \rightarrow \mathrm{EKE}: \quad \mathbf{VEDF} = -\frac{g}{\rho_0}\overline{\rho_a' w'}$$

Data	Data Source
Satellite Altimeter Data	CMEMS
Current Data (Reanalysis)	GLORYS12V1
Wind Data (Reanalysis)	ERA5, ERA-Interim

Motivation

Significant **positive EKE anomalies** in the southwest region of the Kerguelen Plateau **in austral winter** in 2017.

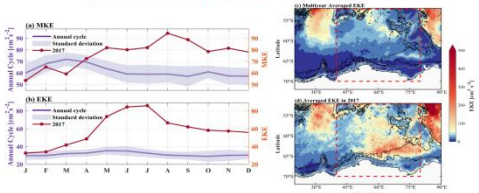

Figure 3. (a)-(b) Seasonal cycles of kinetic energy components and (c)-(d) averaged EKE ($cm^2 s^{-2}$) distributions of climatology and 2017.

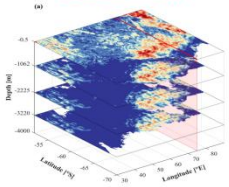

Figure 4. Three-dimensional (longitude-latitude-depth) structure of EKE in June 2017.

What causes the strong EKE anomalies?

Results and Discussion

➢ **Energetics analysis**

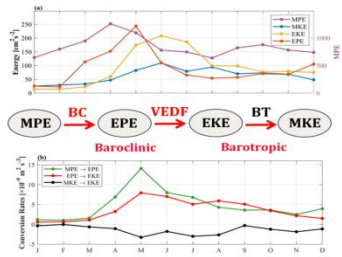

Figure 5. Monthly depth-integrated (upper 500 m) energy densities (a) and conversions (b) over the subregion (60°-80°E, 60°-65°S) in 2017.

Baroclinic Conversion - primary energy source for EKE

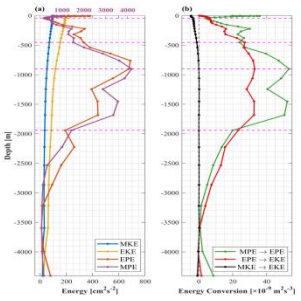

Figure 6. Vertical profiles of energy components (a) and conversions (b) averaged over the subregion in May 2017.

➢ **Possible Mechanisms for the Baroclinic Conversion**

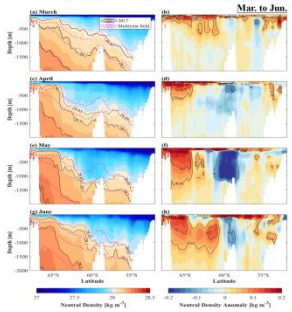

Figure 7. Transects of neutral density (γ_n, kg m^{-3}) and its anomaly at 75°E. The magenta curves represent climatology.

Notable intensities of BC in the depth range of the Circumpolar Deep Water (CDW)

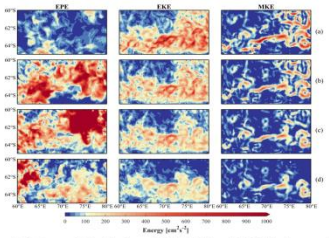

Figure 8. Horizontal distribution of EPE, EKE, and MKE in four typical layers (a-d) in May 2017.

Key Points

- The subpolar region southwest of the Kerguelen Plateau is characterized by the anomalous strong Eddy Kinetic Energy (EKE) observed in 2017.
- The regional positive anomalies in EKE can be **predominantly attributed to enhanced baroclinic instability**, with inverse barotropic energy conversion.
- The enhanced baroclinic instability is mainly caused by **an anomalous intrusion of the Circumpolar Deep Water**, particularly at depths between 500 and 2000 meters.

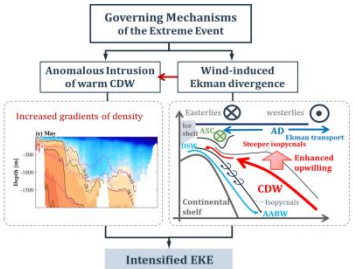

Figure 9. Schematic of mechanisms of the anomalous EKE event in 2017.

Acknowledgment and Reference

Acknowledgment:
This work is funded by the Shanghai Frontiers Science Center of Polar Research.

Reference:
Kang, D., and Curchitser, E. N. (2015). Energetics of Eddy-Mean Flow Interactions in the Gulf Stream Region. Journal of Physical Oceanography, 45(4), 1103-1120.

For more details:

He, Y., Zhou, M., & Kang, D. (2024). Strong Eddy Kinetic Energy Anomalies Induced by Baroclinic Instability in the Southwest Region of the Kerguelen Plateau, East Antarctica. Journal of Geophysical Research: Oceans, 129(6). https://doi.org/10.1029/2023jc020667

Contact:

yunzhuhe_nicole@sjtu.edu.cn

Deep winter mixed layer anchored by meandering ACC: Cross-basin variations

Zihan Song[1,2], Shang-Ping Xie[3]*, Lixiao Xu[1]*, Xiao-Tong Zheng[1], Xiaopei Lin[1], Yu-Fan Geng[1]

1. Ocean University of China; 2. Abdus Salam International Centre for Theoretical Physics, Italy;
3. Scripps Institution of Oceanography, USA

1 Motivation: What drives cross-basin variations in winter MLDs in the Southern Ocean ?

- Climate models simulate **an overly broad distribution in winter mixed layer depth (MLD)** in the Southern Ocean[1].

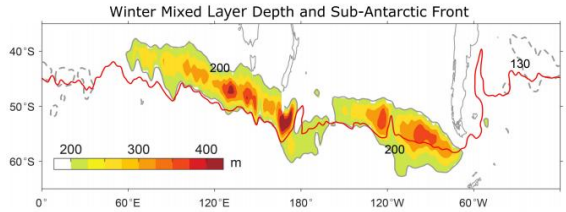

- In observations, **cross-basin variations** are pronounced:

1) MLDs in the Indo-Pacific (>300 m) vs. Atlantic (<150 m).

2) Deep mixed layers in the Indian sector is bounded by the Subantarctic Front (SAF), compared to the broad distribution southeast Pacific.

2 Hypothesis: Zonal variations in ACC differentiate ocean heat loss and background stratification

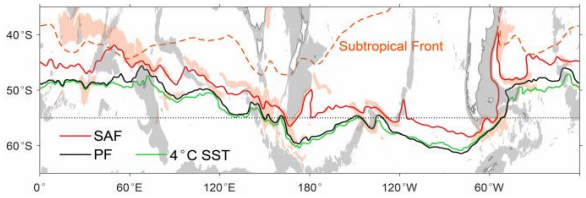

Zonal variations in ACC's latitudinal position and frontal intensity. Sub-Antarctic Front (SAF, -0.01 dyn m), Polar Fronts (PF, -0.42 dyn m); Large horizontal gradients in dynamic height (> 0.3 dyn m/100 km) are shaded in orange

■ 2.1 Meandering ACC (fronts) paths

southward / northward shifts from Indian to Pacific / Atlantic

↓

Warm / cold advection

↓

Warmer Pacific / colder Atlantic sectors

↓

Air-sea temperature difference (ΔT = SST - Ta) and ocean heat loss ?

equatorward (~ 45°S) / poleward (~56°S) position in Indian and Atlantic / Pacific

↓

Eddies from subtropical gyres & solar radiation

↓

strong / weak background stratification

■ 2.2 Varying frontal intensity

- Stronger ACC fronts in the Indian and Atlantic sectors
- Oceanic fronts amplify the air-sea heat exchange rate

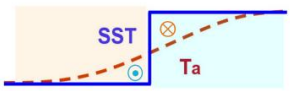

[2]Adapted from *Xie 2023*

4 Deep MLDs: Indian vs. Pacific sectors

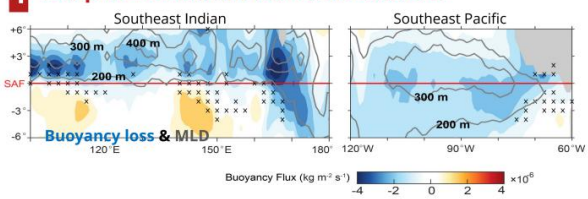

- Indian: **Large-scale (~25 W m^{-2})** ocean heat loss superimposed by **Frontal-scale (40-50 W m^{-2})** heat loss
- Pacific: Dominated by large-scale heat loss

3 Surface ocean heat loss patterns at two scales

Large scale Frontal scale

$$SST(SHF) \xrightarrow{\text{spatial mean filter}} SST_L(SHF_L) + SST_F(SHF_F)$$

■ 3.1 Large-scale SHF from observation

- Broad ocean heat loss (gain) in the Pacific (Atlantic) basin
- Peak heat loss **shifts westwards** along ACC from the peak SST

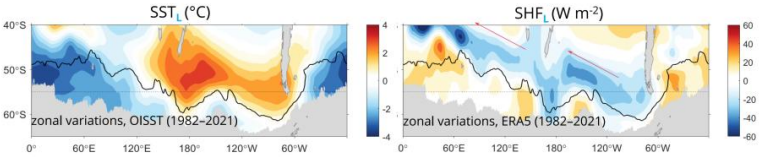

■ 3.2 Large-scale SHF from AGCM simulation

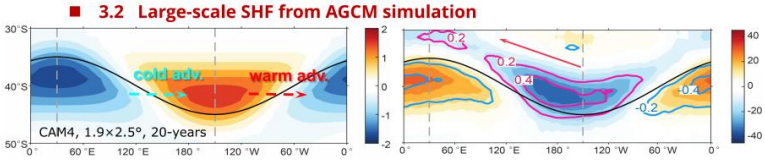

Symmetric SST forcing (°C) **Asymmetric** SHF & ΔT (contours)

- **Heat advection by westerlies** contributes to a larger ocean heat loss in the southeast Indian sector

■ 3.3 Frontal-scale pattern

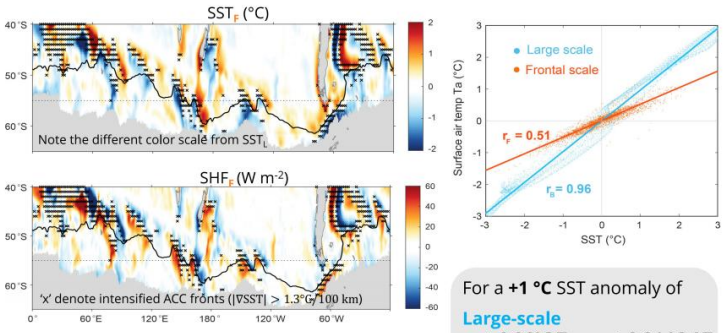

- Intense ocean heat loss (gain) on the warm (cold) flank of fronts
- Vanishingly small in southeast Pacific.
- SST$_F$ variations are **more efficiently** (**~12 times larger** than SST$_L$) to induce surface heat flux

For a **+1 °C** SST anomaly of

Large-scale
~ + 0.96°C Ta ~ **+ 0.04 °C ΔT**

Frontal-scale
~ + 0.51°C Ta ~ **+ 0.49 °C ΔT**

6 Conclusion

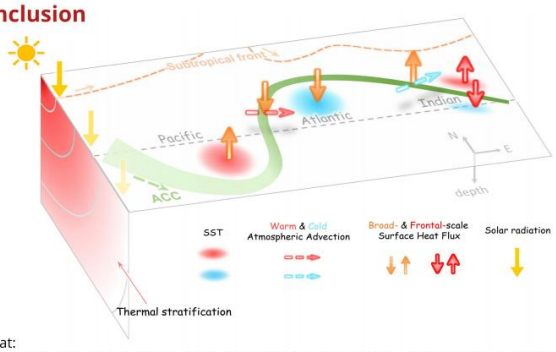

More details at:
Song, Z., S. Xie, L. Xu, X. Zheng, X. Lin, and Y. Geng, 2024: Deep winter mixed layer anchored by the meandering Antarctic Circumpolar Current: Cross-basin variations. *J. Climate*, https://doi.org/10.1175/JCLI-D-23-0174.1.

2024 | INTERNATIONAL SYMPOSIUM ON POLAR OCEAN AND GLOBAL CHANGE

SCHOOL OF OCEANOGRAPHY
SHANGHAI JIAO TONG UNIVERSITY
上海交通大学 海洋学院

Intrusions of the Circumpolar Deep Water and Wind-driven Mechanisms in the Amundsen Sea, West Antarctica

Ziang Li 李子昂 [1], Chuning Wang 王楚宁 [1], Zhaoru Zhang 张召儒[1, 2], Meng Zhou 周朦 [1, 2*]

1.School of Oceanography, Shanghai Jiao Tong University, Shanghai 200240, China;
2.Center for Polar Ecological Conservation, Polar Research Institute of China, Shanghai 200136, China

Introduction

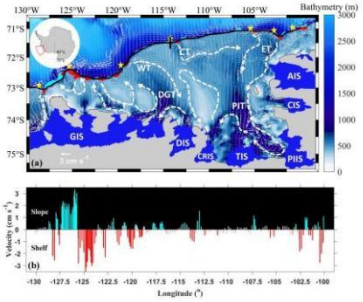

Figure 1. Bathymetry of the Amundsen Sea and its vicinity. (a) mCDW transport paths in the Amundsen Sea. (b) Distribution of cross-shelf break flows along the longitude. The flows exceeding +/- 0.5 cm s^{-1} was colored; red and cyan denote the direction onshore and offshore, respectively.

- Ice shelves in Amundsen Sea are in a rapid basal melting stage due to the Circumpolar Deep Water (CDW) intrusion which can be transported into the vicinity of ice shelves by sea troughs across the continental shelf.In Amundsen Sea, there are no strong easterly winds or even westerly winds that dominate most of the time on the slope; the Antarctic Slope Current (ASC) is weak here, and replaced by an eastward undercurrent.
- Previous studies have shown that the undercurrent consists of the CDW, which is deflected southward by interactions with the topography as it encounters the trough to form the cross-shelf break CDW intrusion. And the wind fields are the potential driver of the undercurrent.
- In this study, through a numerical model based on the Regional Ocean Modelling System (ROMS), we propose a mechanism for wind-driven CDW intrusion, suggesting that CDW intrusion is driven by large-scale barotropic process and regulated by local baroclinicity.

Key Points

- The interaction between local baroclinic effect and topography promotes cross-shelf break CDW intrusion.
- The variation of density gradient along-isobath at intrusion sites is influenced by the intensity of upstream eastward undercurrent.
- Both baroclinic and barotropic effects jointly regulating the strength of the eastward undercurrent by the wind fields.
- The wind fields impose a seasonal-scale internal constraint mechanism on the strength of the eastward undercurrent.

Results

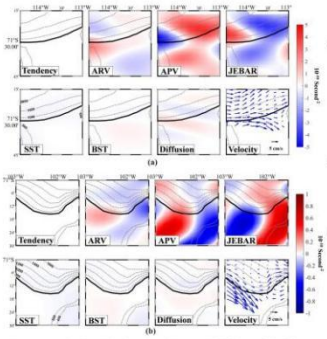

figure 2. Vorticity budget and flow fields in intrusion site (a) CT, (b) ET and their vicinities.

- Depth-averaged 2D vorticity equation (vector formula):

$$\underbrace{\vec{\xi}_t}_{Tendency} \underbrace{+\vec{U}\cdot\nabla\left(\frac{f}{D}\right)}_{APV} = \underbrace{-\vec{U}\cdot\nabla\left(\frac{\vec{\xi}}{D}\right)}_{ARV} \underbrace{+J\left(\chi, D^{-1}\right)}_{JEBAR} \underbrace{+\nabla\times\left(\frac{\vec{\tau}_s}{D}\right)}_{SST} \underbrace{-\nabla\times\left(\frac{\vec{\tau}_b}{D}\right)}_{BST} \underbrace{-\nabla\times\left(\vec{visc}\right)}_{VIS}$$

$$JEBAR = J\left(\chi, D^{-1}\right) = \left|\frac{\partial\left(\chi, D^{-1}\right)}{\partial(x\,y)}\right| = -\frac{1}{D^2}\left(\frac{\partial\chi}{\partial x}\frac{\partial D}{\partial y} - \frac{\partial\chi}{\partial y}\frac{\partial D}{\partial x}\right) = -\frac{1}{D^2}\left(\frac{\partial\chi}{\partial n}\frac{\partial D}{\partial \tau}\right)$$

- The positive **APV** term was almost balanced by the negative **JEBAR** term in the CDW intrusion sites on the shelf break (as **figure 2** shows); and the JEBAR effect is regarded as the driving mechanism for cross-shelf break CDW intrusion.
- As **figure 3** shows, the relationship between eastward undercurrent, JEBAR effect and CDW intrusion is: → Stronger undercurrent → More CDW intrusion → Undercurrent Expansion → More density transport → Stronger JEBAR effect

$$Pt_W(X) = P_W(x > X) = \int_X^{\infty} f_W(x)\mathrm{d}x,\ Pt_C(X) = P_C(x > X) = \int_X^{\infty} f_C(x)\mathrm{d}x.$$

- Extreme percentile (EP) of the wind fields: $EP(X) = P(Pt_W > X, Pt_C < X)$.
- Through the time series analysis and extreme event analysis of wind field and eastward undercurrent, it is suggested that wind events characterized by strong westerly winds and weak wind stress curl are expected to enhance the undercurrent.
- Through sensitivity tests based on wind fields, it is suggested that increasing the westerly wind and reducing the wind stress curl can respectively enhance the intensity of eastward undercurrent (as **figure 5** shows).
- Westerly winds: north-south SSH gradients drive an eastward geostrophic flow.
- Wind stress curl: Sv transport geostrophic component squeezes the local isopycnals.
- Science the intensity of westerly winds and wind stress curl is normally positively correlated in the Amundsen Sea,there is an internal constraint of wind fields on the undercurrent.

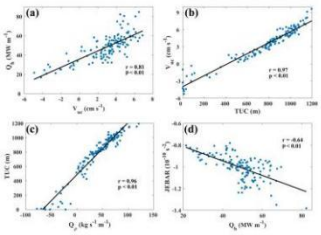

figure 3. The physical connection between upstream and downstream in all intrusion sites.

$$v_E = V_0\, e^{az}\sin\left(\frac{\pi}{4} + az\right),\ a = \sqrt{\frac{f}{2A_z}}, V_0 = \frac{\tau_y}{\rho\sqrt{fA_z}},$$

$$V_E = \int_{-H}^{0} v_E dz,$$

$$\beta\int_{-H}^{0}\rho v dz = \frac{\partial\tau_y}{\partial x} - \frac{\partial\tau_x}{\partial y},$$

$$V = \int_{-H}^{0} v dz,$$

$$V_g = V - V_E = \frac{1}{\beta\rho_0}\left(\frac{\partial\tau_y}{\partial x} - \frac{\partial\tau_x}{\partial y}\right) + V_0\frac{e^{-aH}}{2a}\left[\sin\left(\frac{\pi}{4} - aH\right) - \cos\left(\frac{\pi}{4} - aH\right)\right]$$

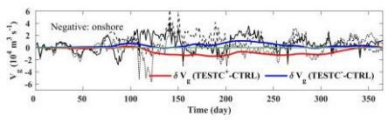

figure 6. Sensitivity test results of geostrophic Sverdrup transport (Vg).

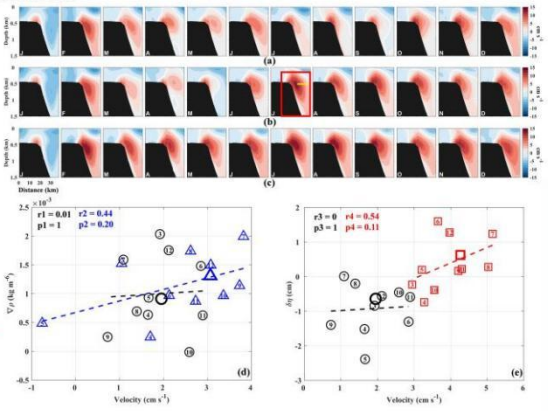

figure 5. The results of sensitivity experiments based on wind fields. Undercurrent near CT outputted from (a) CTRL, (b) TESTC- and (c) TESTW+

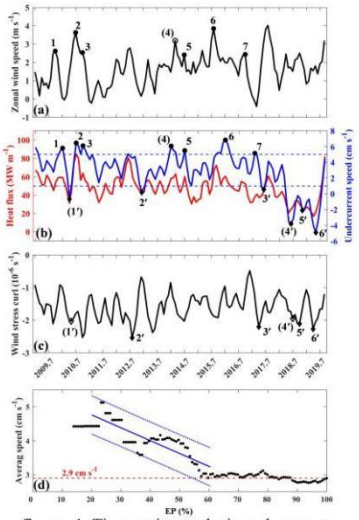

figure 4. Time series analysis and extreme event analysis of wind fields and eastward undercurrents.

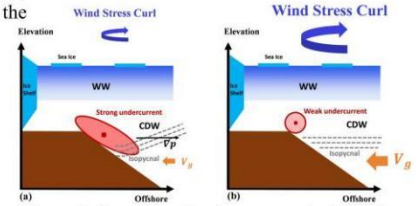

Figure 7. Two types of undercurrent and wind fields.

Conclusion

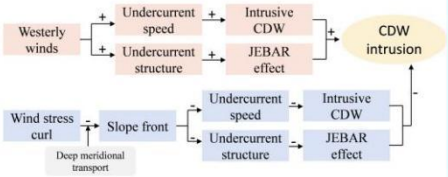

Spatial scales of kinetic energy and its transfer in the Arctic Ocean

Caili Liu[1,2], *Qiang Wang*[1]*, *Sergey Danilov*[1], *Nikolay Koldunov*[1], *Vasco Müller*[1], *Xinyue Li*[1], *Dmitry Sidorenko*[1], *Shaoqing Zhang*[2]

1 Alfred-Wegener-Institut, Helmholtz-Zentrum für Polar- und Meeresforschung (AWI), Germany 2 Ocean University of China, China

\(^o^)/~ *Presenter contact via emails: caili.liu@awi.de cc to liucaili@stu.ouc.edu.cn*

Summarizing information: This work investigates the scale-dependence KE of an eddy-rich modeled Arctic Ocean. The filtered KE at 2D field partitions the general circulations and eddy in spatial, and energy transfers further show an inverse-cascade and annual cycle at mixed layer and depp waters.

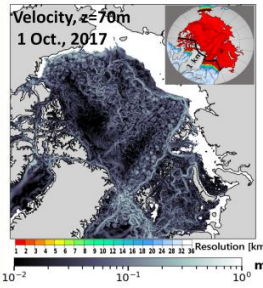

Data: Eddy resolved simulations of FESOM2 (Danilov et al., 2017), with resolution ~ 1 km in the Arctic. Initialized from the PHC3 climatology, spin up of 2010-2013 (of 1 km) and 4.5km from 1958-2010, finnaly 2014-2020 for analysis, ERA5 serves as the atm-forcings.

It shows that eddy flows are ubiquitous in the Arctic Ocean.

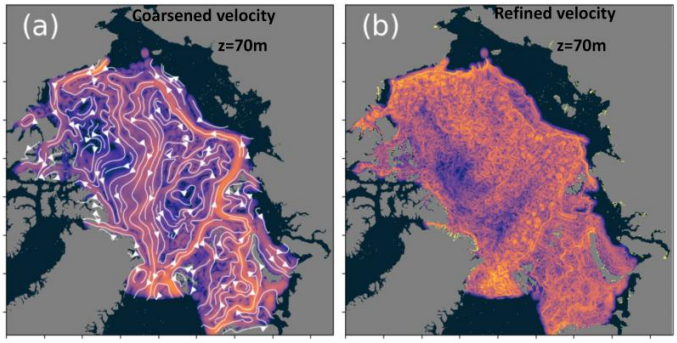

Methodology

Spatial scale-decomposition by means of coarse-graining method (Aluie et al., 2018), in which the convolution approach is applied for filtering.

Example of coarse-graining. Gyre-scale and mesoscale flows (01 Oct., 2017). *Velocity for spatials scales larger than 100 km (a) and the refined components (b).*

Main results (1) Kinetic energy power density over scales

The KE spectra scaling for the both of 70 m and 400 m detect slopes between -5/3 and -3 against scales, which ranges from 100 to 5 km, that is, a typical power-law scaling range for mesoscales and smaller scales in the geophysical flow .

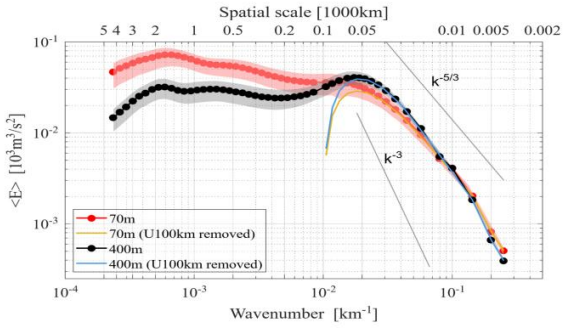

Main results (2) Energy transfer

$$\Pi = -\rho_0[(\overline{u^2} - \overline{u}^2)\overline{u}_x + (\overline{uv} - \overline{u}\,\overline{v})(\overline{u}_y + \overline{v}_x) + (\overline{v^2} - \overline{v}^2)\overline{v}_y]$$

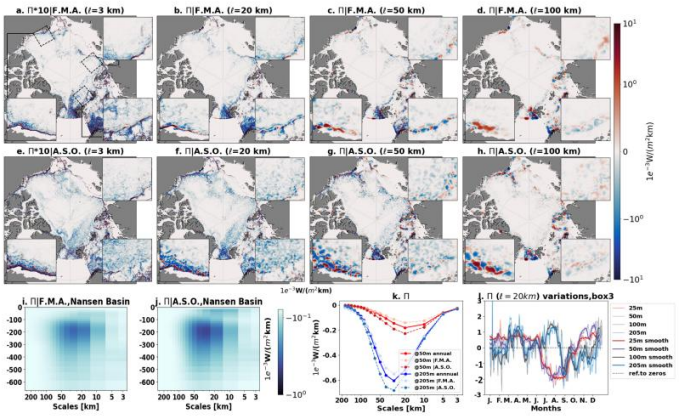

Acknowledgement

Foundings of the German Federal Ministry for Education and Research (BMBF) within the EPICA project (Grant No. 3F0889A), the AWI INSPIRES program and the Helmholtz Climate Initiative REKLIM (Regional Climate Change and Human). The computation was provided by the Jülich Supercomputing Centre. Caili Liu was awarded by China Scholarship Coucil (CSC, Grant 202206330003) scholarship.

Cite it as: *Liu, C., Wang, Q., et al. (2024). Spatial scales of kinetic energy in the Arctic Ocean, JGR-Oceans. doi:10.1029/2023JC020013*

ALFRED-WEGENER-INSTITUT
HELMHOLTZ-ZENTRUM FÜR POLAR- UND MEERESFORSCHUNG

Unraveling Spatio-Temporal Patterns in Global Sea Surface Temperatures with Dynamic Mode Decomposition

Menghao Dong[1], Cheng Sun*[1], Tian Wei[1], Zijing Guo[1], Wei Lou[1], Zichen Song[1], Linfeng Shi[1]

1. State Key Laboratory of Remote Sensing Science, Faculty of Geographical Science, Beijing Normal University, Beijing, China

Background

- Unraveling the large-scale spatial and temporal characteristics of global SST is essential and meaningful for understanding climate variability and climate prediction.
- Traditional methods, limited by assumptions of orthogonality, hinder our ability to fully capture the dynamics of global SST.
- A new method, Dynamic Mode Decomposition (DMD), has been proposed and applied to extract dynamic information from flow field data.

Method & Results

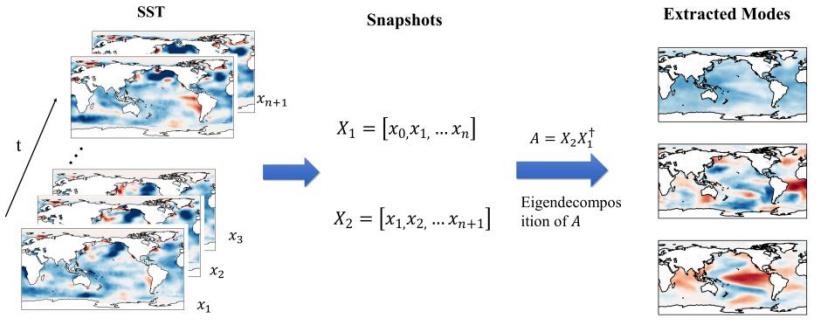

Figure 1. Schematic illustration of the Dynamic Mode Decomposition (DMD) method.

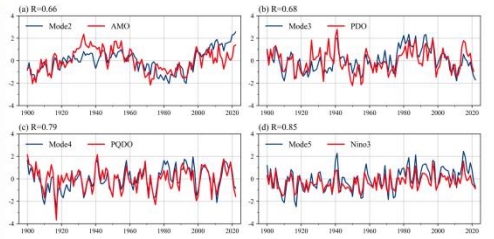

Figure 3. Standardized time series of DMD modes (blue) and the SST pattern indices (red). (a) Mode2 time series and the AMO index. (b) Mode3 and the PDO index. (c) Mode4 and detrended PQDO index. (d) Mode5 and Niño3 index.

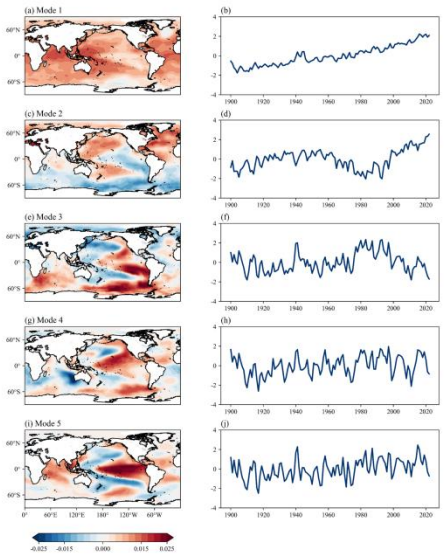

Figure 2. The patterns (left) and the corresponding standardized time series (right) extracted from annual global SST anomalies by dynamic model decomposition based on ERSSTv5 for the period 1900-2022.

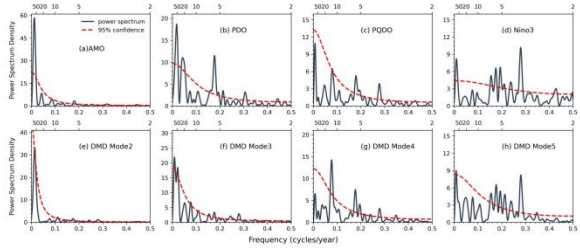

Figure 4. Power spectrum analysis of the indices includes (a) AMO, (b) PDO, (c) PQDO, (d) Niño3 and DMD time series for Mode2 to 5(e-h). The dark solid line represents the power spectrum, the red dash line indicates the 95% significance test for red noise.

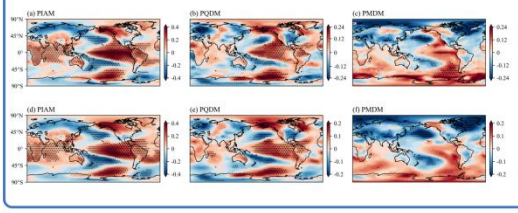

Figure 5. Regression maps of DMD time series with 2m temperature (a-c; unit: ° C) and 850 hPa temperature (b-d; unit: ° C) for the period 1900-2012. (a) PIAM time series and 2m temperature preprocessed by a 7-year high-pass filter. (b) PQDM time series and 2m temperature data preprocessed by an 8-16 years band-pass filter (c) PMDM time series and temperature data with linear trend removed and subjected to a 20-year low-pass filter. (d-f) same as (a-c), but for 850 hPa temperature.

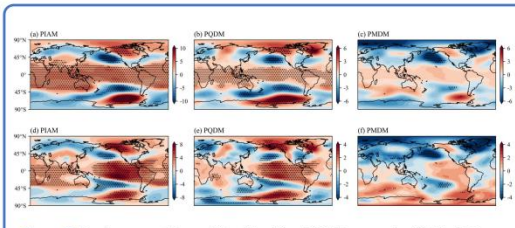

Figure 6. (a-c) same as Figure 4 (a-c), but for 500 hPa geopotential height. (d-f) same as Figure 4(d-f), but for the atmosphere thickness (unit: m)

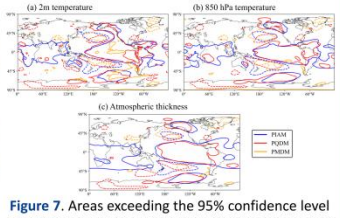

Figure 7. Areas exceeding the 95% confidence level significance test (based on the effective freedom of degree) for the regression

Conclusions

- DMD technique note only extracted global warming and AMO-like modes but also separated Pacific SST modes with similar spatial features but different dynamics.
- Spectral analysis shows that these Pacific modes have distinct periodicities: Pacific Multi-decadal Mode (PMDM, ~50 years), Quasi-decadal Mode (PQDM, 8-16 years), and Interannual Mode (PIAM, 2-8 years).
- The three Pacific modes exhibit significant differences in their impacts on global air temperature.

Amazon drought amplifies SST warming in the North Tropical Atlantic

Wei Lou[1], Cheng Sun*[1], Fred Kucharski[2], Jianping Li[3,4], Yusen Liu[1]

[1] State Key Laboratory of Remote Sensing Science, Faculty of Geographical Science, Beijing Normal University, Beijing 100875, China
[2] Abdus Salam International Centre for Theoretical Physics, Trieste, Italy
[3] Frontiers Science Center for Deep Ocean Multispheres and Earth System/Key Laboratory of Physical Oceanography/ Academy of the Future Ocean, Ocean University of China, Qingdao 266100, China.
[4] Laboratory for Ocean Dynamics and Climate, Pilot Qingdao National Laboratory for Marine Science and Technology, Qingdao 266237, China.

INTRODUCTION

The North Tropical Atlantic (NTA) Sea Surface Temperature (SST) anomaly is a critical component of the climate system, influencing global precipitation patterns and extreme weather events. Previous research on NTA warming has focused primarily on oceanic and atmospheric factors, with little attention to Land-Atmosphere (L-A) coupling factors. The Amazon rainforest, located adjacent to the NTA, is a key player in L-A interactions. Amazon deforestation has led to frequent droughts, reducing soil moisture, and warming the local climate. The impact of the Amazon rainforest on the NTA remains unclear, but its geographical proximity warrants further investigation. In this study, we present observational and modeling evidence that Amazon drought drives rapid warming of the NTA SST.

DATA AND MENTHODS

- **Data**

Variable	Sources	Time
Atmospheric and Surface heat flux	ERA5	1983–2019 Monthly
SST	Ersstv5	
Soil moisture	Terra Climate	
PDSI	sc_PDSIpm	

- **CMIP6**

This study selected the first available ensemble member of the historical simulation of each model, with a variant label of r1i1p1f1.

- **Definitions of main Indices**

Index	Definition
NTA SST	(0° –15° N,10° W–80° W)
ASM/APDSI	(5° S–5° N,45° W–65° W)

- **Methods**

Pearson correlation, Bootstrap resampling, Regression, Partial correlation, Multivariate linear regression analysis, Theil-Sen trend, Taylor Diagram, Two-tailed Student's t-test

- **Experimental design**

We designed two sets of experiments to isolate the climatic impact of decreased soil moisture: a control experiment (CTRL) and a sensitivity experiment (SM_Neg). In both experiments, prescribed soil moisture is imposed within a defined domain (5° S–5° N, 65° W–45° W) at each time step. Outside the domain, climatological monthly varying soil moisture is applied to the land surface to ensure that the difference in soil moisture between the two experiments was confined to the Amazon region, highlighting the impact of soil moisture drying in the Amazon. CTRL: The available soil moisture (both top soil layer and root zone) is prescribed using a monthly climatology. SM_Neg: The available soil moisture in the top soil layer is prescribed as the climatology superimposed with an anomaly term. This anomaly is defined as the product of the observed linear trend value, a 37-year time range (1983–2019) and a scaling factor. The difference between the SM_Neg and CTRL experiments isolates the climatic effect of decreased soil moisture over the Amazon region.

RESULTS

- **The cross-seasonal connection between ASM and NTA SST**

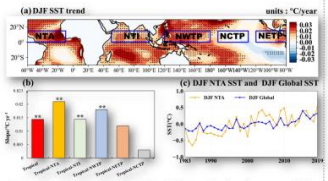

Fig. 1. Trend of NTA SST. (a) is the trend in observed SST during 1983–2019. (b) are the trend values in observed SST in Tropical, NTA, NTI, NWTP, NETP, and NCTP for DJF. (c) is the global mean SST anomaly time series and NTA SST anomaly time series.

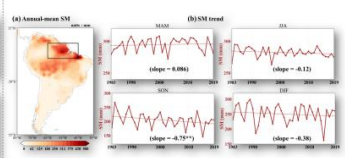

Fig. 2. Trend of ASM. (a) is the annual mean SM during 1983–2019. (b) is the ASM time series for MAM, JJA, SON, DJF.

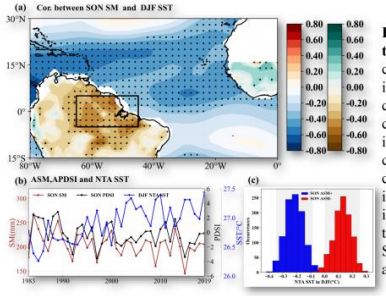

Fig. 3: Lead-lag relationship between the ASM and NTA. The detrended correlation map of the SON Amazon SM index with (a) DJF SST (blue and red color in the figure). The detrended correlation map of the DJF NTA SST index with (a) SON SM (brown and green color in the figure). (b) is the corresponding time series of NTA SST index, ASM index and APDSI index. (c) is the histogram of 10,000 realizations of the bootstrap method for the winter NTA SST anomaly indices of the preceding autumn ASM anomaly.

RESULTS

- **The physical process and modeling evidence associated with the influence of ASM on NTA SST**

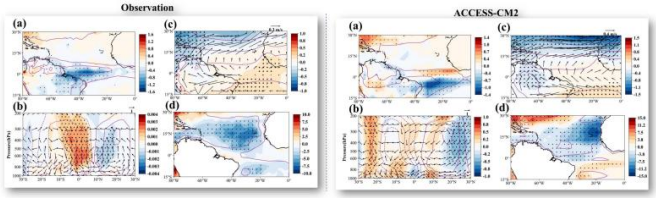

Fig. 4. The physical process of connecting ASM with NTA SST. To visualize the impact of the ASM reduction, all results are multiplied by minus one. (a) is the regression map of the SON ASM index with DJF precipitation. Regression of the DJF (b) meridional–vertical circulation anomalies averaged between 80° W–20° W and vertical velocity anomalies (c) surface pressure and 850 hPa wind and (d) Latent Heat Flux with the SON ASM index. Contours represent DJF-mean climatology. **Fig. 5 is same as Fig.4, but for the simulation results of CMIP6 model (ACCESS-CM2).**

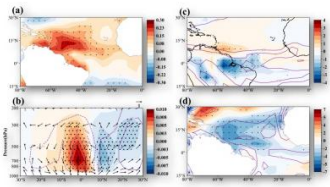

Fig. 6: Simulated results from the sensitivity experiments using ICTPGCM model for the winter season response to the reduction of the Amazon soil moisture. (a) SST, (b) meridional–vertical circulation anomalies averaged between 80° W–20° W and vertical velocity anomalies, (c) precipitation and (d) Latent Heat Flux. Contours represent the DJF-mean climatology of CTRL experiment.

- **A linear model for NTA SST warming**

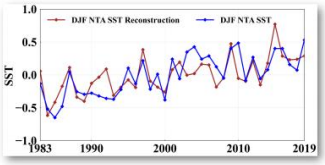

Fig. 7: Multiple Linear Regression (MLR) models constructed based on ASM. The observed and reconstructed SST series of the NTA using the MLR method during 1983–2019.

CONCLUSIONS

- A strong reversed relationship is identified between the interannual variations of winter NTA SST and autumn ASM, with decreased ASM persisting due to positive land-atmosphere feedback, leading to weakened ITCZ and Hadley circulation over the Tropical Atlantic.
- The weakened Hadley circulation induces a south-westerly wind anomaly over the NTA, resulting in weakened trade winds, suppressed latent heat release, and subsequent warming of NTA SST through the WES feedback.
- Simulations using CMIP6 fully coupled models and SM-forced mixed layer ocean models corroborate that Amazon drought exacerbates the weakening of the Hadley circulation, contributing to the warming of NTA SST.
- A multiple regression model constructed to analyze these interactions shows strong correlation with observed data (r = 0.72), indicating significant reconstruction skill for predicting NTA SST trend.

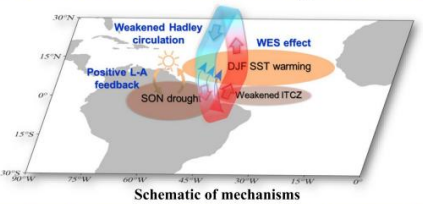

Schematic of mechanisms

Lou, W., Sun, C., Kucharski, F. et al. Amazon drought amplifies SST warming in the North Tropical Atlantic. Clim Dyn 62, 9377–9390 (2024). https://doi.org/10.1007/s00382-024-07400-1

Mechanisms and structure of more persistent summer intense Arctic cyclones compared to mid-latitude cyclones

Ruichang Ding[1,2], Jian Shi[1,2,3], Fei Huang[1,2,3*], Wenqin Zhuo[1,2], Ruihuang Xie[1,2,3], Shumeng Zhang[1,2,3]

[1] Physical Oceanography Laboratory/Frontier Science Center for Deep Ocean Multispheres and Earth System, Qingdao 266000, China
[2] College of Oceanic and Atmospheric Sciences, Ocean University of China, Qingdao 266000, China
[3] Laboratory for Ocean Dynamics and Climate, Qingdao Marine Science and Technology Center, Qingdao 266000, China

Correspoding author: Fei Huang, huangf@ouc.edu.cn

Introduction

Intense Arctic Cyclones (IACs) are significant extreme weather processes in the Arctic, but the understanding of their structural dynamics and intensification mechanisms lags behind that of mid-latitude cyclones. The rapid reduction of Arctic sea ice in summer, coupled with increasing socio-economic activities, necessitates exploring the physical mechanisms related to the intensification and structural evolution of IACs to address potential threats posed by these cyclones. In this study, we utilize a cyclone identification and tracking algorithm based on sea level pressure to identify and track Arctic cyclones. We establish an Arctic cyclone intensity threshold, which is defined as the 5th percentile of the probability density spectrum of the hourly minimum pressure in the Arctic region (north of 60° N) for different months. A cyclone is considered an IACs if its central pressure is lower than the monthly threshold when identified.

Statistical charateristics of IACs

On average, there are 4 IACs affecting the Arctic region IACh summer, with 2.3 of them originating from mid-latitude. Although there is no significant decadal trend in the frequency of IACs, the duration for which IACs maintain extreme intensity in the Arctic region has significantly increased, indicating that the potential threats posed by IACs may be more persistent.

Nearly all IACs rIACh their peak intensity in the Arctic region, indicating that cyclones can develop at high latitudes. We analyzed the circulation characteristics before and after IACs rIAChed peak intensity from a synoptic perspective. In the subpolar region, the extension of the low-level frontal zone poleward enhances atmospheric baroclinicity, while the intensification of the upper-level polar vortex causes the jet stream axis shift poleward, providing additional upper-level dynamical forcing and guiding the cyclone poleward. Thus, despite being at high latitudes, the circulation patterns still support the development and intensification of cyclones at these latitudes.

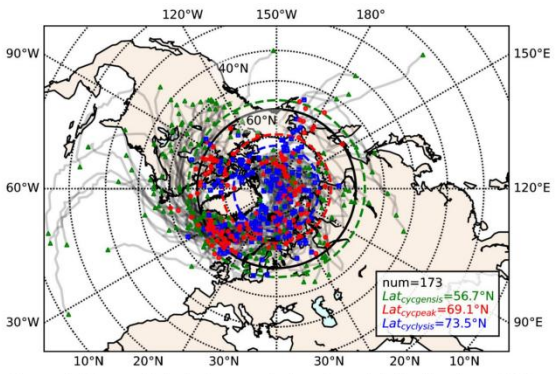

Figure 1. The statistical characteristics of spatial distribution ofIACs.

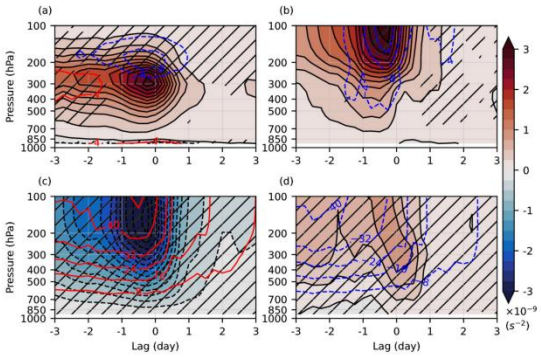

Figure 3. Composite vertical cross–section profiles of (a) vorticity advection (VADV) term, (b) temperature advection (TADV) term, (c) adiabatic heating (ADIA) term and (d) diabatic heating (DIA) term in Z-O equaiton.

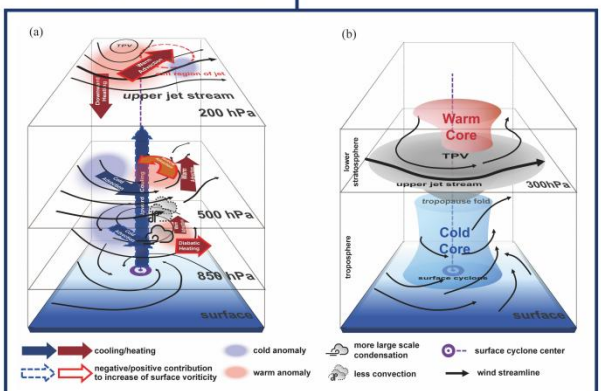

Figure 3. Schematic diagram of the intensification and structural evelution mechanisms of IACs.

Unique vertical structure of IACs

Though the intensification process of IACs is similar to that of mid-latitude cyclones, IACs exhibit a unique symmetrical vertical structure, characterized by a cold core in the troposphere and a warm core in the stratosphere. Diagnosing the atmospheric heating rates reveals that IACs experience adiabatic warming in the stratosphere due to the advection of the upper-level polar vortex across the tropopause, while strong upward motion in the troposphere causes adiabatic cooling. Due to the lack of convective heating in the polar region, IACs are prone to developing a vertical structure with a warm core in the stratosphere and a cold core in the troposphere after they mature.

Diagnostic analysis of intensification

We analyzed the impact of different forcing terms on the changes in vorticity during the intensification process of cyclones using the Zwack-Okossi(Z–O) diagnostic equation. Before IACs strengthen to their peak intensity, positive vorticity advection, positive temperature advection, and adiabatic heating have a positive effect on the minimum vorticity, while adiabatic cooling has a negative effect.

$$\frac{\partial \zeta_{gl}}{\partial t} = P_d \int_{p_t}^{p_l} (-\vec{V}\cdot\nabla\zeta_a)\,dp - P_d \int_{p_t}^{p_l} \frac{R}{f}\left[\int_{p}^{p_l} \nabla^2(-\vec{V}\cdot\nabla T + \frac{\dot{Q}}{c_p} + S\omega)\right] dp$$

(A) (B) (C) (D)

Summary

In summary, our study systematically examines the fundamental characteristics and general mechanisms governing the development and intensification of IACs. We compare and contrast these features with strong mid-latitude cyclones, employing the Z–O equation to dissect the contributions of various forcing processes to IACs intensification. Our findings underscore the significance of the baroclinic atmosphere and the corresponding upper level circulation configuration as crucial condition for intensification of IACs. Emphasizing the unique vertical structure of tropospheric cold core and stratospheric warm core of IACs, we elucidate their evolutionary mechanism.

Climatology of Arctic surface radiation and its links to driving factors

Meihua Wang[1,2], Lei Liu[1,2,] Hailing Xie[1, 2,*], Hao Zhou[1, 2], Jing Su[3], Xuejin Sun[1, 2]*

[1]College of Meteorology and Oceanography, National University of Defense Technology, Changsha, China
[2] High Impact Weather Key Laboratory of CMA, Changsha, China
[3]Key Laboratory for Semi-Arid Climate Change of the Ministry of Education, College of Atmospheric Sciences, Lanzhou University, Lanzhou, China

INTRODUCTION

Arctic surface temperature keeps 2-3 times of increasing rates than global warming speeds, and this phenomenon is called Arctic amplification (ACIA, 2005; Screen and Simmonds, 2010; Dai, 2021). Amplified warming over the Arctic is typically associated with the radiative and non-radiative feedback processes (Langen et al., 2012; Taylor et al., 2013). These processes influence the Arctic surface temperature by perturbations to the Arctic surface radiation (ASR) budget. It is therefore important to investigate the ASR budget for better understanding the physical causes of Arctic amplification.

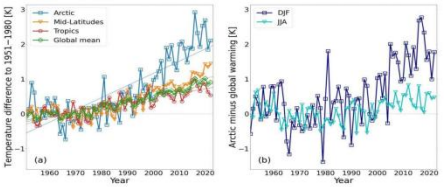

Fig. 1 The changes in Arctic surface temperature (Wendish et al., 2023).

Scientific question:

1. What are the factors that drive the temporal variability in the Arctic surface radiation?

2. Which one is the dominant factor affecting the Arctic surface radiation at regionally scale?

3. Can the model simulations capture the spatio-temporal characteristics of Arctic surface radiation?

METHODS

Datasets:

CERES (Monthly, 1°× 1°); ISCCP (Monthly, 1°× 1°)

ERA5 (Monthly, 1°× 1°); CMIP6 (Monthly)

Temporal Coverage: 2001.1-2014.12

Methods:

- Mann-Kendall (M-K) test is used to compute the long-term trend of Arctic surface radiation and its driving factors;
- Stepwise regression method is used to perform a multilinear regression analysis to establish a stable relationship between Arctic surface radiation anomalies and predictors anomalies.

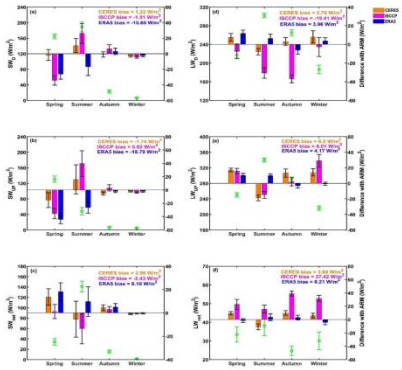

Fig. 2 The seasonal means of surface (a-c) shortwave (SW) and (d-f) longwave (LW) radiation from ground-based observations and their differences with various radiative products over the Arctic during 2001-2014.

RESULTS

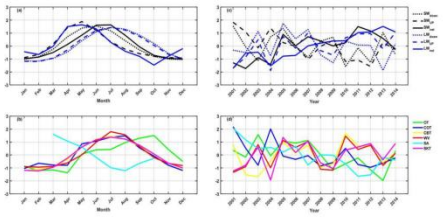

Fig. 3 The (a, b) seasonal and (c, d) annual variations in standardized

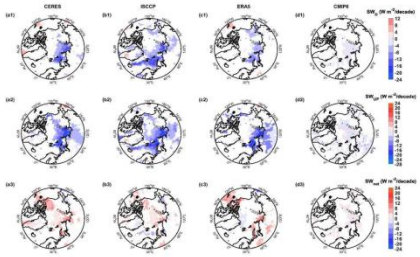

Fig. 4 The spatial trends of surface SW radiation among various radiative products over the Arctic during 2001-2014.

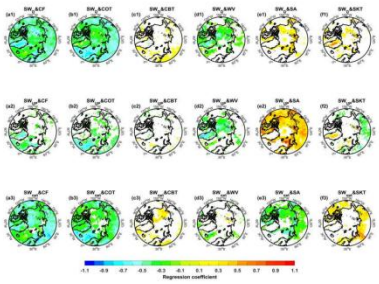

Fig. 5 The spatial patterns of regression coefficients on surface SW radiation and its impacts factors over the Arctic during 2001-2014.

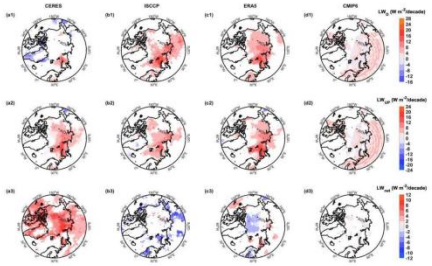

Fig. 6 The spatial trends of surface LW radiation among various radiative products over the Arctic during 2001-2014.

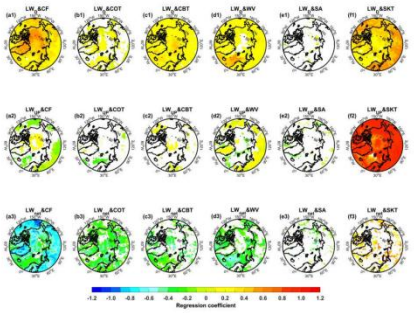

Fig. 7 The spatial patterns of regression coefficients on surface LW radiation and its impacts factors over the Arctic during 2001-2014.

CONCLUSIONS

1. **Compared with CERES-EBAF observations, ISCCP-FH, ERA5, and CMIP6 difficultly reproduce the long-term trends of the ASR, especially for longwave (LW).**
2. **Arctic surface net shortwave (SW) and LW radiation derived from CERES-EBAF show a positive trend ($p < 0.05$) of 3.5 and 4.3 W m-2/decade, respectively.**
3. **Trends of the ASR are tightly related to the climatic factors, which has a profound regional discrepancy.**

——Wang et al., CD, Under Review

REFERENCES

ACIA (2005) Arctic Climate Impact Assessment. Cambridge Univ Press pp 1000.

Screen JA, Simmonds I (2010) The central role of diminishing sea ice in recent Arctic temperature amplification. Nature 464(7293):1334-1337. https://doi.org/10.1038/nature09051.

Taylor PC, Cai M, Hu A, Meehl J, Washington W, Zhang GJ (2013) A decomposition of feedback contributions to polar warming amplification. J Clim 26:7023-7043. https://doi.org/10.1175/JCLI-D-12-00696.1.

E-mail：Meihua Wang: wangmh16@lzu.edu.cn **Lei Liu**: liulei17c@nudt.edu.cn **Hailing Xie**: xiehl11@lzu.edu.cn

College of Meteorology and Oceanography, National University of Defense Technology, Changsha, China

Recent impact of reduced Arctic sea-ice on the winter North Atlantic jet stream and its quantitative contributions compared to pre-industrial level

Jie Jiang[1], Shengping He[2,3], Ke Fan[1]*

[1] School of Atmospheric Sciences, Sun Yat-sen University, and Southern Marine Science and Engineering Guangdong Laboratory (Zhuhai), Zhuhai 519082, China

[2] Geophysical Institute, University of Bergen and Bjerknes Centre for Climate Research, Bergen, Norway

[3] Nansen Environmental and Remote Sensing Center, Bergen, Norway

Introduction

- Arctic sea ice (ArcSIC) has declined rapidly over the past 40 years. But the impact mechanisms of ArcSIC on mid-latitude circulation remain controversial.
- In this study, we simulate the winter North Atlantic jet stream (NAJS) in response to Arctic sea-ice loss.
- Explores possible reasons in simulating ice-loss-induced NAJS changes.
- Quantifies the contributions of external, internal forcing, and ArcSIC loss to NAJS response.

Data and Methods

- Polar Amplification Model Inter-comparison Project (PAMIP). The differences between the ensemble-mean pdSIC and piArcSIC simulations represent "pure" contribution of reduced ArcSIC.
- The difference between 1979–2008 and 1870–1880 in CMIP6 multi-model ensemble mean represent the "pure" contribution of external forcing.
- The relative contributions of external forcing, internal variability, and Arctic sea-ice loss:

$$A_{EX} = \frac{\Delta I_{EX}}{\Delta I_{OBS}} \times 100\%$$

$$A_{IV} = \frac{\Delta I_{OBS} - \Delta I_{EX}}{\Delta I_{OBS}} \times 100\%$$

$$A_{ArcSIC} = \frac{\Delta I_{ArcSIC}}{\Delta I_{OBS} - \Delta I_{EX}} \times 100\%$$

Conclusions

- The PAMIP models display robust but weak equatorward shift of the NAJS response to Arctic sea-ice loss.
- The simulation of models is associated with tropospheric baroclinic wave activity and the troposphere–stratosphere coupling.
- Compared to the pre-industrial period, the recent NAJS has accelerated and shifted poleward, which mainly attributed to internal variability.
- Reduced ArcSIC tends to slow down the acceleration and poleward shift of winter NAJS.

Results

Contributions of external forcing and internal variability to NAJS changes

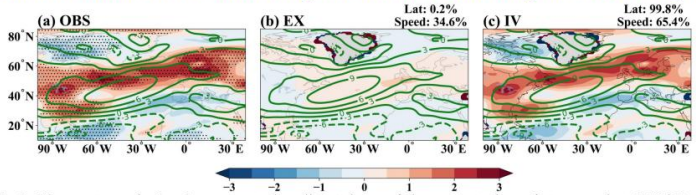

Fig 1. The contours in (a–c) represent the climatology of the present-day winter zonal at 850 hPa. The shading shows the recent zonal wind response compared to the pre-industrial period in (a) observations; (b) CMIP6 multi-model ensemble mean; (c) internal variability ((a) minus (b)).

Contribution of Arctic sea-ice loss in internal variability to NAJS changes

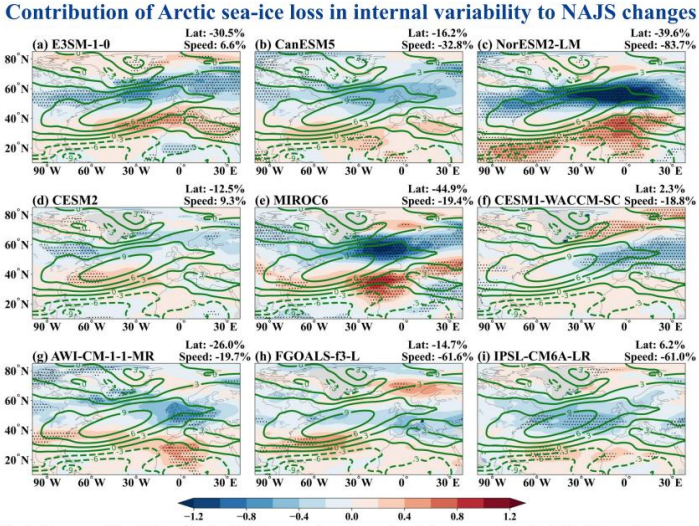

Fig 2. Same as **Fig. 1**, but for ArcSIC-loss-induced zonal wind response in the PAMIP models.

- Compared to the pre-industrial period, the observed westerly winds at 850 hPa during the present-day period show an increase to the north of the NAJS and northern Europe (**Fig. 1a**).
- External forcing accounts for about 34.6% of the observed change in NAJS speed, while its impact on the latitude of NAJS is not significant (**Fig. 1b**).
- The contribution of internal variability to the NAJS changes can be estimated as the difference between the observations and the response to external forcing (**Fig. 1c**), showing that the increase in observed westerlies north of the NAJS is mainly affected by internal variability.
- The ensemble-mean results in PAMIP show that reduced ArcSIC have a major negative impact on the internal variability of NAJS speed and latitude, indicating that without the forcing effect of Arctic sea-ice reduction, the NAJS would further accelerate and shift poleward (**Fig. 2**).

References

[1] Woollings T, Hannachi A, Hoskins B (2010) Variability of the North Atlantic eddy-driven jet stream. Quart J Roy Meteor Soc 136:856–868.
[2] Ye K, Woollings T, Screen JA (2023) European winter climate response to projected Arctic sea-ice loss strongly shaped by change in the North Atlantic jet. Geophys Res Lett 50:e2022GL102005.

Impacts of strengthened Antarctic Circumpolar Current on the Arctic climate

Peixi Wang[1], Yuhui Han[1], Xiaoming Hu[1], Zhenning Li[2], Xichen Li[3], Yingfei Fang[1], Jun Ying[4] and Song Yang[1]

[1]School of Atmospheric Sciences, Sun Yat-sen University, Zhuhai, China
[2]Division of Environment and Sustainability, Hong Kong University of Science and Technology, Hong Kong, China
[3]Institute of Atmospheric Physics, Chinese Academy of Sciences, Beijing, China
[4]Second Institute of Oceanography, Ministry of Natural Resources, Hangzhou, China

Introduction

- Understanding the relationship between the Arctic and Antarctic climates is an important yet a challenging topic.
- However, the impact of climate changes in the high latitudes of the Southern Hemisphere on the Northern Hemisphere, particularly on the Arctic, has received little attention.

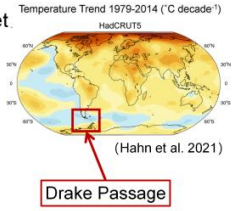

- In this study, we discuss the impact of strengthened Antarctic Circumpolar Current (ACC) on the seasonality of Arctic climate using idealized model simulations.

Model Experiment Design

Model	Experiments	Adding land in Drake Passage	Spinup	CO2 Forcing
CESM	DPO	no	249 years	B_2000 scenarios (250th yr - 349th yr)
	DPC	yes	900 years	B_2000 scenarios (901th yr - 1000th yr)

Results

Response of Seasonal Polar Climatology to Stronger ACC

Δ = DPO - DPC

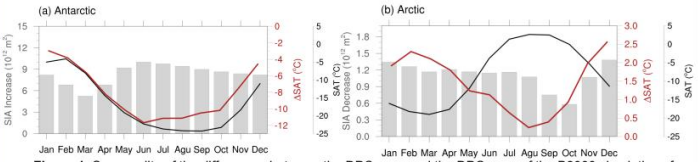

Figure 1. Seasonality of the differences between the DPC case and the DPO case of the B2000 simulations for sea ice area (gray bars), surface air temperature (red line), and the seasonality of climatological-mean surface air temperature (black line) in (a) Antarctic and (b) Arctic.

With strengthened ACC:

- The Antarctic gets colder with more sea ice and the Arctic gets warmer with less sea ice resulted from weaker ACC and Atlantic Meridional Overturning Circulation (AMOC).
- The changes in surface air temperature in the two poles are largest in winter, , a phenomenon referred to as “seasonal phase-locking”.

Role of Oceans in the Seasonal Phase-locking

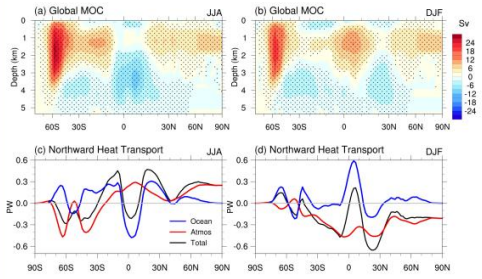

Figure 2. Seasonal differences between the DPO and DPC cases for (a-b) global meridional overturning circulation and (c-d) oceanic (blue line), atmospheric (red line), and total (black line) northward heat transport. Stippling indicates the significant difference at the 95% confidence level based on the Student’s t-test.

With strengthened ACC:

- The southern Meridional Overturning Circulation (MOC) strengthens more significantly in winter than in summer, leading to greater oceanic northward heat transport in winter around the Antarctic .
- The peak of ocean heat transport in the Northern Hemisphere shifts
- northward in DJF, which may induce winter amplified warming.

Results

Seasonality of Surface Energy Budget

Surface Energy Budget: $\Delta LW\_up = \Delta SW\_net + \Delta LW\_down + \Delta LH + \Delta SH - \Delta Dyn$

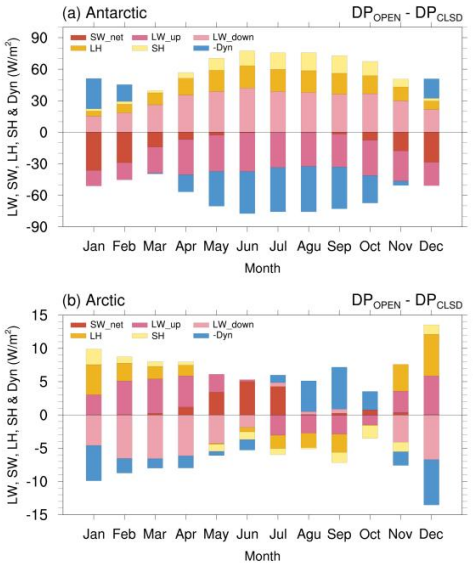

Figure 3. Seasonal differences in surface energy budget between the DPO and DPC cases in (a) the Antarctic and (b) the Arctic. The units for SW_net (red), LW_up (deep pink), LW_down (light pink), LH (brown), SH (yellow), and -Dyn (blue) are in W/m2 (positive values standing for warming).

In the Antarctic, with strengthened ACC:

- The surface solar radiation decreases in summer. Decreased energy reduces the engergy stored in the ocean and cools the atmosphere in the following winter.
- The seasonal energy transfer mechanism amplifies the winter cooling in the Antarctic.

In the Arctic, with strengthened ACC:

- The downward sensible and latent heat fluxes cool the surface more significantly in winter.
- The local atmosphere-ocean-ice interaction contributes to the winter amplification in the Arctic.

Conclusions

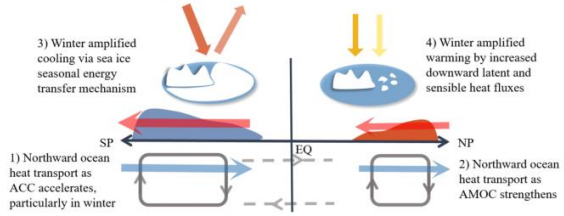

Figure 4. Schematic that depicts the global impacts of strengthened ACC, especially in winter.

- The influence of ACC exhibits a winter amplification effect, with the most significant polar response in winter.
- We attribute the stronger winter-time cooling in the Antarctic to enhanced acceleration of the ACC and the MOC, as well as the seasonal energy transfer mechanism.
- In the Arctic, this winter amplification of surface air warming is attributed to ocean heat transport and downward latent and sensible fluxes.
- This work shows how the small but important topography changes affect global climate.
- Model results highlight the crucial role of ACC in the current climate system and demonstrate the remote influence of ACC on the Arctic climate.

Interdecadal opposite variation of December–January blocking days between the eastern North Atlantic and Ural region around 2008

Yifan Xu[1] Ke Fan[1]* Shengping He[2,3]

[1] School of Atmospheric Sciences, Sun Yat-sen University, and Southern Marine Science and Engineering Guangdong Laboratory (Zhuhai), Zhuhai, 519000, China

[2] Geophysical Institute, University of Bergen and Bjerknes Centre for Climate Research, Bergen, Norway

[3] Nansen Environmental and Remote Sensing Center, Bergen, Norway

- **Based on observational datasets and the simulations from the PAMIP, a pronounced interdecadal variation of the eastern North Atlantic–Ural blocking days dipole pattern in December–January occurs in 2008. Specifically, the blocking days in Ural (eastern North Atlantic–western Europe) regions increase (decrease) after 2008.**
- **Further research shows that the changes in the simultaneous background atmospheric circulation field (westerly winds, vertical shear of zonal winds, and meridional potential vorticity gradient etc.) contribute to the interdecadal variation of the dipole pattern.**
- **Moreover, through the enhanced sea-ice-atmosphere interaction, the rapid decrease in Barents–Kara sea ice, dominated by newly formed sea ice, and the interdecadal variations of North Atlantic sea surface temperature anomalies combine to influence significantly the dipole pattern.**

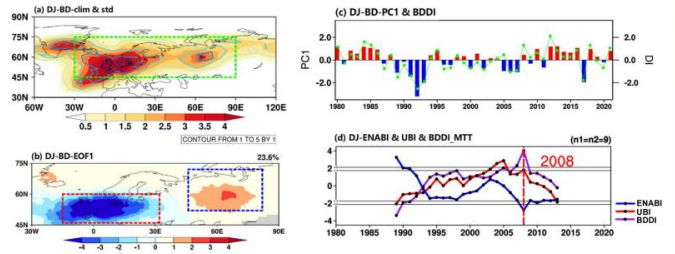

Figure 1. (a) Climatology (shading, unit: d) and standard deviation (contours, unit: d) of blocking days in December–January during 1980–2021. (b) The spatial field and (c) its normalized time series (bar) in the analysis of the first mode (EOF1) of the eastern North Atlantic–Ural blocking days anomalies and blocking days dipole pattern index (polyline) in December–January during 1980–2021. (d) Moving *t*-test of the December–January blocking days index: eastern North Atlantic–western Europe (blue); Urals (red); dipole pattern (Urals minus eastern North Atlantic–western Europe; purple). The blue box in (b) indicates the Urals region, and the red box indicates the eastern North Atlantic–western Europe region.

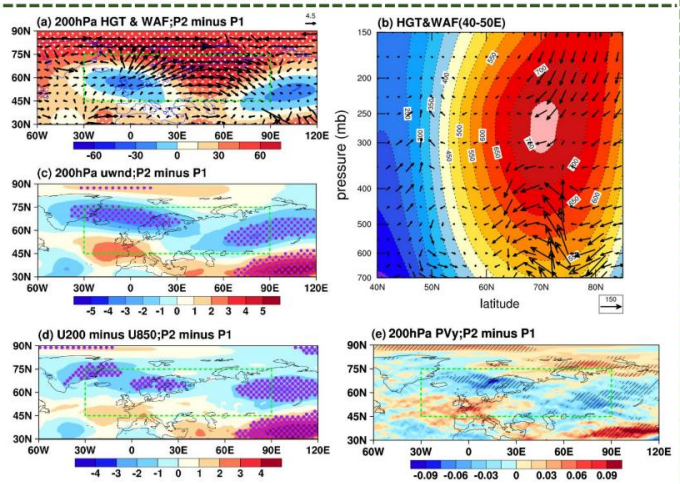

Figure 2. Interdecadal difference field (2008–2021 minus 1980–2007) of December–January (a) 200-hPa geopotential height (shading, unit: gpm) and wave activity flux (arrows, unit: $m^2\ s^{-2}$). (b) Latitude–height profile of interdecadal difference field of the geopotential height (shading, unit: gpm) and wave activity flux (arrows, unit: $m^2\ s^{-2}$) with a zonal mean (40° –50° E). Interdecadal difference field (2008–2021 minus 1980–2007) of December–January (c) 200-hPa westerly wind (unit: m s^{-1}), (d) vertical shear of zonal wind (m s^{-1}), and (e) 200-hPa meridional potential vorticity gradient (unit: 10^{-5} PVU m^{-1}). Dots in (a, c, d) and slashes in (e) indicate that the difference field exceeds the 90% confidence level based on a two-tailed Student's *t*-test.

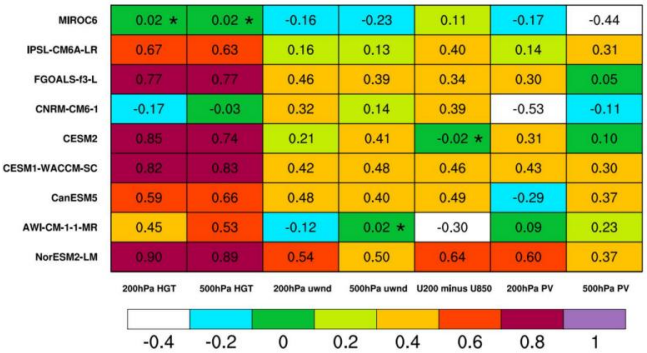

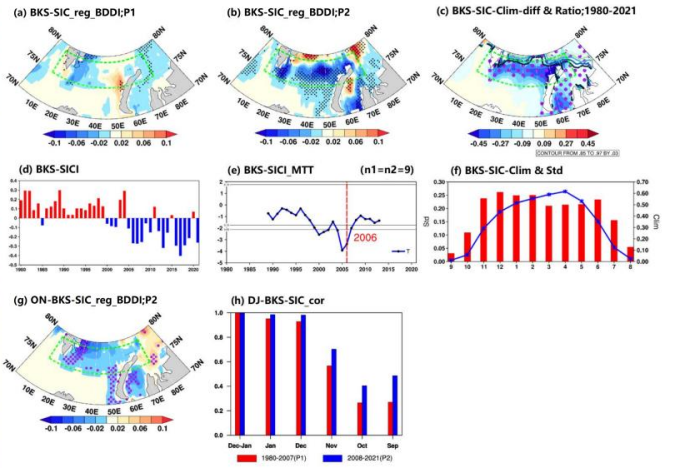

Figure 3. Simultaneous BKS sea-ice concentration (SIC) of the December–January blocking days dipole pattern index regression in (a) 1980–2007 and (b) 2008–2021. (c) Interdecadal differences (2008–2021 minus 1980–2007; shading) of December–January BKS sea ice and the proportion of newly formed sea ice in the BKS during December–January in 1980–2021 (newly formed SIC/SIC; contour). (d) The BKS SIC index and (e) its moving *t*-test. (f) Monthly SIC climatology (polyline) and standard deviations (bars) in the BKS during 1980–2021. (g) Previous October–November BKS SIC of the December–January blocking days dipole pattern index regression in 2008–2021. (h) The correlation coefficient of the December–January BKS SIC index with the simultaneous December–January average, January, December and the previous autumn (November, October, September). The dots in (a–c, g) indicate statistical significance at the greater than 90% confidence level based on a two-tailed Student's *t*-test. The green box in (a–c, g) indicates the BKS region.

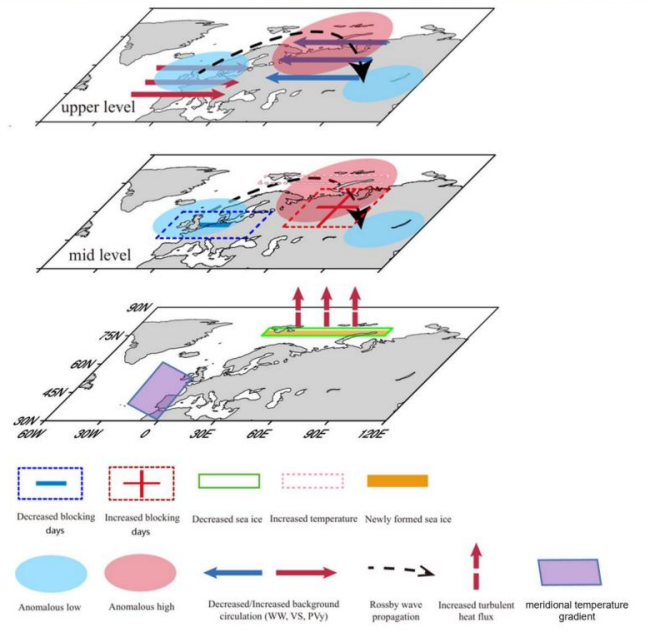

Figure 5. Schematic of the mechanism through which the sea ice in the Barents–Kara Sea and North Atlantic SST influence the interdecadal variation of the blocking days dipole pattern in the eastern North Atlantic–Urals region during December–January in 2008.

Figure 4. The spatial (eastern North Atlantic–Urals; 45° –75° N, 30° W–90° E) correlation coefficients between observed (2008–2021 minus 1980–2007) and PAMIP-simulated (modern minus pre-industrial; AWI-CM-1-1-MR, CanESM5, CESM1-WACCM-SC, CESM2, CNRM-CM6-1, FGOALS-f3-L, IPSL-CM6A-LR, MIROC6, NorESM2-LM) difference fields of background circulation in December–January: 200-hPa and 500-hPa geopotential height (unit: gpm); 200-hPa and 500-hPa westerly wind (unit: m s^{-1}); vertical shear of zonal wind (200-hPa westerly wind minus 850-hPa westerly wind, unit: m s^{-1}); 200-hPa and 500-hPa potential vorticity (unit: PVU). An asterisk indicates that the correlation coefficient does not exceed the confidence level of 95% based on a two-tailed Student's *t*-test.

Impact of Early-winter Antarctic Sea Ice Reduction on Antarctic Stratospheric Polar Vortex

Jibin Song[1] Jiankai Zhang[1,*]

1. College of Atmospheric Sciences, Lanzhou University, Lanzhou 730000, China

Abstract: This research uses the ERA5 reanalysis dataset and the WACCM-SC model to investigate the following questions: (1) What are the impacts and mechanisms of Antarctic sea ice changes on the Antarctic stratospheric polar vortex? (2) Are the effects of sea ice changes on planetary waves different in different regions? Our results indicate that the Antarctic sea ice reduction during early austral winter weakens the Antarctic polar vortex (Fig 2), and we further explored the underlying physical mechanisms.

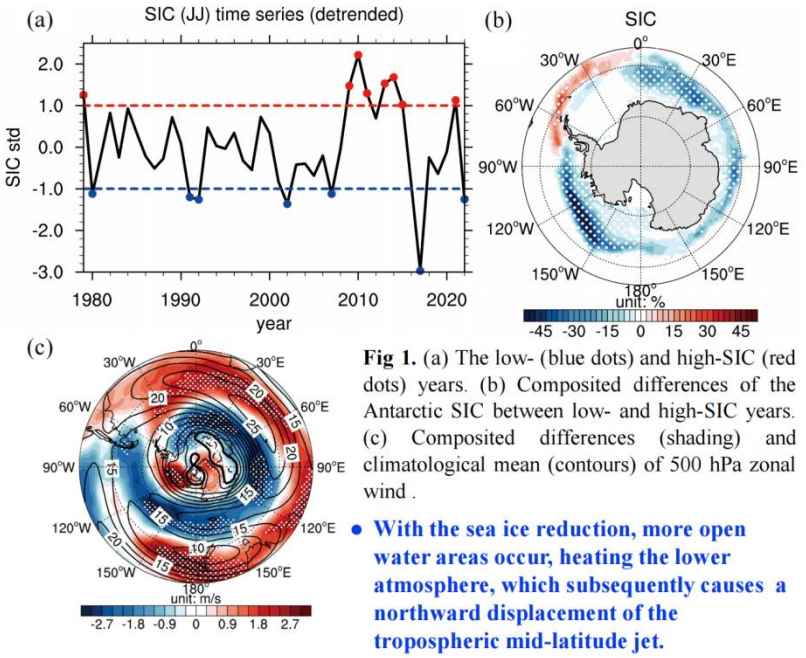

Fig 1. (a) The low- (blue dots) and high-SIC (red dots) years. (b) Composited differences of the Antarctic SIC between low- and high-SIC years. (c) Composited differences (shading) and climatological mean (contours) of 500 hPa zonal wind .

- **With the sea ice reduction, more open water areas occur, heating the lower atmosphere, which subsequently causes a northward displacement of the tropospheric mid-latitude jet.**

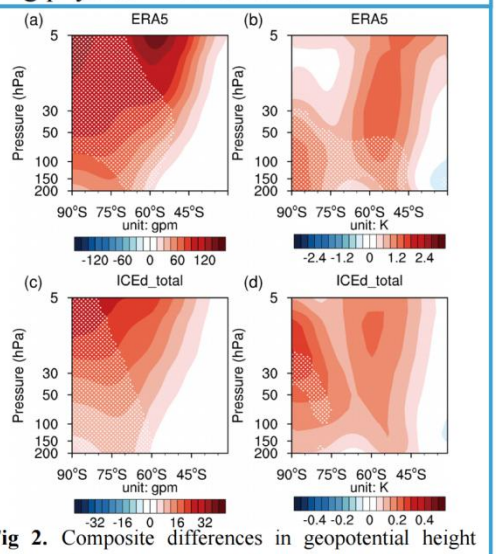

Fig 2. Composite differences in geopotential height (left) and temperature (right) during austral winter, derived from (a-b) the ERA5 dataset and (c-d) the WACCM-SC simulations.

- **The Antarctic sea ice reduction results in a weaker Antarctic polar vortex.**

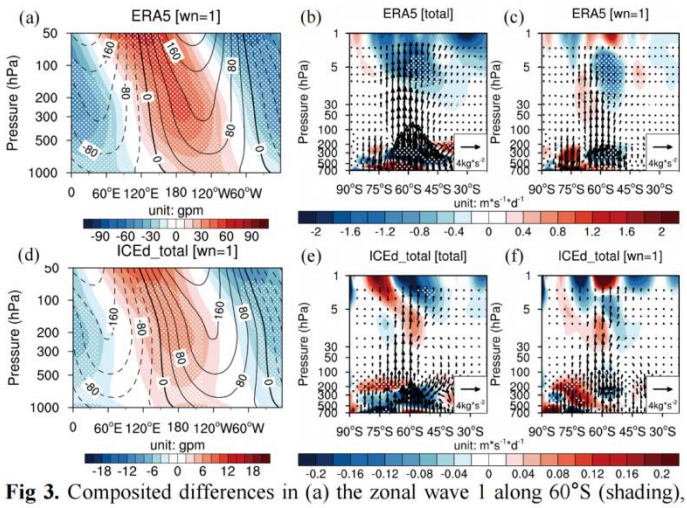

Fig 3. Composited differences in (a) the zonal wave 1 along 60°S (shading), (b) EP-flux (vector) and its convergence (shading) and (c) its wave 1 component during early austral winter between low- and high-SIC scenarios. (a-c) derived from the ERA5 dataset, (d-f) derived from the WACCM-SC simulations.

- **The sea ice reduction strengthens planetary wave activity in the troposphere and more waves propagate upward into the stratosphere, ultimately weakens the stratospheric polar vortex.**

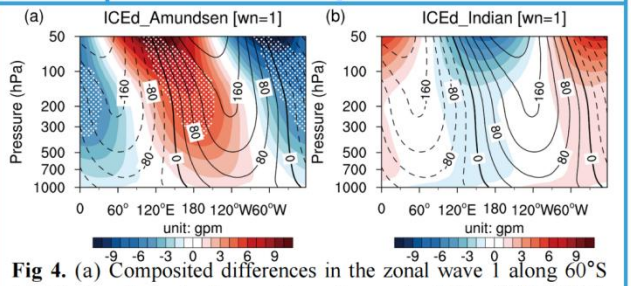

Fig 4. (a) Composited differences in the zonal wave 1 along 60°S (shading), derived from Amundsen-sector-SIC (90°-180°W) simulations. (b) same as (a), but derived from Indian-sector-SIC (0°-60°E) simulations.

- **The sea ice reduction in the Amundsen Sea sector enhances the planetary wave activity, whereas in the Indian Ocean sector, has the opposite effect.**

Summary:

- **The sea ice reduction in early austral winter contributes to the weakening of the Antarctic stratospheric polar vortex during austral winter by affecting tropospheric planetary wave activity.**
- **The sea ice reduction in the Amundsen Sea sector enhances the planetary wave activity, whereas in the Indian Ocean sector, has the opposite effect.**

*jkzhang@lzu.edu.cn, songjb2024@lzu.edu.cn